Oxidierte Phospholipide und ihre Funktion in neuronaler Erregbarkeit in primären sensorischen Neuronen

Oxidized phospholipids and their role in neuronal excitation of primary sensory neurons

Doctoral thesis for a doctoral degree
at the Graduate School of Life Sciences,
Julius-Maximilians-Universität Würzburg,
Section Neuroscience and Clinical Sciences

submitted by

Corinna Martin

from

Rüsselsheim

Würzburg, 29.01.2018

Submitted on: …………………………………………………...……..

Members of the Promotionskomitee:

Chairperson: **Prof. Thomas Dandekar**

Primary Supervisor: **PD Dr. Robert Blum**

Supervisor (Second):   **Prof. Dr. Heike Rittner**

Supervisor (Third):   **Prof. Dr. Erhard Wischmeyer**

Date of Public Defence: …………………………………….……

Date of Receipt of Certificates: …………………………………

Abbreviations

AITC	Allyl isothiocyanate
AP	Action potential
ATP	Adenosine triphosphate
BCTC	4-(3-Chloro-2-pyridinyl)-N-[4-(1,1-dimethylethyl)phenyl]-1-piperazinecarboxamide
BK	Bradykinin
Ca^{2+}	Calcium ions
DRG	Dorsal root ganglion
DMEM	Dulbecco's Modified Eagle's Medium
E. Coli	*Escherichia coli*
ER	Endoplasmic Reticulum
FCS	Fetal calf serum
Forsk	Forskolin
G418	Geniticin
HC-030031	2-(1,3-Dimethyl-2,6-dioxo-1,2,3,6-tetrahydro-7H-purin-7-yl)-N-(4-isopropylphenyl) acetamide
HEK293	Human embryonic kidney cells
HEK293$_{rTRPV1}$	Human embryonic kidney cells expressing rat TRPV1
HEK293$_{hTRPA1}$	Human embryonic kidney cells expressing human TRPA1
His	Histamine
IS	Inflammatory soup
KO	Knock out
MP	Membrane potential
$Na_V1.7$	Voltage-gated sodium channel 1.7
$Na_V1.8$	Voltage-gated sodium channel 1.8
$Na_V1.9$	Voltage-gated sodium channel 1.9
$Na_V1.9$ -/-	Knock out of the voltage-gated sodium channel 1.9
ND7/23	Mouse neuroblastoma X Rat neuron hybrid
NGF	Neuronal growth factor
OxPAPC	Oxidized PAPC
PAPC	1-palmitoyl-2-arachidonoyl-sn-glycero-3-phosphocholine
PCR	Polymerase chain reaction
PGE$_2$	Prostaglandin E2
PGPC	1-Palmitoyl-2-glutarylphosphatidylcholine
Pen./Strep.	Penicillin/Streptomycin

POVPC	1-(palmitoyl)-2-(5-oxovaleroyl)phosphatidylcholine
RMP	Resting membrane potential
ROS	Reactive Oxygen Species
TRPA1	Transient receptor potential channel ankyrin type 1
TRPV1	Transient receptor potential channel vanilloid type 1
VGSC	Voltage gated sodium channel
Wt	Wild typ

Table of contents

List of figures

List of tables

Zusammenfassung

Im Zuge einer Studie über Entzündungsschmerz hat unsere Arbeitsgruppe oxidierte Phospholipide (OxPL) als neue endogene Entzündungsmediatoren entdeckt. Diese werden im entzündeten Gewebe produziert und vermitteln ihre schmerzinduzierende Funktion durch Aktivierung von sogenannten transienten Rezeptorpotentialkanälen TRPA1 und TRPV1. Beide Ionenkanäle werden von afferenten Nozizeptoren exprimiert und sind Sensoren für chemische Reize. In dieser Arbeit wurde mithilfe von Calcium Imaging und elektrophysiologischen Messungen gezeigt, dass oxidierte Phospholipide TRPA1 und TRPV1 aktivieren und eine erhöhte Erregbarkeit in sensorischen Neuronen der Hinterwurzelganglien (DRG Neuronen) auslösen. Hierbei aktivieren oxidierte Phospholipide TRPA1 stärker als TRPV1 und induzieren langanhaltende, nicht-selektive Einwärtsströme. Ein Bestandteil von OxPL, das Oxidationsprodukt PGPC, aktiviert zudem eine Mutante von TRPA1, die nicht die Bindungsstelle für elektrophile Agonisten trägt. Dies lässt vermuten, dass OxPL die TRP Kanäle über einen indirekten, mechanischen Mechanismus aktivieren. Als nächstes wurde der Einfluss von OxPL auf die Erregbarkeit von sensorischen Neuronen untersucht. Schnelles Calcium Imaging zeigte, dass eine akute Stimulation mit OxPL zu wiederholten spike-ähnlichen Signalen in DRG Neuronen führt. Diese waren nur in Neuronen mit kleinem Durchmessern zu finden und deren Aktivierung konnte sowohl durch Antagonisten gegen TRPA1/V1 als auch mit Inhibitoren spannungsgesteuerter N-Typ Kalziumkänale blockiert werden. Elektrophysiologische Untersuchungen zeigten, dass eine Strominjektion mit gleichzeitiger lokaler Applikation von OxPL zur Erhöhung der Aktionspotentialsrate in kleinen DRG Neuronen führt. Deshalb wurde untersucht, ob der spannungsgesteuerte Natriumkanal $Na_V1.9$ für die durch OxPL induzierten Kalziumspikes und Aktionspotentiale verantwortlich ist, da er an der unterschwelligen Erregbarkeit von Neuronen beteiligt ist. Es konnte jedoch kein Unterschied beim Ruhemembranpotential oder der OxPL induzierten Aktionspotentialsrate zwischen den wt und $Na_V1.9$-defizienten ($Na_V1.9$ KO) Neuronen festgestellt werden. Um zu verstehen, ob $Na_V1.9$ unter inflammatorischen Bedingungen in die OxPL induzierte Erregungskaskade integriert wird, wurden die sensorischen Neurone mit inflammatorischen Mediatoren vorbehandelt und anschließend mit OxPL stimuliert. Dies führte sowohl zu einer stark erhöhten Kalziumspike- als auch Aktionspotentialfrequenz im wt, während die $Na_V1.9$ KO Neurone sich wie unter nicht inflammatorischen Bedingungen verhielten. Unter inflammatorischen Bedingungen konnte zudem eine Erniedrigung des Ruhemembranpotentials im Vergleich zwischen $Na_V1.9$ KO und wt Neuronen beobachtet werden. Das lässt vermuten, dass $Na_V1.9$ seine Ruheaktivität nur unter Entzündungsbedingungen zeigt.

In dieser Arbeit wurde gezeigt, dass OxPL endogene Agonisten sind, die kleine DRG Neurone, ein zelluläres Model für Nozizeptoren, über TRPA1 und TRPV1 aktivieren. Dieser Effekt wird unter Entzündungsbedingungen verstärkt. Hierbei spielt der unterschwellig aktive Kanal $Na_V1.9$ eine essentielle Vermittlerrolle, indem er die Auslösung von Aktionspotentialen nach einem OxPL Stimulus erleichtert. Da Mutationen im menschlichen Na1.9 Kanal zu einem erhöhten oder sogar fehlendem Schmerzempfinden führen können, gibt diese Studie einen neuen Einblick in den Mechanismus mit dem $Na_V1.9$ Stimuli endogener, reizauslösender Substanzen unter Entzündungsbedingungen amplifiziert.

Abstract

Recently, our research group identified in a study novel proalgesic targets in acute and chronic inflammatory pain: oxidized phospholipids (OxPL). OxPL, endogenous chemical irritants, are generated in inflamed tissue and mediate their pain-inducing function by activating the transient receptor potential channels TRPA1 and TRPV1. Both channels are sensors for chemical stimuli on primary afferent nociceptors and are involved in nociception. Here, with the help of calcium imaging and *whole cell* patch clamp recording techniques, it was found that OxPL metabolites acutely activate TRPA1 and TRPV1 ion channels to excite DRG neurons. OxPL species act predominantly via TRPA1 ion channels and mediate long-lasting non-selective inward currents. Notably, one pure OxPL compound, PGPC, activated a TRPA1 mutant lacking the binding site for electrophilic agonists, suggesting that OxPL activate TRP ion channels by an indirect mechanical mechanism. Next, it was investigated how OxPL influence the excitability of primary sensory neurons. Acute stimulation and fast calcium imaging revealed that OxPL elicit repetitive, spike-like calcium transients in small-diameter DRG neurons, which were fully blocked by antagonists against TRPA1/V1 and N-type voltage-gated calcium channels.

In search of a mechanism that drives repetitive spiking of DRG neurons, it was asked whether $Na_V1.9$, a voltage-gated sodium channel involved in subthreshold excitability and nociception, is needed to trigger OxPL-induced calcium spikes and action potential firing. In electrophysiological recordings, both the combination of local application of OxPL and current injection were required to efficiently increase the action potential (AP) frequency of small-diameter sensory neurons. However, no difference was monitored in the resting membrane potential or OxPL-induced AP firing rate between wt and $Na_V1.9$-deficient small diameter DRG neurons. To see whether $Na_V1.9$ needs inflammatory conditions to be integrated in the OxPL-induced excitation cascade, sensory neurons were pretreated with a mixture of inflammatory mediators before OxPL application. Under inflammatory conditions both the AP and the calcium-spike frequency were drastically enhanced in response to an acute OxPL stimulus. Notably, this potentiation of OxPL stimuli was entirely lost in $Na_V1.9$ deficient sensory neurons. Under inflammatory conditions, the resting membrane potential of $Na_V1.9$-deficient neurons was more negative compared to wt neurons, suggesting that $Na_V1.9$ shows resting activity only under inflammatory conditions.

In conclusion, OxPL are endogenous irritants that induce excitability in small-diameter DRG neurons, a cellular model of nociceptors, via TRP activation. This effect is potentiated under inflammatory conditions. Under these conditions, $Na_V1.9$ functions as essential mediator as it eases the initiation of excitability after OxPL stimulation.

As mutants in the human $Na_V1.9$ mediate an enhanced or painless perception, this study provides new insight into the mechanism on how $Na_V1.9$ amplifies stimuli of endogenous irritants under inflammatory conditions.

1   Introduction

1.1.   Pain and nociception

The International Association for the Study of Pain (IASP) defines pain as "unpleasant sensory and emotional experience associated with actual or potential tissue damage, or described in terms of such damage". Hereby, pain is an important and necessary protective mechanism of the body to avoid further harm for survival (Dubin and Patapoutian, 2010). The sensors of the pain pathway are peripheral sensory neurons, so called nociceptors. Their basic function is the detection and notification of harmful stimuli as noxious chemicals or high temperatures. Without any stimulation inducing action potential firing, nociceptors are electrically silent (Woolf and Ma, 2007).
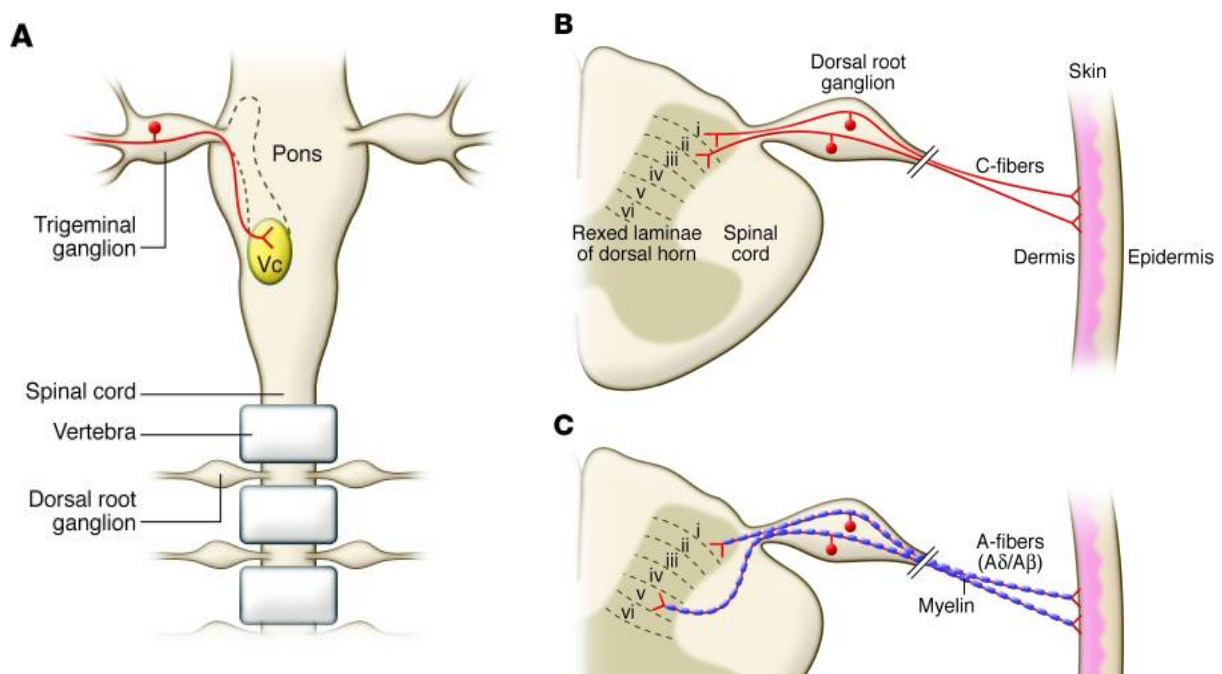
Figure 1: Nociceptors are the sensors of the pain pathway. Somatosensory neurons of the pain pathway are located in peripheral ganglia. **(A)** Trigeminal ganglion neurons have a pronounced projection to the trigeminal brainstem sensory subnucleus caudalis (Vc). **(B)** Most sensory neurons reside in dorsal root ganglia and are small-diameter neurons that form unmyelinated small-diameter axons (C-fibres). Their afferent projection forms glutamatergic synapses to laminae I/II of the dorsal horn in the spinal cord. **(C)** Nociceptors forming myelinated A-fibers project to laminae I and V in the spinal cord. Images taken from Dubin & Patapoutian, 2010.

Nociceptors of the skin are pseudo unipolar neurons and reside in peripheral sensory ganglia (trigeminal ganglia (TG) or dorsal root ganglia (DRG). Axonal projections formed by these neurons can be divided in small-diameter unmyelinated C-fibers surrounded by Schwann cells with conduction velocities of 0.4-1.4 m/s and myelinated A-fibers, responsible for the fast-onset pain, with a conduction velocity of 5–30 m/s (Djouhri and Lawson, 2004). Here, their classification is based on their conduction velocity and threshold to detect heat/cold, mechanical and chemical stimuli (Raja et al., 1988; Kumazawa et al., 1996).

The neurotrophin nerve growth factor (NGF) is of great importance for the development and function of sensory neurons. During the early development, nociceptors require NGF action for growth, survival and maturation. NGF binds to the tropomyosin receptor kinase A (TrkA), a tyrosine kinase receptor mainly expressed by peptidergic C-fiber neurons and in a subtype of A-fiber neurons (Averill et al., 1995; Huang and Reichardt, 2001; Patapoutian and Reichardt, 2001). These nociceptors are restricted to the small and medium diameter DRG neuron population even though larger sensory neurons express TrkA receptors as well (Wright and Snider, 1995; Patapoutian and Reichardt, 2001). In adult nociceptors, NGF retains its specifity for some small peptidergic neurons where high-affinity NGF receptors are expressed (Verge et al., 1989) and has an impact on the sensitivity to methanol, capsaicin and cooling effects (Story et al., 2003; Babes et al., 2004). A-fiber neurons express TrkB, the receptor brain-derived neurotrophic factor (BDNF), and/or TrkC, the receptor for Neurotrophin 3 (NT3) (McMahon et al., 1994).

Most DRG neurons are pseudo-unipolar with one peripheral axon innervating the skin while the central axon is connected to second-order neurons located in the dorsal horn of the spinal cord (Fig. 1). Hereby the DRG axon forms branches to innervate the spinal segments in the caudal and rostral direction (Dubin and Patapoutian, 2010), where they end in laminae I, II and V of the dorsal horn (Millan, 1999; Basbaum et al., 2009). Therefrom, sensory information is transferred to the medulla, the mesencephalon and thalamus, from where somatosensory signals are projected to anterior cingulate cortices (Millan, 1999). The transmission of nociceptive signals is regulated by local inhibitory and excitatory interneurons located in the dorsal horn and by stimulatory and inhibitory pathways emerging in the brain. This regulatory pathway is of great importance to the prioritization of pain perception in comparison to competing events like behavioral demands or homeostatic requisition (Heinricher et al., 2009). Nociceptors have excitatory properties and use glutamate as their primary neurotransmitter as well as other chemical substances or modulators important for efferent and synaptic signaling (Basbaum et al., 2009).

Action potential firing of nociceptors can induce somatic biochemical changes to alter gene expression and functional properties of nociceptors (Woolf and Costigan, 1999; Cheng and Ji, 2008; Dubin and Patapoutian, 2010). For investigation of molecular and regulative mechanisms induced by noxious stimuli, the cell body of nociceptors is a useful cellular model for examining neuronal function and plasticity changes in nociceptive signaling (Malin et al., 2007; Cummins et al., 2009).

1.2.　Inflammation

Inflammation is an adaptive and beneficial response mechanism of the body to restore homeostasis after tissue damage or infection. Triggers of inflammation are infections, tissue injury and tissue stress. The physiological purpose of inflammation is the defense against infection, the tissue-repair response leading to healing of the damaged tissue and furthermore the adaption to stress as well as the recovery of the homeostatic state (Medzhitov, 2008). Characteristic hallmarks of inflammation are heat, redness, swelling, pain or loss of function of the affected area (Fig. 2), leading to hyperalgesia, an increased sensitivity to a noxious stimulus.
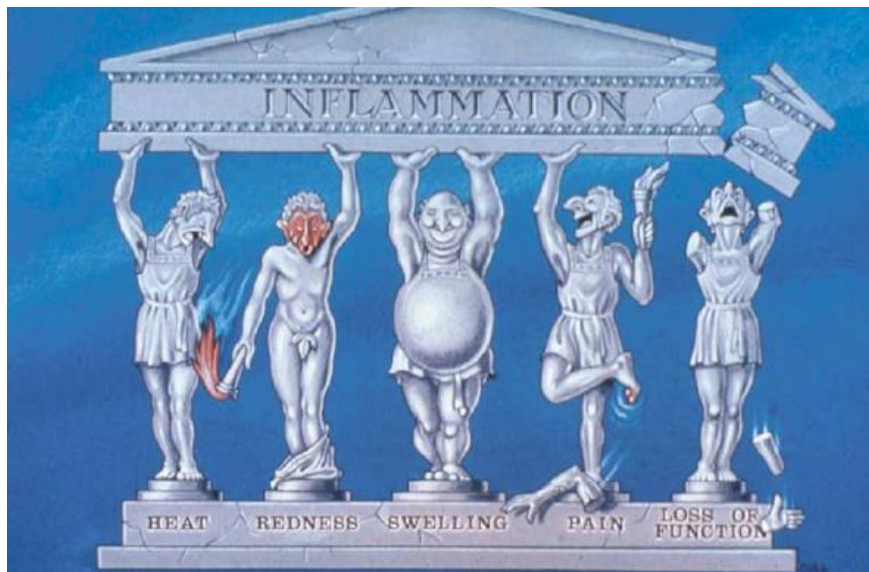
Figure 2: The five characteristics of inflammation: Heat, redness, swelling, pain and loss of function. http://www.drdebe.com/blog/2014/7/9/inflammaging

During inflammation immune cells and blood components infiltrate into the damaged or infected area (Kumar and Sharma, 2008). Hereby, macrophages and mast cells detect tissue injury and by producing and releasing inflammation mediators like chemokines or cytokines they in turn activate neutrophils. Leukocytes such as neutrophils degrade the invading agents by producing reactive oxygen species (ROS), cathepsin G or elastase (Akopian, 2011; Gangadharan and Kuner, 2013a).

16
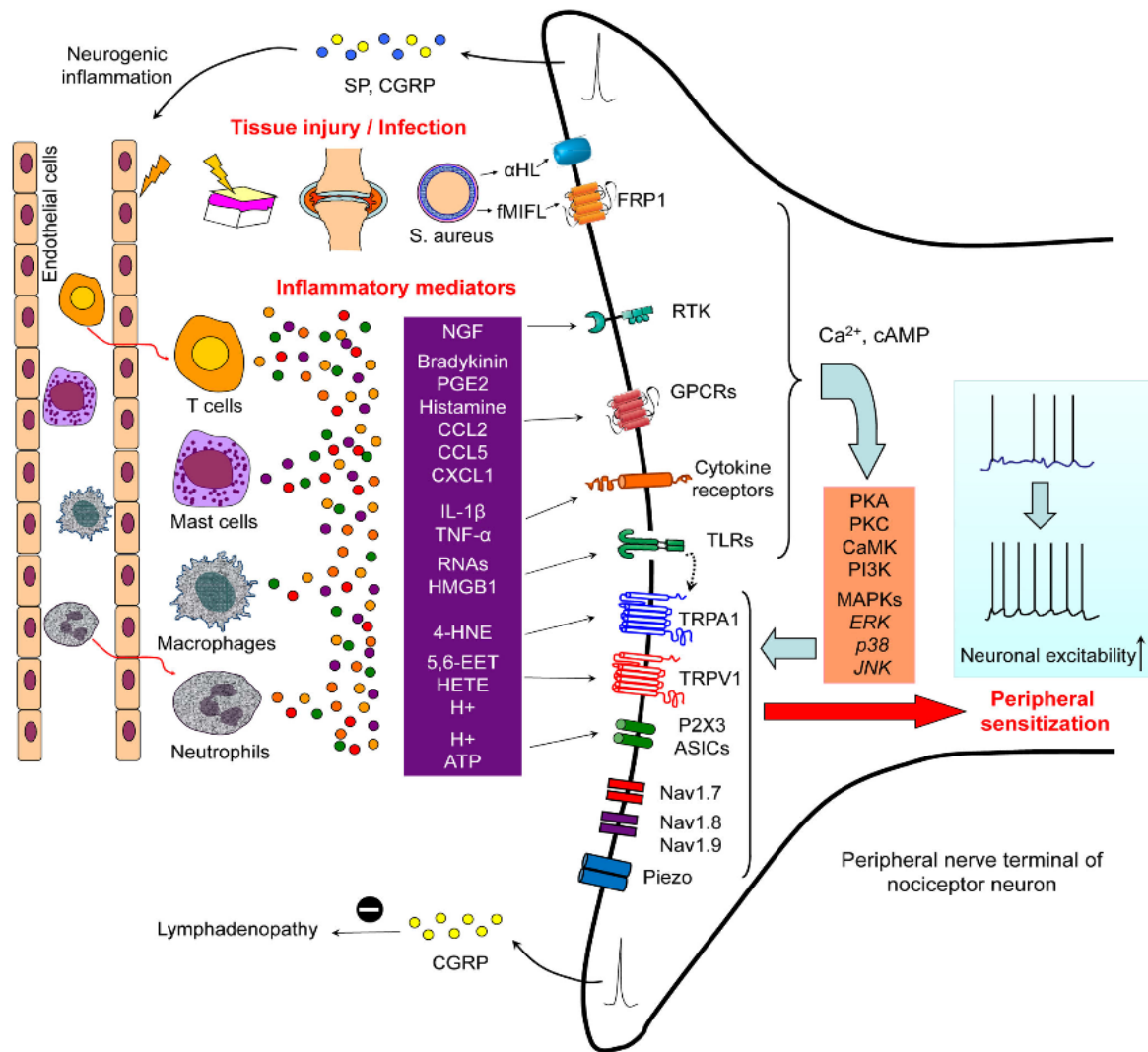
Figure 3: Overview of the release of inflammation mediators after tissue damage and their effect on nociceptors and their receptors. Immune cells like macrophages or leukocytes infiltrate into the damaged area and release a broad range of inflammation mediators which interact on receptors expressed by peripheral sensory neurons (Ji et al., 2014).

ROS are pronociceptive mediators, which are produced by existing or infiltrating leukocytes via e.g. NADPH oxidase complexes. Furthermore ROS can oxidize lipids and phospholipids in plasma membranes as well as reactive sites of proteins, where they can in particular interact with sulfhydryl groups. ROS and their downstream products are pronociceptive through activation of irritant receptors such as the transient receptor potential ion channels (Andersson et al.; Liu and Ji), of which the family members transient receptor potential vanilloid 1 (TRPV1) or ankyrin 1 (TRPA1) receptors are of outstanding importance. Released inflammation mediators act on a complex regulatory signaling network (Fig. 3).

The transmission of nociceptive signals by peripheral nociceptors is straight forward. Nerve injury or tissue damage as well as inflammation mediators excite nociceptors by activation of a diverse set of signaling cascades, receptors and ion channels to increase the membrane potential. Voltage-gated ion channels sense the increase of membrane potentials, generate action potentials to transmit nociceptive signals to the central nervous system (Akopian, 2011). Pain signals are important physiological protection signals.

These signals can be pronounced during inflammation and other pathologic processes. The understanding of the molecular mechanism underlying the perception of harmful stimuli is of outstanding clinical importance. For treatment of inflammatory pain, nonsteroidal anti-inflammatory drugs (NSAIDs) such as aspirin or ibuprofen became common. NSAIDs are among the most widely used painkillers worldwide. These compounds disable the production of prostaglandins by inhibition of cyclooxygenases-1 and -2 (Vane, 1971; Flower et al., 1972). However, despite their unequivocal effectiveness, serious side effects like gastric bleeding, renal failure or heart attacks restrict NSAID usage. Furthermore, NSAIDs have a poor effectiveness on patients with severe pain syndromes indicating the need for alternative treatment options (Sostres et al., 2010). Other potent pain reducing drugs are opioids. However, pain treatment with opioids should be only temporary as opioids bear the risk of inducing addiction behavior and patients treated with opioids might suffer from drowsiness and respiratory depression (Stein and Baerwald, 2014).

1.3. Inflammation mediators and their receptors

In the peripheral nerve terminal of nociceptors there are several types of receptors and ion channels: First, the transduction proteins for the transduction of noxious stimuli that lead to membrane depolarization. Commonly, the generation of excitatory receptor potentials is mediated by a Na^+ or Ca^{2+} influx into the nociceptor. Metabotropic G-protein coupled receptors, TRP ion channels as well as, other ionotropic ion channels, or tyrosine kinase-linked receptors detect nociceptive stimuli. The potency of depolarizing receptor potentials depends on the electrical excitability of the nociceptors and is regulated by voltage-gated sodium channels and different types of potassium-permeable ion channels. These types of excitation mediators are also responsible for the conversion of receptor potentials into action potentials due to their voltage-dependent activation characteristic (Petho and Reeh, 2012).

Various stimuli can interact with all these receptors and ion channels and increase the excitability of nociceptors and therefore increase the potency to generate a higher action potential firing frequency in response to an adequate stimulus. This process called nociceptor sensitization contributes to hyperalgesia and is mediated by a broad range of endogenous substances that are produced during inflammation.

The sensitization of nociceptors causes an elevated responsiveness to mechanical, chemical or thermal stimulation. One of the most potent pain-inducing agents produced under inflammatory conditions, is bradykinin (Edery and Lewis, 1962; Hargreaves et al., 1988). It is mediated by various effects of the arachidonic acid-cyclooxygenase pathway (Petho et al., 2001). Bradykinin, an oligopeptide, interacts with B1 and B2 bradykinin receptors; both belong to the family of G protein-coupled plasma membrane receptors. Hereby, the B2 receptor seems to be responsible for the mediation of acute effects.
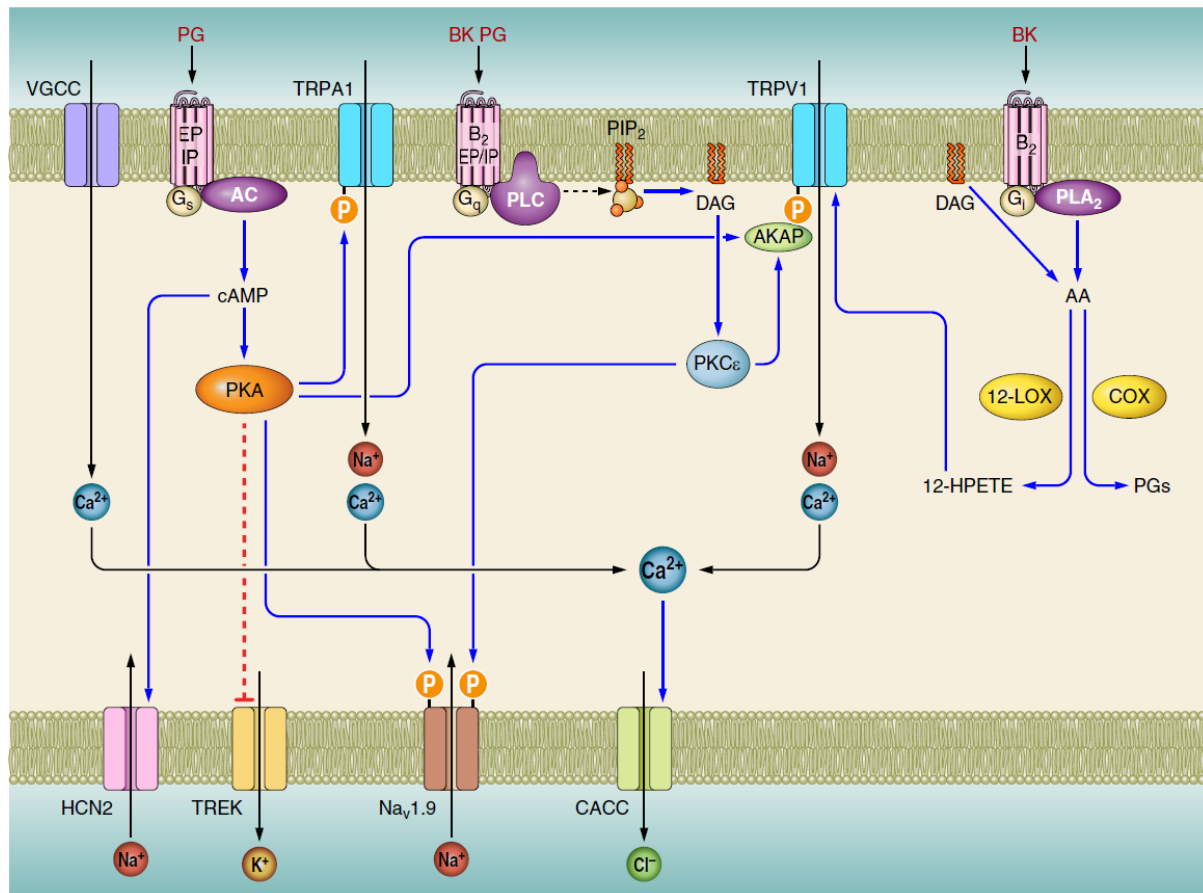
Figure 4: Signal transduction pathways induced by prostaglandins and bradykinin in peripheral sensory neurons of nociceptors. The blue arrow indicates activation, synthesis of a substance or stimulation of a target. Red line shows the inhibition of a target. Dashed black arrows indicate cleavage of a substance. CACC: calcium-activated Cl⁻-channel, HCN2: hyperpolarization-activated cyclic nucleotide-gated channel, TREK: mechanosensitive K⁺-channel, TRPA1: transient receptor potential channel ankyrin 1, TRPV1: transient receptor potential channel vanilloid 1, VGCC: voltage-gated sodium channel, $Na_V1.9$: voltage-gated sodium channel. After (Petho and Reeh, 2012).

Besides bradykinin, other inflammatory mediators like prostaglandins can interact with channels and receptors on the nociceptor. Prostaglandins consist of a group of arachidonic acid derivatives and have a variety of biological activities.

They are generated by cyclooxygenases (COX) during inflammation and act on a broad range of cell types (Ricciotti and FitzGerald, 2011; Petho and Reeh, 2012). Prostaglandins such as PGE_2 bind to G protein-coupled prostaglandin receptors to mediate nociceptor sensitization (Lin et al., 2006). Prostaglandins can influence the activity of several channels and receptors by initiating cAMP accumulation, PKA activation and additionally PKC activation (Petho and Reeh, 2012). For example, PGE_2 facilitates gating of TRP channels and voltage-gated sodium channels (Rush and Waxman, 2004; Moriyama et al., 2005).

1.4. Transient receptor potential channels

Different types of transient receptor potential (TRP) channels are expressed on C-fibers and act as sensors in the pain pathway (Gangadharan and Kuner, 2013b). The TRP ion channel family is divided into seven subgroups: TRPA (Ankyrin), TRPC (Canonical), TRPML (Mucolipin), TRPM (Melastatin), TRPN (no mechanoreceptor potential C), TRPP (Polycystin), and TRPV (Vanilloid) (Pedersen et al., 2005; Clapham, 2007). Their structure is formed out of tetramers with subunits of six transmembrane domains containing non-selective cation pore modules with high calcium permeability (Latorre et al., 2009). In pain perception, TRPA1 and TRPV1 are of high relevance. Both ion channels can excite peptidergic small-diameter nociceptors, which express the calcitonin gene-related peptide (CGRP) and are additionally expressed by non-peptidergic isolectin 4-positive nociceptors (Barabas et al., 2012; Eberhardt et al., 2012a).

The transient receptor potential channel vanilloid 1 (TRPV1, Fig. 5) is a crucial thermosensor and is also a high affinity receptor for capsaicin, a hot pepper compound (Caterina et al., 1997; Tominaga et al., 1998; Jordt et al., 2000). Furthermore, TRPV1 can be activated by a broad spectrum of chemical compounds such as oxidized linoleic acid metabolites including 9-hydroxy-10E- and 13-hydroxy-10E,12Z-octadecadienoic acid (9-HODE and 13-HODE). Both metabolites are released in inflammation or after exposure to heat (Trevisani et al., 2007; Patwardhan et al., 2010).

The TRPA1 channel differs from other TRP members due to its numerous NH_2-terminal ankyrin repeats (Fig. 5). A prototypical agonist of TRPA1 is allyl isothiocyanate (AITC), a compound of mustard oil (Bandell et al., 2004; Jordt et al., 2004). Exogenously applied AITC can lead to the activation of peripheral C-fibers and induces acute pain signals (Bautista et al., 2006). A broad range of substances can interact with TRPA1, mostly electrophiles and oxidizing agents.
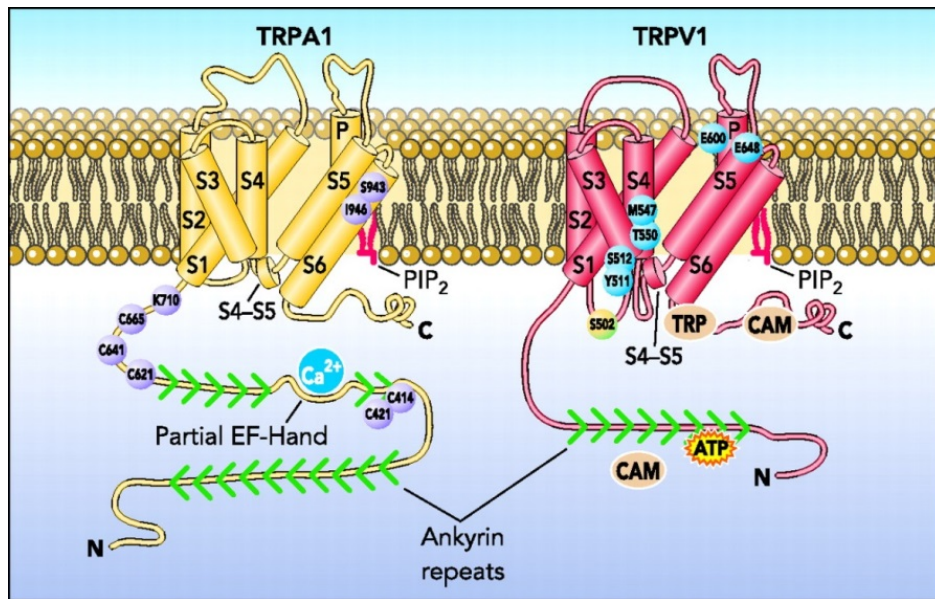
Figure 5: The structure and ligand interaction of the transient receptor potential channels TRPA1 and TRPV1 (Bessac and Jordt, 2008). TRPA1 carries around 15 Ankyrin repeats in its intracellular N-terminal domain. The N-terminus also contains critical lysine and cysteine residues (grey) that form the interaction site for certain agonists. In TRPV1, the reactive binding site is close to the intracellular part of the membrane. Agonists such as vanilloids activate the channel at this site. The structure of both channels was modeled according to an X-ray crystal structure of $K_V1.2$, a potassium channel (Bessac and Jordt, 2008).
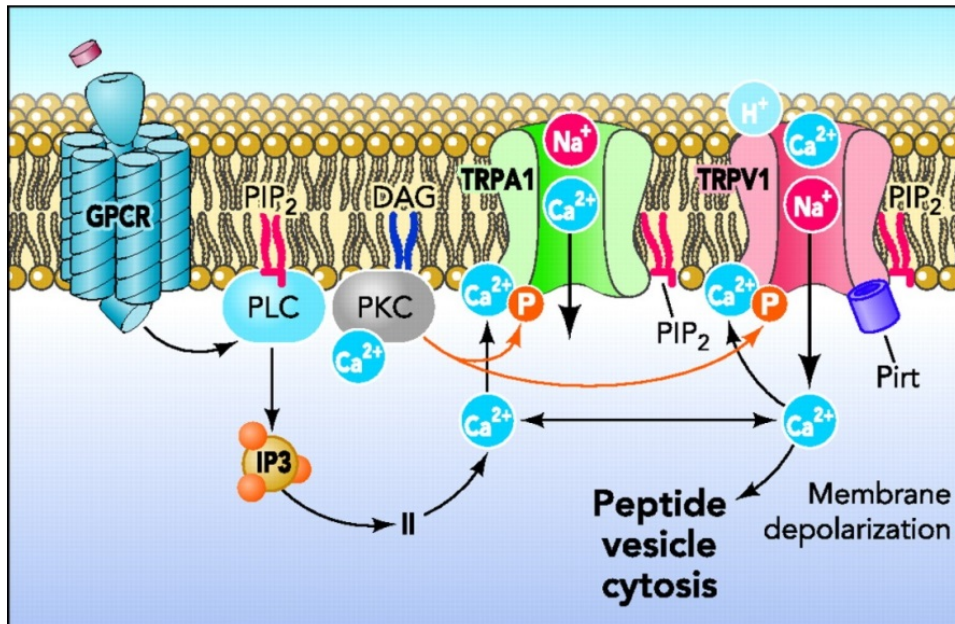
Figure 6: TRP channels are activated by inflammatory signal pathways. (Bessac and Jordt, 2008). The sensitization of TRPV1 and TRPA1 during inflammation is mediated by various PLC- and PKC-coupled receptor pathways. These receptors include receptors for bradykinin and histamine as well as NGF. TRPA1 and TRPV1 activity is also affected by calcium release from intracellular calcium stores.

Its activation can be blocked by ruthenium red and HC-030031 (Atzori et al., 1992; Andre et al., 2008). TRPA1 responds to both endogenous and exogenous irritants like 4-hydroxynonenal (4-HNE), a downstream metabolite of OxPL found in complete Freund's adjuvant (CFA)-induced hind paw inflammation (Pflucke et al., 2013). TRPA1 responds to both endogenous and exogenous irritants like 4-hydroxynonenal (4-HNE), a downstream metabolite of OxPL found in complete Freund's adjuvant (CFA)-induced hind paw inflammation (Pflucke et al., 2013). It was shown that TRPA1 is also triggered by cold, at least in a subpopulation of peptidergic sensory neurons (Story et al., 2003).

There is structural evidence that activation of TRPA1 by AITC occurs via a reversible covalent modification of the channel at three critical cysteine residues in the N-terminal ion channel domain. Strong electrophiles can interact with these cysteine residues in the channel due to a Michael addition and Schiff base formation (Pereira et al., 1973). Additionally, it was investigated that TRPA1 can be inhibited by N-methyl-maleimide, which binds irreversible to the cysteine residues of the channel protein and keeps the channel in its active state (Hinman et al., 2006). Pain-inducing endogenous ligands for TRPA1 are not well defined. In the course of this study our research group found that the new endogenous irritant oxidized phospholipids activate TRPA1 and TRPV1.

1.5. Oxidized Phospholipids

Phospholipids containing polyunsaturated fatty acids are highly prone to modification by ROS after tissue damage (Catala, 2009). After tissue injury or during inflammation, phospholipids such as 1-palmitoyl-2-arachidonoyl-sn-glycero-3-phosphocholine (PAPC) can be modified via reaction with ROS released by activated immune cells. Through lipid peroxidation and following fragmentation of the products, the oxidation of one PAPC molecule can induce the formation of a variety of oxidized phospholipids with most diverse bioactivities. In atherosclerosis oxidized phospholipids (OxPL) facilitate amongst others the adhesion of monocytes to endothelial cells and the generation of plaques (Hansson and Hermansson, 2011b; Lee et al., 2012b; Zeller and Srivastava, 2014).

Furthermore OxPL are engaged in converting macrophages into foam cells, which contain oxidized LDL (OxLDL) and produce chemokines (Hansson and Hermansson, 2011a; Lee et al., 2012a; Zeller and Srivastava, 2014). OxPAPC (oxidized 1-palmitoyl-2- arachidonoyl-sn-glycero-3-phosphocholine), a mixture of oxidation products formed by lipid peroxidation of PAPC, is one of the best characterized OxPL, though its overall role in inflammatory pain is unknown (Bochkov et al., 2010). It contains amongst other OxPL metabolites POVPC (1-palmitoyl-2-(5-oxovaleroyl)-sn-glycero-3-phosphocholine) and the acid PGPC (1-palmitoyl-2-glutaryl-sn-glycero-3-phosphocholine) (Bretscher et al., 2015).

OxPL mediate a diverse spectrum of bioactivities. For instance, OxPL are involved in the inhibition of lipopolysaccharide-induced activation of toll-like receptors (Bochkov et al., 2010). Furthermore, OxPL are suggested to assume a role in acute inflammation (sepsis or acute lung injury) (Imai et al., 2008), neurodegenerative diseases like Alzheimer´s or Parkinson´s and chronic inflammation (Furnkranz et al., 2005; Usui et al., 2009). The peroxidation of phospholipids can lead to an enrichment of lysoforms resulting from both enzymatic and non-enzymatic hydrolysis.
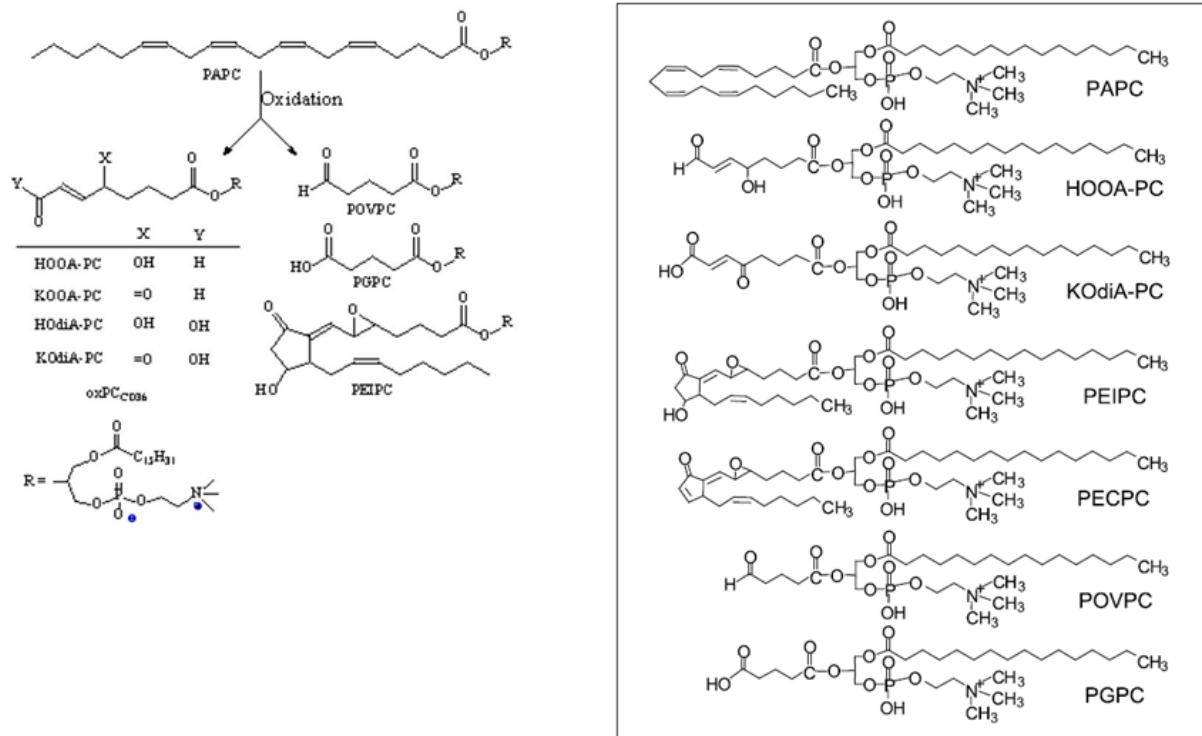
Figure 7: Production and structure of oxidized phospholipids and its components (modified after Bochkov et al. 2010). Oxidized phospholipids are generated by oxidation of PAPC with reactive oxygen species. Oxidation of phospholipids and subsequent reactions form a broad variety of oxidized phospholipids with most diverse bioactivities.

Lysophospholipids can both bind and activate G protein-coupled receptors as well as Lysophosphatidic acid receptors 1 and 4 (LPA1 to LPA4) (Anliker and Chun, 2004; Tomura et al., 2005). It has already been shown that OxPAPC and the component PEIPC facilitate the prostaglandin E2 receptor 2 and prostaglandin D2 *receptor* 1, leading to inflammation by mediation enhancement of cAMP levels (Li et al., 2006). Furthermore, OxPL and in particular its components PGPC and POVPC stimulate peroxisome proliferator-activated receptors (PPAR) and toll-like receptor 4 (Lee et al., 2000; Davies et al., 2001; Walton et al., 2003). In addition, OxPL have a role in interacting with scavenger receptors CD36 and SR-BI; both are important for the detection of apoptotic cells and the production of foam cells (Podrez et al., 2002; Bochkov et al., 2010).

In summary, OxPL have a broad pharmacological spectrum and have a role in several receptor-mediated mechanisms with an activation of quite a few signaling pathways (Bochkov et al., 2010).
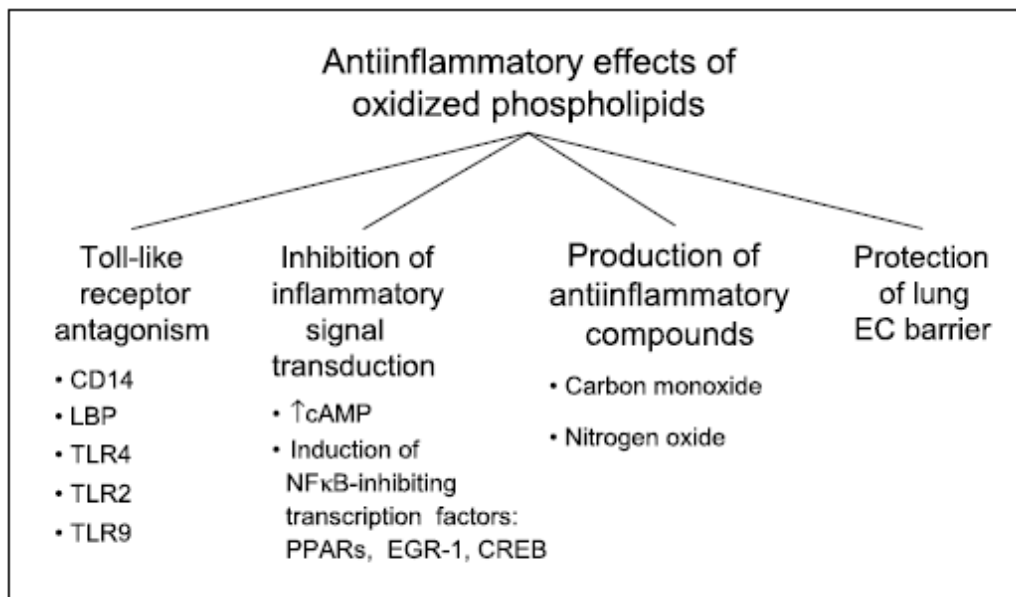
Figure 8: Anti-inflammatory effects and mechanisms of OxPL.

1.6. The voltage-gated sodium channel $Na_V1.9$

The transmission and transduction of nociceptive signals after inflammation or injury is depended on an enhanced excitability of sensory neurons. In this, voltage-gated sodium channels have a critical role. They may influence increased responsiveness to endogenous pronociceptive irritants such as OxPL. Voltage-gated sodium channels have a conserved structure of 24 transmembrane segments arranged into four homologous domains (DI-DIV). Each domain consists out of six transmembrane segments (S1-S6) (Catterall et al., 2005). There are nine genes encoding for the pore-forming alpha-subunit of the channels (SCN1A-SCN5A; SCN8A-SCN11A). The voltage-sensing domain can be found in S4 domains, while the segments S5 and S6 contribute to the pore domain. The channel pore is selective for sodium ions.

$Na_v1.8$ and $Na_v1.9$ are resistant to micromolar concentrations of TTX (TTX-R), while $Na_v1.1$, $Na_v1.6$, and $Na_v1.7$ are inhibited by nanomolar concentrations of the neurotoxin tetrodotoxin (TTX-Sensitive, TTX-S). The three VGSC $Na_V1.7$, $Na_v1.8$ and $Na_v1.9$ are in particular expressed on peripheral neurons and all three channels have been shown to have an important role in human pain disorders (Faber et al., 2012; Dib-Hajj et al., 2013; Huang et al., 2013; Leipold et al., 2013; Leipold et al., 2015).

While Na$_V$1.7 and Na$_V$1.8 are responsible for the generation of action potentials, the function of Na$_V$1.9 in the pain pathway is not entirely understood (Basbaum et al., 2009; Dib-Hajj et al., 2015). Na$_V$1.9 is highly abundant in dorsal root ganglion neurons with a size smaller than 30 µm and in trigeminal ganglia from rats (Dib-Hajj et al., 1998; Dib-Hajj et al., 2002; Rugiero et al., 2003). The recent discovery of rare mutations in the gene encoding for Na$_V$1.9 in individuals suffering from either a complete loss of pain perception, episodic pain syndromes, or painful peripheral neuropathy highlighted the importance of Na$_V$1.9 in nociception (Woods et al.; Leipold et al., 2013; Zhang et al., 2013; Huang et al., 2014; Han et al., 2015; Huang et al., 2017).
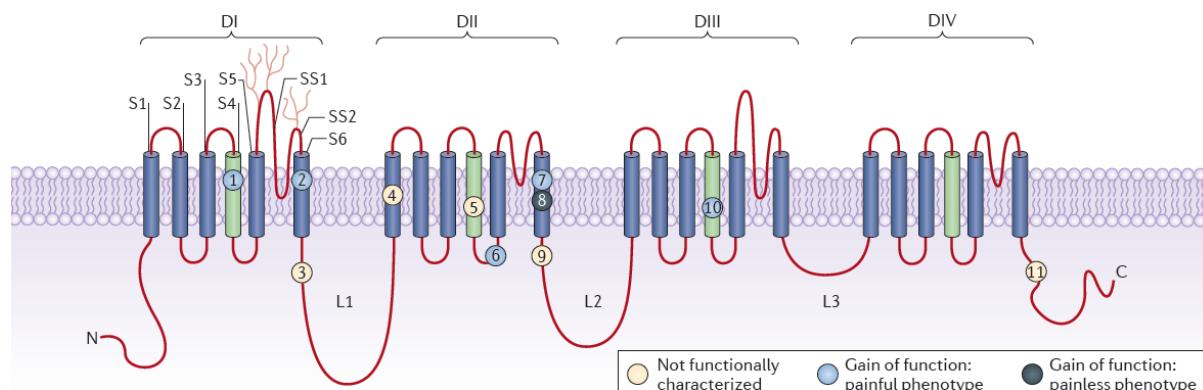
Figure 9: Structure of the VGSC Na$_V$1.9 and the consequence of mutations in the channel (Dib-Hajj et al., 2015). The channel has four homologous domains (DI-DIV) and each domain consists out of six transmembrane segments. Mutations lead to either a painful (light blue) or painless phenotype (dark blue).

Na$_V$1.9 mediated currents were detected in C-Fibers of the peripheral axon and the somata of the dorsal root ganglion neurons. A unique characteristic of Na$_V$1.9 is that the channel is responsible for excitation effects in the range close to the resting membrane potential (RMP) (Maingret et al., 2008; Basbaum et al., 2009). Notably, Na$_V$1.9 is not only active in sensory neurons, but also in developing motoneurons where the channel controls cell-autonomous, spontaneous excitability (Subramanian et al., 2012). It was also suggested that Na$_V$1.9 mediates fast excitability in hippocampal neurons in response to fast neurotrophin stimuli (Blum et al., 2002). However, compared to DRG neurons, expression levels of Na$_V$1.9 are rather weak in motoneurons and hippocampal neurons. Here, the Na$_V$1.9 encoding mRNA is 70-150 times lower in comparison to those observed in DRG neurons (Subramanian et al., 2012). Characteristic for the Na$_V$1.9 channel is a slow closing kinetics leading to the assumption that the channel is not involved in action potential firing but provides a persistent sodium current to elongate below-threshold depolarization. Furthermore, active Na$_V$1.9 can reduce the threshold for repetitive firing of DRG neurons (Maingret et al., 2008; Basbaum et al., 2009).

2 Aim of this thesis

Inflammatory mediators are released in inflamed tissue where they sensitize and stimulate nociceptors. Oxidized phospholipids (OxPL) are endogenous pain-inducing irritants. OxPL mediate their pain-inducing function through activation of the transient receptor potential channels TRPA1 and TRPV1; both are polymodal chemoreceptors and are mediators of pain-inducing signals. The aims of this thesis were:

- The identification and analysis of target receptors of OxPL-induced effects on nociceptors *in vitro* and the mechanism of OxPL activation on TRPA1 and TRPV1 ion channels.

- The investigation of physiological responses induced by individual OxPL compounds.

- The deciphering of the neuronal excitation cascade induced by OxPL in small-diameter neurons, a cellular model for nociceptors. As OxPL were found to be rather weak excitants for nociceptors, it was also asked whether the subthreshold active voltage-gated sodium channel $Na_V1.9$ might act as an amplifier of TRP-responses induced by OxPL stimuli.
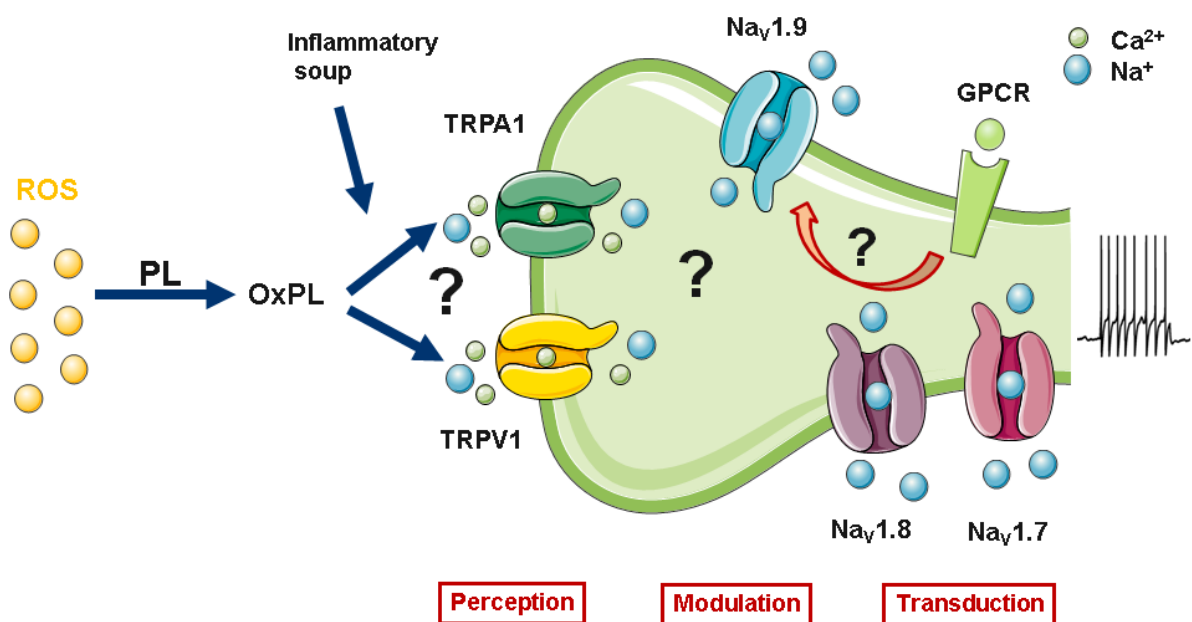
Figure 10: Working model. During inflammation, OxPL are produced and stimulate TRPA1 and/or TRPV1. TRP-responses might be amplified by $Na_V1.9$-mediated persistent sodium currents. Activation of $Na_V1.9$ might increase the ease with which action potentials are elicited through the activity of $Na_V1.7$ and $Na_V1.8$.

3 Material and methods

3.1. Material

3.1.1. Chemicals

For the experiments, chemical products of the following companies have been used.

Table 1: Chemicals.

Chemical	Company	Productno.
2-Propanol	Sigma-Aldrich	33539
Adenosine 5′-triphosphate magnesium salt	Sigma-Aldrich	A9187
Agarose	Biozym	840004
AITC	Sigma-Aldrich	36682
Ampicillin	Carl Roth	K029.1
Aqua Poly/Mount	Polysciences Inc.	18606
β-mercaptoethanol	Merck Millipore	8057401000
Bradykinin	CaymanChemical Company	15539
Bromphenol blue	Sigma-Aldrich	B-8026
Calcium chloride dihydrate	Merck Millipore	102382
Capsaicin	Capsaicin	M2028
Chloroform	Sigma-Aldrich	288306
CTAB	Sigma-Aldrich	855820
D(+)-Glucose-Monohydrat	Merck MIllipore	K38291142
Dimethylsulfoxid	Carl Roth	4720.2
DMEM/F-12, GlutaMAX™ Supplement	Thermo Fisher Scientific	31331093
DMEM, high glucose, GlutaMAX™	Thermo Fisher Scientific	31966047
DMSO	Sigma-Aldrich	276855
DTT	Invitrogen-Gibco	P2325
Dulbecco´s PBS without Ca^{2+}/Mg^{2+}	Invitrogen-Gibco	14190144
dATP 100 mM	Thermo Fisher Scientific	10216018
dCTP 100 mM	Fermentas	10217016
dGTP 100 mM	Fermentas	10218014
dTTP 100 mM	Fermentas	10219012
ECL Prime WB Detection Reagent	GE Healthcare	RPN2232
EDTA acid	Sigma-Aldrich	E6758

EGTA	Sigma-Aldrich	E3889
Ethanol	Sigma-Aldrich	32205
Ethidium bromide	Sigma-Aldrich	E1510
F12 medium	Invitrogen-Gibco	21765-029
Fetal bovine serum	Invitrogen-Gibco	10500-064
Forskolin	Sigma-Aldrich	F6886
Fura-2, AM	Thermo Fisher Scientific	F1201
Gene RulerTM 100 kb DNA Ladder	Fermentas	SM0242
Gene RulerTM 1 kb DNA Ladder	Fermentas	SM0311
Geneticin R selective antibiotic	Carl Roth	CP11.3
Gentamicin R selective antibiotic	Thermo Fisher Scientific	15750060
Glycerol	Thermo Fisher Scientific	15514011
Guanosine 5′-triphosphate sodium salt hydrate	Sigma-Aldrich	G8877
HBSS (without Mg^{2+} and Ca^{2+})	Thermo Fisher Scientific	14170-138
HC-030031	Sigma-Aldrich	H4415-10MG
HEPES Pufferan, >99.5% cell pure	Carl Roth	HN77.4
High performance chemiluminescence HyperfilmTM	GE Healthcare	28906836
Histamine	Sigma-Aldrich	H7125
Horse Serum	Thermo Fisher Scientific	16050122
Hygromycin B	Sigma-Aldrich	H0654
Immuno-Blot PVDF membrane	BioRad	1620177
LB Broth	Sigma-Aldrich	L3022
Liberase™ TH Research Grade	Sigma-Aldrich	5401135001
Liberase™ TM Research Grade	Sigma-Aldrich	5401119001
Lipofectamine 2000 Transfection Reagent	Thermo Fisher Scientific	11668019
Magnesium chloride hexahydrate	Merck Millipore	105833
Magnesium sulfate heptahydrate	Merck Millipore	105886
Midori Green Advance DNA Stain	NIPPON Genetics	MG04
NaF	Sigma-Aldrich	S7920
Na-orthovanadate	Sigma-Aldrich	S6508
Na-pyrophosphate	Sigma-Aldrich	S6422
NEBuffer 3.1	New England Biolabs	B7203S
Nerve growth factor	Sigma-Aldrich	N0513

Nonidet P40 Substitute	Sigma-Aldrich	74385-1L
Opti-MEM® Reduced Serum Medium	Thermo Fisher Scientific	31985070
Oregon Green® 488 BAPTA-1, AM	Thermo Fisher Scientific	O6806
Oxidized PAPC	Hycult Biotech	HC4036
Paraformaldehyde	Sigma-Aldrich	P6148
PBS (without Mg^{2+} and Ca^{2+})	Sigma-Aldrich	D8537
Penicillin-Streptomycin	Thermo Fisher Scientific	15070063
PGPC	Avanti Polar Lipids	870602P
Pluronic® F-127	Sigma-Aldrich	P2443
Poly-D, L-ornithine hydrobromide	Sigma-Aldrich	P8638
Poly-L-lysine hydrobromide	Sigma-Aldrich	P2636
Potassium chloride	Merck Millipore	104936
Powdered milk	Carl Roth	T145.3
Precision Plus Protein All Blue Standards	BioRad	1610373
Prostaglandin E2	Sigma-Aldrich	P0409
RNasin® Plus RNase Inhibitor	Promega	N2611
SDS	BioRad	1610302
Sodium bicarbonate	Fluka	71628
Sodium dihydrogen phosphate monohydrate	Merck Millipore	106346
Sodium chloride	Sigma-Aldrich	31434
Sucrose	Sigma-Aldrich	S0389
Tablet of complete Mini EDTA-free	Roche	11836170001
Taq buffer advanced 10x	Thermo Fisher Scientific	B33
Taq DNA polymerase	Thermo Fisher Scientific	EP0402
Tris-Base	AppliChem	A2264
TritonTM X-100	Sigma-Aldrich	X100
TrypLE™ Express	Thermo Fisher Scientific	12605036
Trypton	Sigma-Aldrich	T7293
Trypsin inhibitor	Sigma-Aldrich	T0256
Tween®20	Sigma-Aldrich	P1379
Xylene cyanol	Sigma-Aldrich	X4126
Yeast Extract	Merck Millipore	111926
Water-Ampuwa® Aqua ad injectabilia	DeltaSelect	V07AB

3.1.2 Solutions

Blocking solution for immunocytochemistry

1x PBS

10% horse serum

0.3% Triton X-100

0.1% Tween 20

Blocking solution for protein detection after western blot

1x TBS-T

5% powdered milk

Calcium imaging buffer

135 mM NaCl

6 mM KCl

1 mM $MgCl_2$

1 mM $CaCl_2$

10 mM HEPES

5,5 mM Glucose

DNA loading buffer 6x (10 ml)

6 ml 50% glycerol

2 ml H_2O dest.

1 ml 2% bromophenol blue

1 ml 2% xylene cyanol solution

DRG cell culture medium

DMEM with GlutaMaxTM

F12 Medium

10% FCS

1% Penicillin/Streptomycin

100 µg/mL NGF

Electrophoresis buffer 10x (1 l)

30.3 g Tris base;

144 g glycine;

10 g SDS

pH adjustment to 8.45

External buffer (DRG neurons)

120 mM NaCl

3 mM KCl

2.5 mM $CaCl_2$

1 mM $MgCl_2$

30 mM HEPES

15 mM glucose

adjust pH to 7.4 with NaOH

External buffer (HEK293/HEK$_{rTRPV1}$)

140 mM NaCl

5 mM CsCl

2 mM $MgCl_2$

1 mM $CaCl_2$

10 mM HEPES

10 mM glucose

Adjust pH to 7.4 with NaOH

HEK 293 cell culture medium

DMEM with GlutaMaxTM

10% FCS

1% Penicillin/Streptomycin

400 µg/mL Hygromycin (TRPA1)

400 µg/mL Geneticin (TRPV1)

Internal buffer (DRG neurons)

125 mM KCl

8 mM NaCl

1 mM $CaCl_2$

1 mM $MgCl_2$

0.4 mM Na_2-GTP

4 mM Mg-ATP

10 mM EGTA

10 mM HEPES

Adjust to pH 7.3 with KOH

Internal solution (all HEK293 cell lines)	140 mM $CsCl_2$,
	4 mM $MgCl_2$,
	10 mM HEPES
	10 mM EGTA
	Adjust pH to 7.3 with CsOH
Lysis buffer	1% NP40
	150 mM NaCl
	50 mM HEPES
	10 mM sodium pyrophosphate
	1 mM NaF
	10% glycerol
NMDG-buffer (HEK293$_{hTRPA1}$)	75 mM NMDG
	75 mM NaCl
	2.5 mM CsCl
	1 mM $MgCl_2$
	10 mM HEPES
	10 mM Glucose
	Adjust pH with HCl to 7.4
PBS 10x (1 l)	80 g NaCl
	2 g KCl,
	2.4 g KH_2PO_4
	14.4 g Na_2HPO_4,
	H_2O bidest. autoclaved
PFA 4% (100 ml)	4 g paraformaldehyde
	dissolved in 50 ml H_2O at 60°C,
	few drops of 2 M NaOH, filtered;
	45 ml 0.2 M Na_2HPO_4,
	5 ml 0.2 M NaH_2PO_4;
	pH adjustment to 7.4

3.2. Methods

3.2.1. Isolation of DNA

For DNA isolation and genotyping mouse tails or ear biopsies of three-week old mice were dispersed in 500 µl DNA lysis buffer containing 20 µl of 20mg/ml proteinase K at 60°C in a shaker at 550 rpm overnight. 300 µl of 5% SDS and 120 µl 3 M NaCl were added and the samples mixed until the solution became homogenous. Samples were centrifuged for 10 min at 4°C and 14 000 rpm. The upper phase of each sample was transferred to a new reaction and chloroform clearance was repeated until the phase became completely clear.

1 ml of 100% ethanol was added to the supernatant and tubes were mixed carefully until the white DNA precipitate became visible. Mouse samples were centrifuged for 10 min at 4°C and 14 000 rpm and the pellet was washed with 70% ethanol. The supernatant was discarded and the pellet dried at RT for 5 min. The DNA was resolved in 100 µl Tris pH 8.0 and stored at 4°C.

3.2.2. Primers

Table 2: Primers.

Primer	Sequence
Na$_V$1.9_antisense	5'-AACAGTCTTACGCTGTTCCGATG-3'
Na$_V$1.9_sense	5-ATGTGGCACTGGGCTTGAACTC-3
neomycin gene	5-CTCGTCGTGACCCATGGCGAT-3

3.2.3. Polymerase chain reaction

PCR (polymerase chain reaction) was performed using Taq polymerase and PCR reaction buffer from 5´ Prime. Each reaction contained 1 µl DNA as template, forward and reverse primer, 2 mM dNTPs, 10x PCR buffer, Taq polymerase and sterile distilled water (Ampuwa). The DNA amplification process occurred in Eppendorf´s Mastercycler® PCR machine. PCR was used for genotyping of the mouse line Na$_V$1.9 KO. The reaction mix and PCR program for each genotyping experiment is shown in Table 3 and 4. After PCR procession, DNA fragments were analysed on a 2% agarose gel by agarose gel electrophoresis.

Table 3: PCR reagents for genotyping.

Reagents	Volume [µl]
DNA	1
dNTP (2 mM)	2.5
PCR buffer (10x)	2.5
Each primer (20pMol)	0.25
Taq	0.3
water	17.95
total reaction volume	**25**

Table 4: PCR protocol for $Na_V1.9$ genotyping.

Segment	Temperature	Time	Cycle
pre-denaturation	94 °C	2 min	1x
denaturation	94 °C	30 s	
annealing	60 °C	15 s	
elongation	72 °C	1 min	35x amplification
post-elongation	72 °C	10 min	1x
cooling	4 °C	∞	1x

3.2.4. Agarose gel electrophoresis

Agarose gel electrophoresis was used for separation of DNA fragments in a 2% agarose gel containing agarose, 1xTAE and 0.4 µg/ml ethidium bromide or Midorri green. DNA samples were mixed with 6x DNA loading dye and loaded on the gel. Furthermore a DNA size marker with the size of 1 kb was loaded on the gel. The gel was run in 1x TAE for 30 min at 120 V. The visualization of DNA bands was performed at 368 nm and documented with a photo.

3.2.5. Cell Culture

HEK293-cells, HEK293$_{hTRPA1}$ and HEK293$_{rTRPV1}$ were cultured in DMEM with 10% fetal bovine serum (FBS) and 1% Penicillin/Streptomycin at 37°C and 5% CO_2 in T75 or T25 cell culture flasks in a standard cell culture incubator. At a confluency of 80-90%, cells were washed two times TrpLExpress (10x diluted in 1x PBS) and detached with the same dilution. Trypsinization was stopped by adding cell culture medium. The detached cells were centrifuged to remove residual trypsin and a defined part of the cell solution was transferred into new T75 or T25 cell culture flasks containing fresh cell culture medium.

For selection of an hTRPA1 expression cassette, medium for HEK293$_{hTRPA1}$ cells contained Hygromycin (400 µg/ml), medium for HEK293$_{rTRPV1}$ cells contained Geniticin (400 µg/ml).

For experiments, cells were cultivated on 10 mm glass cover slips which were coated with 0.1 mg/ml Poly-L-Lysin or Poly-D-Lysin. Glass coating was performed for at least one hour at 37°C in a standard cell culture incubator or overnight at 4°C. Coated cover slips were washed three times with H_2O (Ampuwa aqua dest.). Notably, all $HEK293_{hTRPA1}$ and $HEK293_{rTRPV1}$ cells used for this thesis are stable expressing either hTRPA1 or rTRPV1. For transfection with the TRPA1-3C mutant, 1 μg DNA and 2 μL Lipofectamine were incubated for 30 min at RT and then carefully added to HEK293 cells. Cells were cultured overnight and measured after 24 h.

3.2.6. Culture of primary sensory neurons

For dorsal root ganglion (DRG) dissection, the cover slips were prepared freshly two hours before dissection with Poly-L-Lysine and incubated for at least one hour at 37°C and 5% CO_2 in a standard cell culture incubator. Enzymes (Liberase™ TH Research Grade/ Liberase™ TM Research Grade) were dissolved in 2.6 mL aqua dest. and frozen in 90 μl samples. For digestion, 1400 μl DMEM and 1.4% sterile EDTA were added. DRG neurons were cultivated in a mixture of DMEM and Ham´s F-12 (1:1), 10% FCS, 1% Penicillin/Streptomycin and 100 ng/ml NGF at 37°C and 5% CO_2 in a standard cell culture incubator overnight. For dissection, the mouse was euthanatized with CO_2 and decapitation and rough separation of the back bone was executed. From cranial to caudal the rips were removed along the backbone and the backbone transected above the spinal cord. The spinal cord was kept in DMEM. DRG neurons were taken out with the help of two fine tweezers (size 5). DRG neurons were stored in 35 mm Petri-dishes in DMEM for preparation. For calcium imaging and electrophysiology at least 12 to 20 DRG neurons were necessary to sustain appropriate densities of cells.

The nerve bundles and connective tissues were removed from the ganglion and the ganglions stored in a 2 ml Eppendorf tube on ice. For digestion of the cell body, the cell suspension was centrifuged at 3000 rpm for 3 min. The supernatant was discarded carefully and the first enzyme mix (Liberase™ TH Research Grade) prepared as described above was added to the cells. They were incubated at 37°C and 900 rpm in a standard thermo mixer for 25 to 30 min. If the cell suspension appeared bulgy, the supernatant was discarded and the second enzyme mix (Liberase™ TH Research Grade) was added. A second incubation step was done at 37°C and 900 rpm in a standard thermo mixer for 10 min. The supernatant was discarded and further digestion was prevented by addition of 1 ml DRG medium without NGF. The cells were centrifuged at 3000 rpm for 3 min and the supernatant was discarded. 700 μl DRG medium were added and the cells were triturated with a 1000 μl pipette tip for 10-20 times. Cells were centrifuged at 3000 rpm for 3 min and collected in 200 μl medium containing NGF. Cells were plated at appropriate densities and settled down for 1 h.

Afterwards, DRG medium with NGF (10 µg/ml) was added carefully to the cells and a slight panning was carried out. The medium was removed and 2 ml medium were added. Finally, the cells were incubated at 37°C and 5% CO_2 in a standard cell culture incubator overnight.

3.2.7. Immunocytochemistry

For immunocytochemistry, cells on cover slips were fixed with pre-warmed 4% PFA (paraformaldehyde) for 15 minutes at RT, washed three times with 1x PBS and incubated in blocking solution containing 1x PBS, 10% HS (horse serum), 0.1% Tween 20 and 0.3% Triton X-100. During blocking the samples were kept at room temperature for 1 h. Afterwards, they were transferred into a dark wet chamber and covered with 75 µl of the primary antibody in blocking solution. The primary antibody was incubated for 3 hours.

Then, cells were washed eight times with a washing solution containing 1x PBS, 0.1% Tween 20 and 0.1% Triton X-100. Next, 75 µl of the secondary antibody in blocking solution were added for 1.5 hours. After this, coverslips were washed for eight times with washing solution and incubated with 80 µl of 0.4 µg/ml DAPI in 1x PBS for 5 min. Subsequently, cells were washed three times with 1x PBS and the cover glass was dipped in aqua dest. and dried. Cover glasses with the cells upside down were embedded in aqua polymount on an object slides and fixed with nail polish. The slides were analyzed by confocal microscopy and stored at 4°C in slide boxes or folders for light protection afterwards.

3.2.8. Agonist and antagonist preparation

All OxPLs (OxPAPC; PGPC; POVPC) were solved in chloroform as 10 mM stock solution and stored in glass vials to prevent reactions with plastic material. The chloroform was evaporated via the use of nitrogen gas to prevent further oxidation. Afterwards, the glass vials were stored at -20 °C until usage. For experiments, OxPL were freshly solved in the appropriate buffer including the amount of chloroform they were previously solved in and mixed for 2 min with the help of a vortex. Capsaicin, AITC, HC-030031, BCTC and carvacrol were solved as 10 mM stock solution in DMSO and stored at -20 °C in Eppendorf tubes. For usage, they were thawed and diluted in the appropriate buffer.

3.2.9. Calcium imaging

For Ca^{2+} imaging, a buffer containing 135 mM NaCl, 6 mM KCl, 1 mM $MgCl_2$, 1 mM $CaCl_2$, 10 mM HEPES and 5,5 mM Glucose was used. The osmolarity of the solution was controlled with the Micro-Osmometer TypOM806 from Vogel.

For slow imaging, the calcium indicator Fura-2-AM was prepared as 2 mM stock solution by adding 500 µl of 20% Pluronic® F-127 solved in DMSO to 1 mg Fura-2-AM. 3 µl aliquots were made and for dye loading, 1 ml of calcium imaging buffer was added. Cells were incubated for 30 minutes at 37°C and 5% CO_2 in a standard cell culture incubator. The cover slips were transferred to a special chamber. Measurements were performed at RT using a Nikon TE2000-E microscope. Fura-2 AM was excited for 60–90ms with 340/380 nm with a Lambda DG4/17 wavelength switch (Sutter Instruments). Time-lapse image series were acquired at intervals of 2 s with a cooled EMCCD Andor iXon camera (Andor Technology) controlled by NIS Elements Software (Nikon) with a 10x CFI S-Fluor objective (N.A. 0.5; Nikon, Martin and Stoffer et al., 2018).

For fast imaging, the high-affinity calcium indicator Oregon Green 488 BAPTA-1, AM was prepared as 5 mM stock solution by adding 8.9 µl of 20% Pluronic® F-127 solved in DMSO. The solution was incubated for three minutes in a sonifier water bath (Bandelin) and 0.5 µl aliquots were made. For dye loading of cells, 500 µl of calcium imaging buffer was added to one aliquot of Oregon Green 488 BAPTA-1, AM. Cells on cover glasses were incubated for 15 minutes at 37°C and 5% CO_2 in a standard cell culture incubator. Subsequently the cover glasses were transferred to the imaging setup containing an upright fixed microscope (BXWI, Olympus) equipped with a CoolLED (Visitron Systems) and an X-cite 120Q excitation light source (Lumen dynamics).

The microscope system was controlled by a remote control SM7 (Luigs and Neumann), while imaging was performed in an imaging chamber under continuous perfusion with calcium buffer warmed to 25°C using a SH-27B In-line Solution Heater (Warner Instrument Cooperation) regulated over Automatic temperature controller (Warner Instrument Cooperation) and a Bridge 500 under the control of Bad Controller V (Luigs & Neumann). For steady flow of the solution, the Minipuls 3 Peristaltic Pump (Gilson) was used and images were captured with the Rolera-XR camera (Qimaging) operated by the StreamPix 4 software (Norpix). During imaging of Ca^{2+} dynamics, the following parameters were applied: frame size limited to 2000, 100 ms exposure, at a speed of 5 Hz. Oregon Green was excited at a wave length of 470 nm. For analysis fluorescent intensities in defined regions of interest (ROIs) were obtained using the ImageJ 1.42l software. The change in fluorescence intensity was measured over time using the Time Series Analyzer V2 0 tool. Results were transferred to Microsoft Excel 2003 for further calculations. Here, background noise was subtracted from each ROI at each time point using the average of three background ROIs.

To display relative changes of fluorescence intensity over the time (ΔF/F0), fluorescence intensity at each time point (FROI) was set in correlation to the basic fluorescence intensity (F_0) using the following formula: $(\Delta F/F_0) = (F_{ROI} - F_0) / F_0$.

Afterwards peak analysis was done with OriginPro 9.0.OG software (OriginLab Corporation). For this, a baseline was defined and peaks with amplitude of at least 10% increase over background were defined to represent a calcium transient.

3.2.10. Electrophysiology

Patch clamp measurements were performed with HEKA EPC-10 USB and controlled by patch master software (HEKA Electronic, Lamprecht, Germany). Measurements were sampled continuously at 5 kHz every second. Currents were filtered at 2.9 kHz. For measurements of currents at constant voltage, cells were clamped at -60 mV in *whole cell* configuration (Hamill et al., 1981). Agonists were applied with a second pipette controlled by a pneumatic drug ejection system (0.3 s, 0.2 bar; PDES-02DX, npi electronic, Tamm, Germany). All pipette electrodes consisted of silver wires, which were chlorinated for better conductance. Pipettes with 2.5-5 MΩ resistances were pulled from borosilicate glass (GB 150-8P, Science Products, Hofheim, Germany) with a P-97 micropipette puller (Sutter Instruments, Novato, CA, USA). Measurements were analyzed with Igor Pro 6.37 and Origin 2016. For electrophysiological measurements of HEK293 cells and DRG neurons, the cover slips with grown cells were transferred to an appropriate chamber. For HEK293 an external buffer was used containing 140 mM NaCl, 5 mM CsCl, 2 mM $MgCl_2$, 1 mM $CaCl_2$, 10 mM HEPES and 10 mM glucose (pH 7.4, NaOH). As internal solution a buffer with 140 mM $CsCl_2$, 4 mM $MgCl_2$, 10 mM HEPES and 10 mM EGTA (pH 7.3, CsOH) was applied. For dorsal root ganglion (DRG) an external buffer containing 120 mM NaCl, 3 mM KCl, 2.5 mM $CaCl_2$, 1 mM $MgCl_2$, 30 mM HEPES and 15 mM glucose (pH 7.4 with NaOH) was used (Leipold et al., 2013). The pipette solution contained 125 mM KCl, 8 mM NaCl, 1 mM $CaCl_2$, 1 mM $MgCl_2$, 0.4 mM Na_2-GTP, 4 mM Mg-ATP, 10 mM EGTA and 10 mM HEPES (pH 7.3 with KOH). Current clamp recordings were acquired in the *whole-cell* configuration from isolated DRG neurons with an electrical capacitance of less than 30 pF, to delimit the recordings to C-fibre neurons only. The exchange of bath solutions occurred via a perfusion pipette, which was located near the cell during the measurement. DRGs were placed in a recording chamber.

3.2.11. DHE-dye

For analysis of ROS production induced by OxPAPC, 100.000 HEK293$_{hTRPA1}$ cells grown for 24 h on coated glass coverslips were loaded with 10 µM dihydroethidium (DHE) for 15 min at 37°C.

Cells were treated with either FCCP (10 µM), H_2O_2 (100 µM), or OxPAPC (10 µM) in calcium imaging buffer (in mM: 135 NaCl, 6 KCl, 1 $MgCl_2$, 1 $CaCl_2$, 10 HEPES, 5.5 Glucose) and were analysed after incubation for 10, 20 and 30 min at 37°C. For control, cells were incubated in calcium imaging buffer only. DHE labels were analysed with life cell imaging in calcium imaging buffer. For this, cells were excited with a LED light source (550 nm, CoolLED) and fluorescence (emission: 574 – 650 nm) was imaged with a CCD-camera (Rolera XR, Qimaging), mounted on an Olympus BX51WI microscope with an Olympus objective (40x water, N.A. 0.8). 20 images (8 bit) were acquired at 10 Hz, at indicated time points. Images were averaged and integrated fluorescence intensity was determined in regions of interest representing individual cells. For image analysis the software ImageJ was used.

3.2.12. OxyBlot

200.000 HEK293$_{hTRPA1}$ cells were cultured for 24 hours. Cells were washed and treated with either H_2O_2 (10 µM or 100 µM), or OxPAPC (10 µM) in calcium imaging buffer, for 10 min at 37°C. Cells were harvested in lysis buffer (1% NP40, 150 mM NaCl, 50 mM HEPES, 10 mM sodium pyrophosphate, 1 mM NaF, 10% glycerol, including protease inhibitors). Protein concentrations were determined with Bio-Rad Protein Assay (BioRad). 5 µg of protein per lane was separated by SDS-PAGE and blotted on PVDF membrane (Immunoblot, BioRad). Western detection was performed with the OxyBlotTM Protein Oxidation Detection Kit (Merck Millipore) and ECL Prime reagent (Amersham).

3.2.13. Statistics

Data are presented as mean ± S.E.M. Measurements were analyzed with a student's t-test. Multiple measurements with one or two variables were analyzed by one-way ANOVA repeated measurements (RM), post hoc test as indicated. Differences were considered significant when $p ≤ 0.05$ (*), $p ≤ 0.01$ (**) or $p ≤ 0.001$ (***). Statistical analysis of data as well as the creation of graphs was performed with OriginPro 9.0 (OriginLab Corporation, Northampton, MA, USA) or Igor Pro 6.37 (WaveMetrics, Inc, Nimbus, Portland, USA).

4 Results

4.1. TRPA1 is a target channel for oxidized phospholipids

Oxidized phospholipids are endogenous irritants produced during inflammation (Oehler et al., 2017). Apart from activating toll-like receptors (Bochkov et al., 2010), their impact on other receptors expressed on nociceptors was at the beginning of this project unknown. Previous experiments performed with a FLIPPR calcium influx assay suggested TRPA1 and TRPV1 as possible target receptor channels of the OxPL mixture OxPAPC (Oehler et al., 2017).

To better define OxPAPC function on the TRP channel TRPA1, a vector expressing recombinant human TRPA1 under a CMV-promoter was transiently expressed in HEK293 cells. Then, OxPAPC-evoked inward currents of the human TRPA1 channel (hTRPA1) were investigated. To see whether OxPAPC-evoked currents were mediated by TRPA1, HC-030031, a small molecule and selective antagonist of TRPA1 was used (McNamara et al., 2007). Furthermore, the TRPA1 agonist AITC was used to control for TRPA1 responsiveness in this experimental assay. TRPA1-mediated currents were measured with the help of *whole cell* patch clamp recording on HEK293$_{hTRPA1}$ cells. For this, a ramp protocol from -100 mV to +100 mV voltage injection was applied. Hereby, a calcium free extracellular bath solution containing N-methyl-*D*-glucamine was used to limit OxPAPC- as well as AITC evoked in-and outward currents (Fischer et al., 2013; Schulze et al., 2013). Either OxPAPC or AITC were added with a concentration of 10 µM via a gravity perfusion system. Furthermore, cells were incubated in HC-030031 with a concentration of 10 µM for 10 min before addition of the agonists, to examine a potential inhibition of a substance evoked current.

OxPAPC induced a long-lasting inward current in HEK293$_{hTRPA1}$ cells and this effect was inhibited by preincubations with the TRPA1 agonist HC-030031 (Fig. 11 A, B). After addition of OxPAPC and the injection of voltage ramps, a linear current voltage relationship was found, indicating a potent activation of TRPA1 by OxPAPC (Fig. 11 D, F). In untransfected control cells no agonist-induced inward currents were observed after OxPAPC application (Fig. 12). The functional expression of TRPA1 was verified by control stimulation with AITC. AITC-evoke currents in HEK293$_{hTRPA1}$ showed a characteristic almost linear I/V-curve progression and the curve crosses the point of origin. This indicates both non-selective in-and outward currents.

These experiments indicate that the OxPL mixture OxPAPC is a potent activator of the human TRPA1.
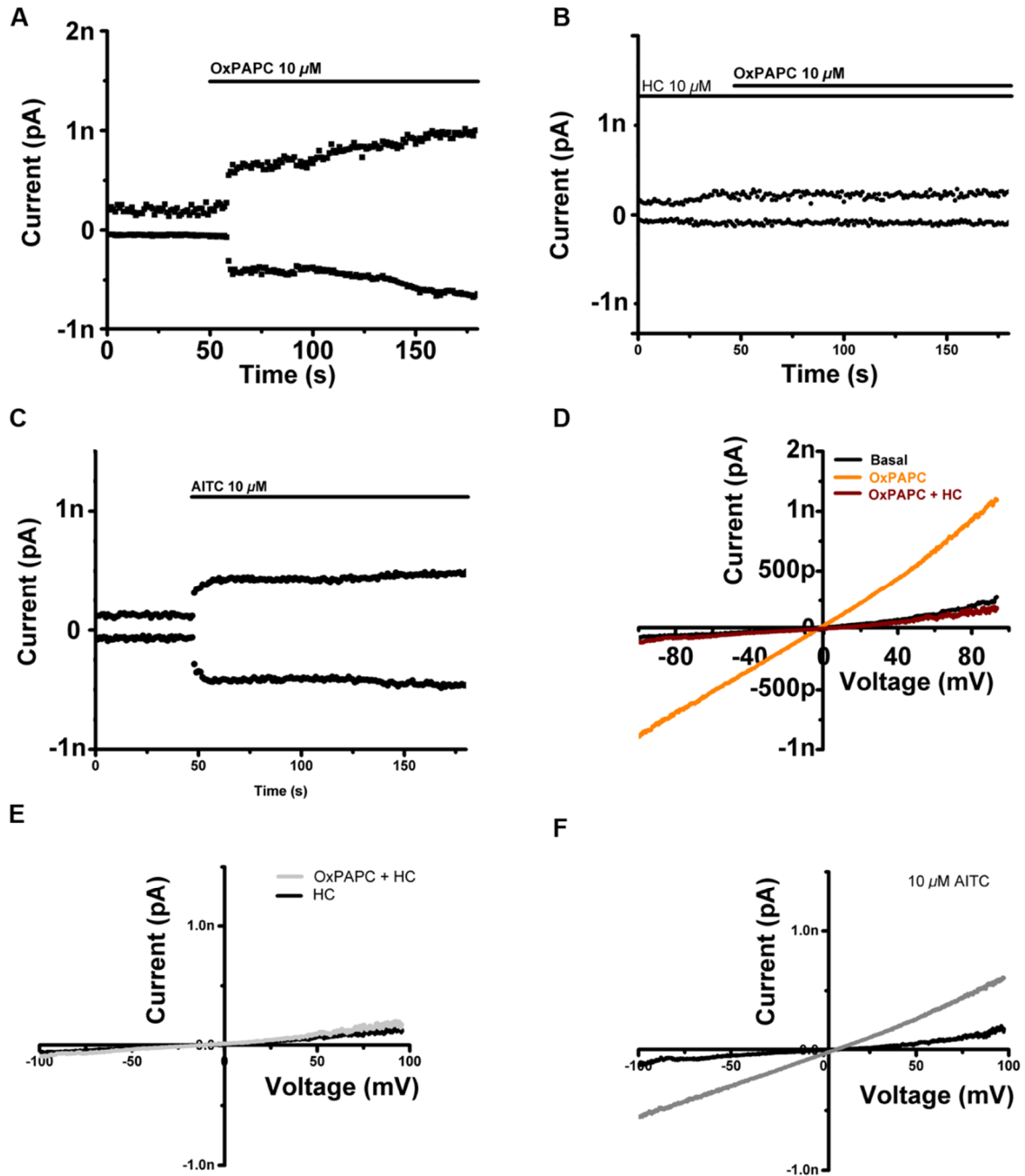
Figure 11: OxPAPC evokes non-selective inward currents in recombinant HEK293 cells expressing hTRPA1. (A) Representative whole-cell patch clamp recording of hTRPA1 after application of 10 µM OxPAPC (A) or of 10 µM OxPAPC to cells pre-incubated in 10 µM HC-030031 (B) or 10 µM AITC (C). (D, E) I/V-curve of hTRPA1 basal (x1) and OxPAPC-induced (x2) currents. Data in (D-F) were extracted from voltage ramps such as in (A-C; modified after(Oehler et al., 2017).
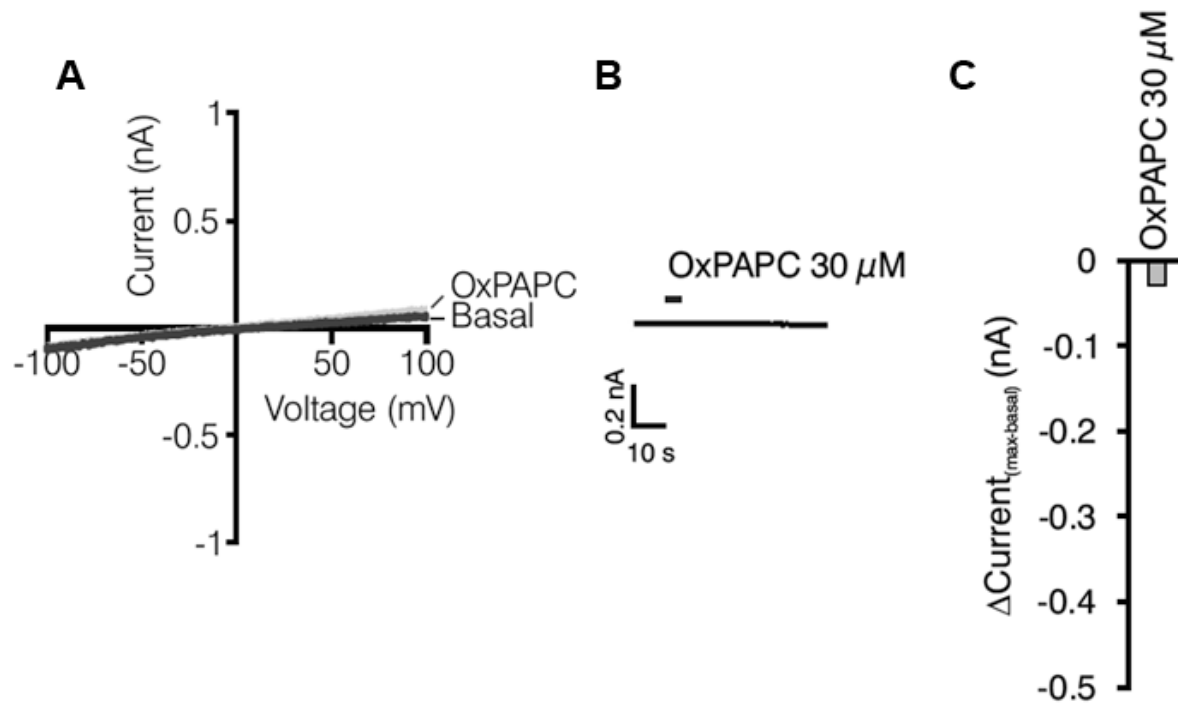
Figure 12: OxPAPC induces no currents in untransfected HEK293 cells. (A) I/V curves, **(B)** current traces and **(C)** ΔCurrent$_{(max-basal)}$ evoked by 30 µM OxPAPC in parental HEK-293 cells are displayed. Voltage was held at –60 mV in current trace analysis and maximum was taken within 2 min after OxPAPC application (modified after Oehler et al., 2017).

4.2. Oxidized phospholipid subcompounds evoke acute currents in HEK293$_{TRPA1}$

While the first experiments revealed TRPA1 current induction by OxPAPC, the kinetic of the activation was of further interest. Furthermore, it was asked whether individual chemically pure subcompounds of the OxPL mixture OxPAPC were able to act via TRPA1 as well. For this set of experiments, a pressure ejection system was used to allow fast agonist application on TRPA1-expressing cells. Thereby, a patch-clamp glass pipette (1 MOhm) was filled with the appropriate agonists in a 3-fold higher concentration (30 µM) compared to perfusion or steady-state agonist applications, leading to a final concentration of about 10 µM at the cell. The application pipette was brought close to the cell with help of a micromanipulator system and the substance was applied 10 s after starting the voltage injection of -60 mV. In total the evoked currents were measured for 60 s (Fig. 13).
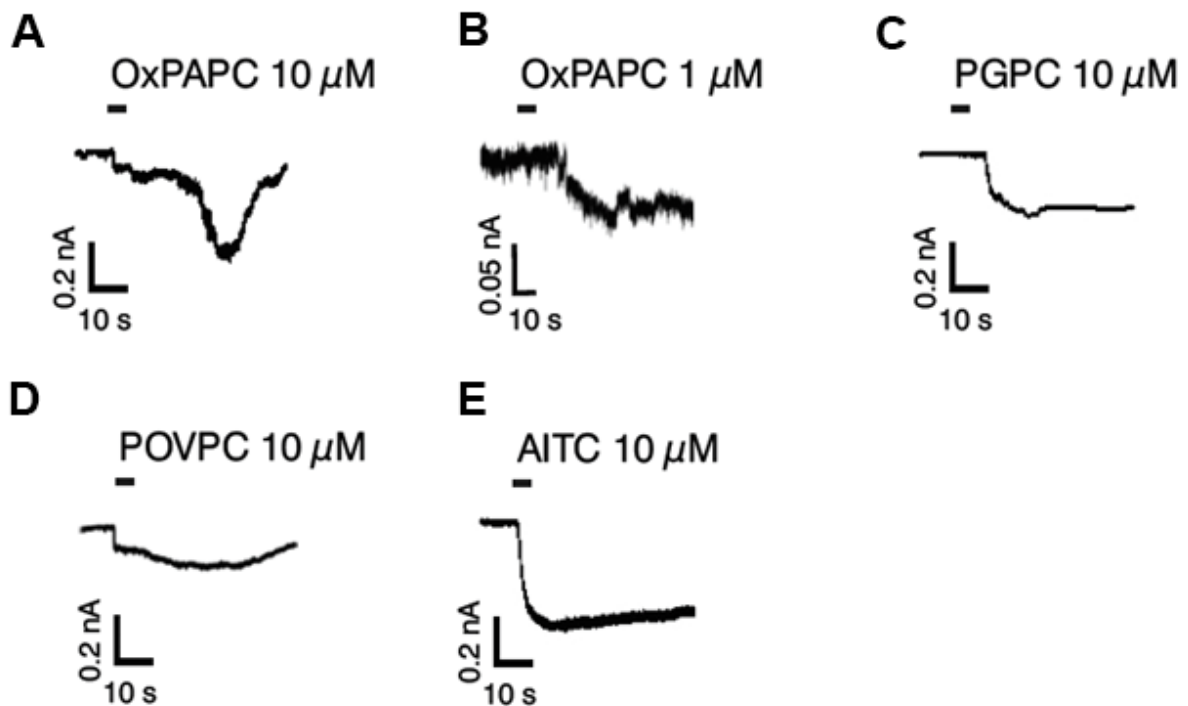
Figure 13: Oxidized phospholipid subcompounds PGPC and POVPC induce acute currents in HEK293$_{hTRPA1}$. (A-D) Injection of -60 mV and the equivalent current response after either OxPAPC (1 µM, 10 µM), PGPC (10 µM) or POVPC (10 µM) stimulation. OxPAPC and its compounds induce a slower activation compared to the agonist for TRPA1 (AITC; E). **(E)** AITC served as positive control for TRPA1 channel activation (modified after Oehler et al.2017).
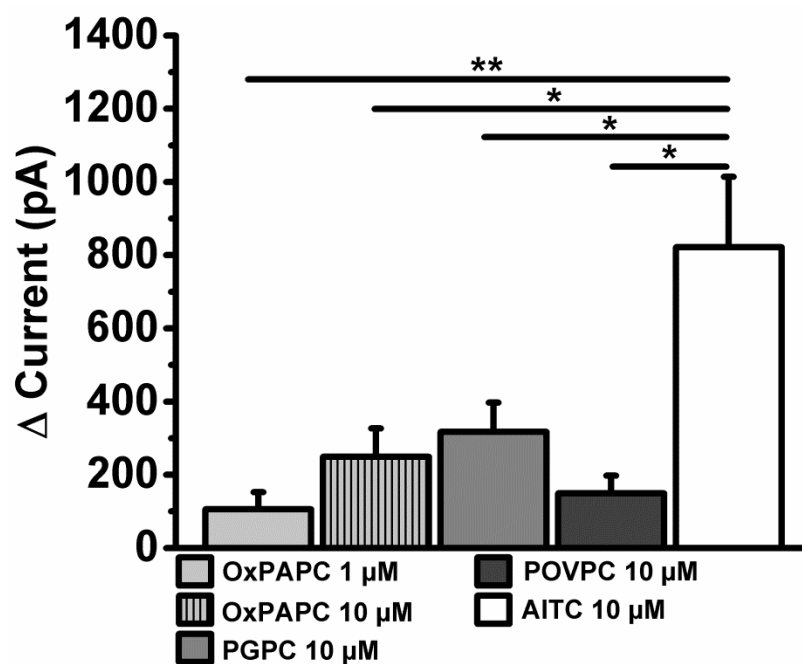
Figure 14: Activation of TRPA1 expressed in HEK293 cells by OxPL and the TRPA1 agonist AITC. OxPL induce influx of currents in HEK293$_{hTRPA1}$ when measured at -60 mV (n = 4-8 separate experiments of 3-4 cultures, separate experiments, mean ± SEM, one-way ANOVA post hoc Holm-Sidak, * p ≤ 0.05; ** p ≤ 0.01).

Analysis of the onset activation of TRPA1-mediated currents initiated by OxPAPC revealed a smaller current within the first seconds compared to the immediate activation onset induced by AITC (Fig. 13). This indicates a delayed activation kinetic of TRPA1 by OxPAPC. OxPAPC activation was concentration dependent: larger currents were observed when using a 10-fold higher OxPAPC concentration (Fig. 13 A, B, n=5). However, PGPC and POVPC showed a more stable and acute induction of currents (Fig. 13 C, D; Fig. 14). In all cases, the OxPL-evoked currents were smaller in comparison to the TRPA1 agonist AITC (Fig. 13).

Table 5: Current induction of the used agonists in HEK293$_{hTRPA1}$ cells.

Agonist	Δ Current	p-Value (to AITC)
OxPAPC (1 µM)	106.26 ± 46.18	0.00922
OxPAPC (10 µM)	249.42 ± 77.12	0.02
PGPC (10 µM)	317.71 ± 79.75	0.036
POVPC (10 µM)	149.38 ± 48.23	0.025
AITC (10 µM)	821.52 ± 192.35	-

In a next experiment it was tested, whether TRPA1-mediated inward currents induced by OxPL or AITC are modified by using polyphosphates (PPP$_i$) in the intracellular patch clamp solution. PPP$_i$, an intracellular mediator was described to inhibit the rapid rundown of TRPA1-mediated inward currents induced by AITC (Kim et al., 2008). The currents and activation conducted with intracellular solution containing PPP$_i$ and stimulation with OxPAPC, PGPC or AITC showed a similar TRPA1 channel response in HEK293 expressing hTRPA1. However, the activation seemed to be more stable, persistent and steady (Fig. 15). Onset and curve progression of TRPA1 currents were similar as those observed in absence of PPP$_i$. This shows that polyphosphates seem to have a minor effect in stabilization of OxPL-induced TRPA1 inward currents.

In summary, these results verify an acute and dose-dependent activation of hTRPA1 by OxPAPC and the OxPAPC subcompounds PGPC and POVPC.
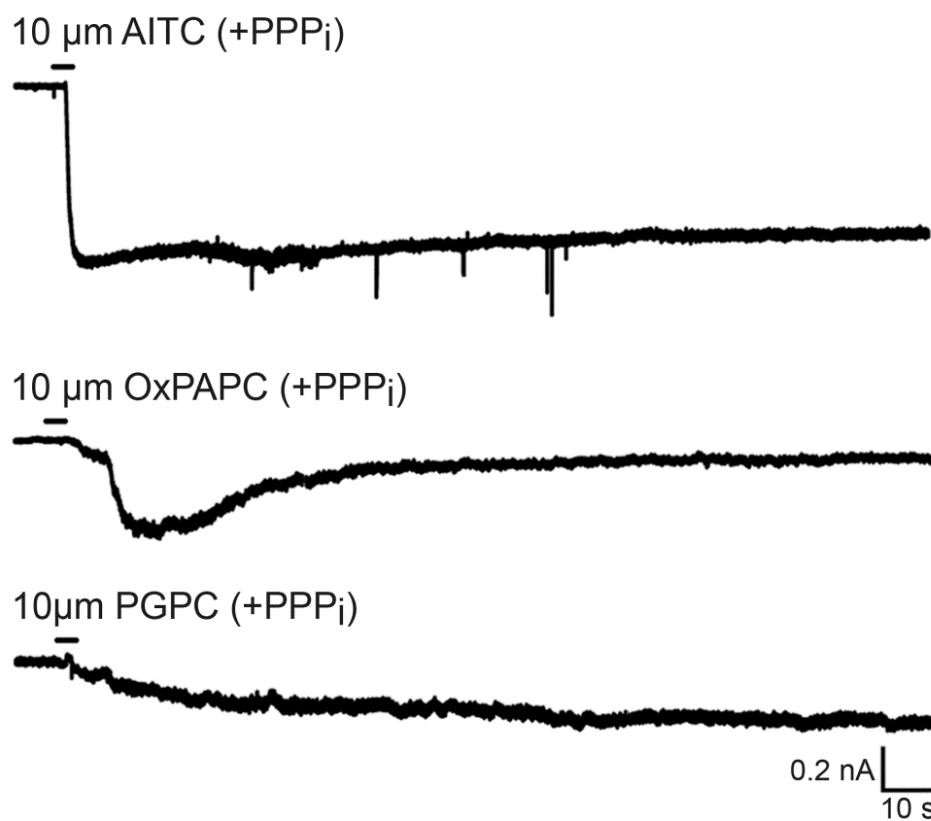
Figure 15: OxPL mediated responses of hTRPA1 expressed in HEK293 cells in the presence of intracellular PPPi. Representative traces of currents recorded at -60 mV and stimulated by local application for 400 ms with the TRPA1 agonist AITC (10 µM), OxPAPC (10 µM) or PGPC (10 µM).

4.3. OxPAPC is neither activating TRPA1 by oxidation nor by ROS production

In vivo, OxPL are formed by reactive oxygen species (ROS) oxidizing 1-Palmitoyl-2-Arachidonoyl-sn-Glycero-3-Phosphocholin (PAPC). This chemical reaction generates also the compounds of OxPAPC might lead the formation of ROS, which are known as potent agonists of TRPA1 (Andersson et al.; Liu and Ji). To examine whether OxPAPC induces ROS formation to indirectly activate TRPA1, we tested whether treatment of TRPA1-expressing HEK293 cells with OxPAPC leads to the production of ROS. To determine ROS production, the fluorescence resulting from oxidation of dihydroethidium by ROS to 2-hydroxyethidium was imaged and quantified (Fig. 17, Fig. 18). Dihydroethidium (DHE) has an emission from 500-530 nm respectively 590-620 while 2-hydroxyethidium, the ROS-dependent oxidation product of DHE, has an emission of 480/567 nm. FCCP, a proton ionophore, which elicits intracellular ROS production by cellular stress due to uncoupling of the ATP synthesis, served as positive control. The substance increases the permeability of the inner mitochondrial membrane for protons, induces apoptosis and thus, increases the internal ROS concentration (Guimarães et al.). Images were averaged and the integrated fluorescence intensity was determined in regions of interest (ROI) representing individual cells (n = 3, 216 cells of 3 cultures; Fig. 16; Fig. 17). After 30 min of incubation in 10 µM FCCP, HEK293$_{hTRPA1}$ cells showed an increased ROS level determined by the integrated density of fluorescence of 115.35 ± 17.18. The experiment revealed an increase of ROS over time reaching its maximum after 30 minutes. The cells incubated in 10 µM OxPAPC for 30 min (49.51 ± 2.61) had a ROS level comparable to the control measurement (39.33 ± 0.25) indicating that OxPAPC does not induce ROS production. Cells incubated with 100 µM H_2O_2 showed an increased fluorescence signal (74.50 ± 5.97) compared to the control (Fig. 16; Fig. 17), as expected.
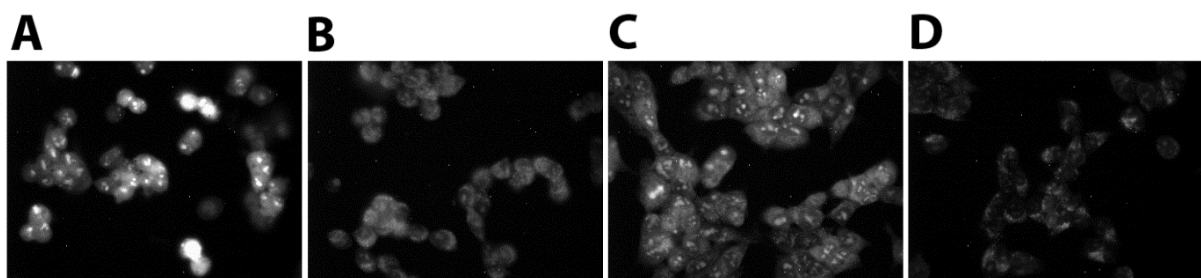
Figure 16: OxPAPC does not induce ROS production in HEK293$_{hTRPA1}$. **(A-D)** Illustrate exemplary 2-hydroxyethidium-derived fluorescence in cells incubated with 10 µM FCCP **(A)**, 10 µM OxPAPC **(B)** and 100 µM H_2O_2 **(C)** and calcium imaging buffer **(D)**. FCCP serves as positive control and HEK293$_{hTRPA1}$ cells incubated in standard bath solution served as negative control (D).
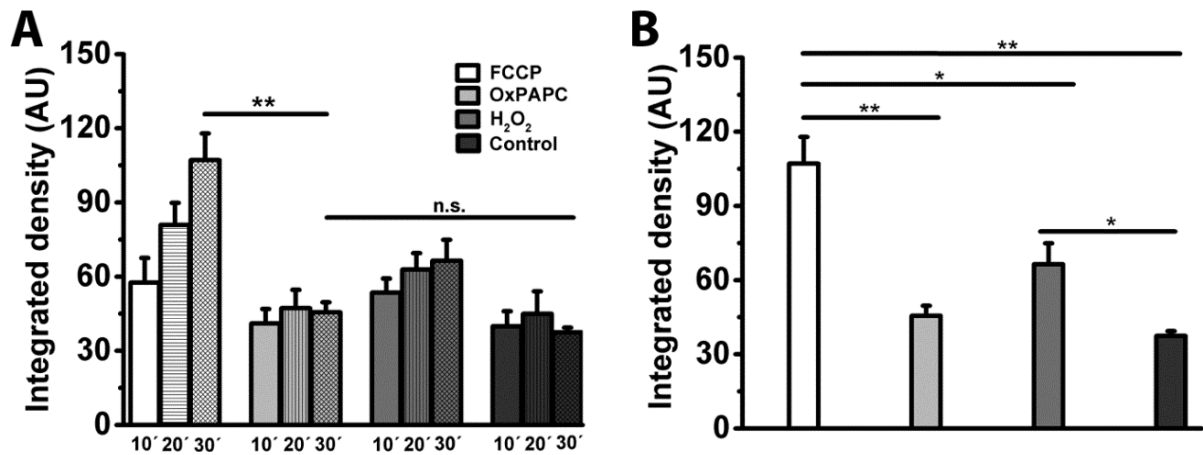
Figure 17: OxPAPC does not induce ROS production in HEK293$_{hTRPA1}$. (A) Increase of integrated density of fluorescence in AU as a function of time (10 min, 20 min, 30 min) after treatment of HEK293$_{hTRPA1}$ cells with either 10 µM FCCP, 10 µM OxPAPC, 100 µM H_2O_2 or untreated control. **(B)** Integrated density after 30 min of pre-treatment with the corresponding substances. FCCP serves as positive control. Cells incubated in bath solution served as negative control ($n = 3$ separate experiments, mean ± SD, one-way ANOVA post hoc Holm-Sidak, * $p \leq 0.05$, ** $p \leq 0.01$).

To test whether 10 µM OxPAPC acts as an oxidant to activate TRPA1, OxPAPC was preincubated with ascorbic acid and ratiometric calcium imaging was performed on HEK293$_{hTRPA1}$ cells using the calcium chelator Fura-2-AM. For this, either a mixture of OxPAPC/ascorbic acid or OxPAPC alone was used to stimulate calcium influx in HEK293$_{hTRPA1}$. No significant effect of ascorbic acid on OxPAPC- induced calcium responses was observed as indicated by a non-significant decrease in the area under the curve (AUC) value after antioxidant treatment (Fig. 18 A).

To investigate whether OxPAPC is affecting hTRPA1 by oxidation, an Oxyblot was performed with HEK293$_{hTRPA1}$ cells and OxPAPC (10 µM). Hereby, H_2O_2 applied in two different concentrations, 10 µM and 100 µM, served as positive control. The cells were incubated for 30 min in the potential ROS producing agents or calcium imaging buffer alone. Then cell protein lysates were harvested and afterwards Oxyblot-based Western blot was performed. Results showed no difference in the degree of oxidation between OxPAPC and untreated treated cells (Fig. 18 B). Negative controls showed no bands on the Oxyblot.

In total, these results indicate that OxPAPC is neither influencing the hTRPA1 channel expressed in HEK293 cells by ROS production nor by oxidation, though antioxidants seem to have a slight inhibition effect.
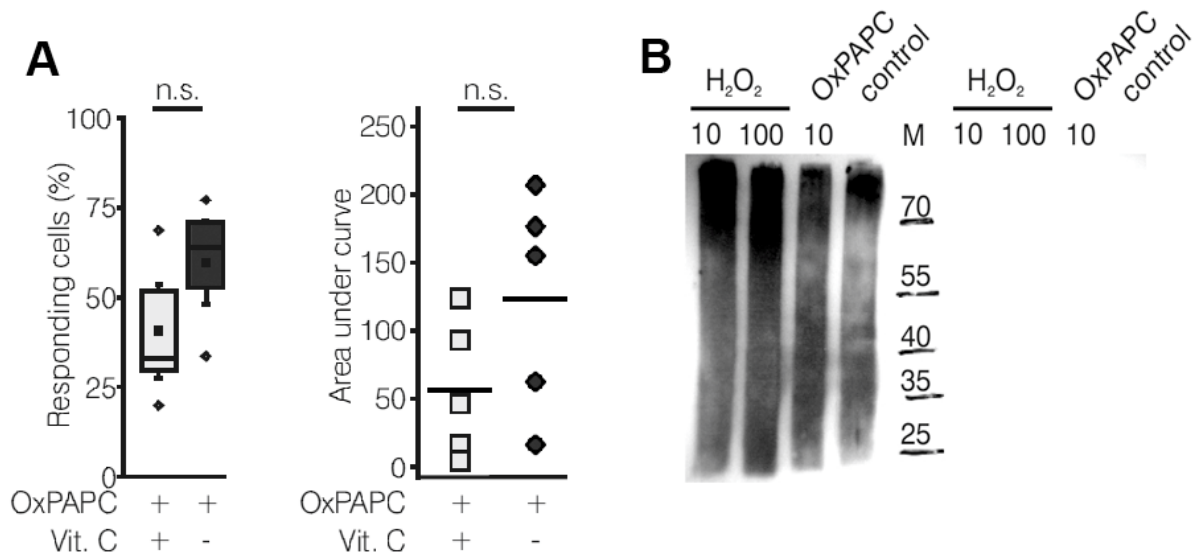
Figure 18: Antioxidants have no significant inhibitory effect on OxPAPC-induced activation of hTRPA1 expressed in HEK293 cells. (A) The percentage number of responding cells and the area under the curve analysis to OxPAPC and Vitamin C stimulation and merely OxPAPC stimulation are displayed (n = 3 separate experiments, mean ± SD, one-way ANOVA post hoc Holm-Sidak, *p ≤ 0.05, **p ≤ 0.01, ns = not significant). **(B)** Representative OxyBlot of HEK293$_{hTRPA1}$ cells treated with different H_2O_2 concentrations (10 µM, 100 µM) or OxPAPC (10 µM). Control cells were incubated in calcium imaging buffer. Column 1-4 display oxidized proteins of HEK293$_{hTRPA1}$-expressing cells stimulated with either 10 µM H_2O_2, 100 µM H_2O_2, 10 µM OxPAPC or calcium imaging buffer. Column 6-9 show total, non-derivated cellular proteins of HEK293$_{hTRPA1}$ stimulated equally to column 1-4 as negative control. Molecular weight markers (column 5) are indicated in kilodaltons in the middle.

4.4. A TRPA1 mutant lacking the electrophile interaction side can be activated by OxPL compounds

As these experiments indicated that neither ROS production nor direct oxidation by OxPAPC caused TRPA1 activation, it was asked whether electrophile activation of TRPA1 might be the only mechanism how OxPL activate TRPA1. Ratiometric calcium imaging experiments were performed using the TRPA1-mutant (C621S/C641S/C665S) lacking the characteristic binding site for electrophilic agonists of TRPA1 (Macpherson et al., 2007; Paulsen et al., 2015). These cysteine residues are unique for this TRP channel and can only be found in the cytosolic N-terminus of TRPA1. The activation of TRPA1 by the three N-terminal cysteine residues requires an electrophilic substance such as AITC (Bautista et al., 2006).

OxPAPC is a mixture of electrophilic and non-electrophilic OxPL with different biological activities. Here, the OxPL OxPAPC and PGPC were tested on their binding behavior on the TRPA1-3C mutant via ratiometric calcium imaging. For this, cells were incubated in the calcium chelator and dye Fura-2-AM solved in calcium imaging buffer and afterwards transferred to an imaging chamber. Agents were applied via a pipette with a volume of 50 µL. Carvacrol (10 µM), a TRPA1 agonist acting through a non-electrophilic binding site in the TRPA1 receptor, served as positive control and demonstrated that the TRPA1 channel function was intact. Both OxPAPC (10 µM) and PGPC (10 µM) induced an influx of calcium into the hTRPA1-3C transfected HEK293 cells (Fig. 19 A-D). AITC served as negative control and failed to induce a calcium influx, showing that indeed the electrophilic binding site was absent. HEK293 cells without expression of any TRP channel served as negative control. In control cells, after stimulation with OxPAPC, PGPC, AITC or Carvacrol no calcium influx was observed (Martin et al., 2018).

Comparing the measurements done with OxPAPC and PGPC, PGPC induces a more acute activation pattern, while the OxPAPC effect seemed to be delayed. The finding that the OxPL PGPC, a non-reactive acidic end product of PAPC oxidation can activate TRPA1-3C verifies that OxPL can activate TRPA1 by a non-electrophilic and non-oxidative mechanism.
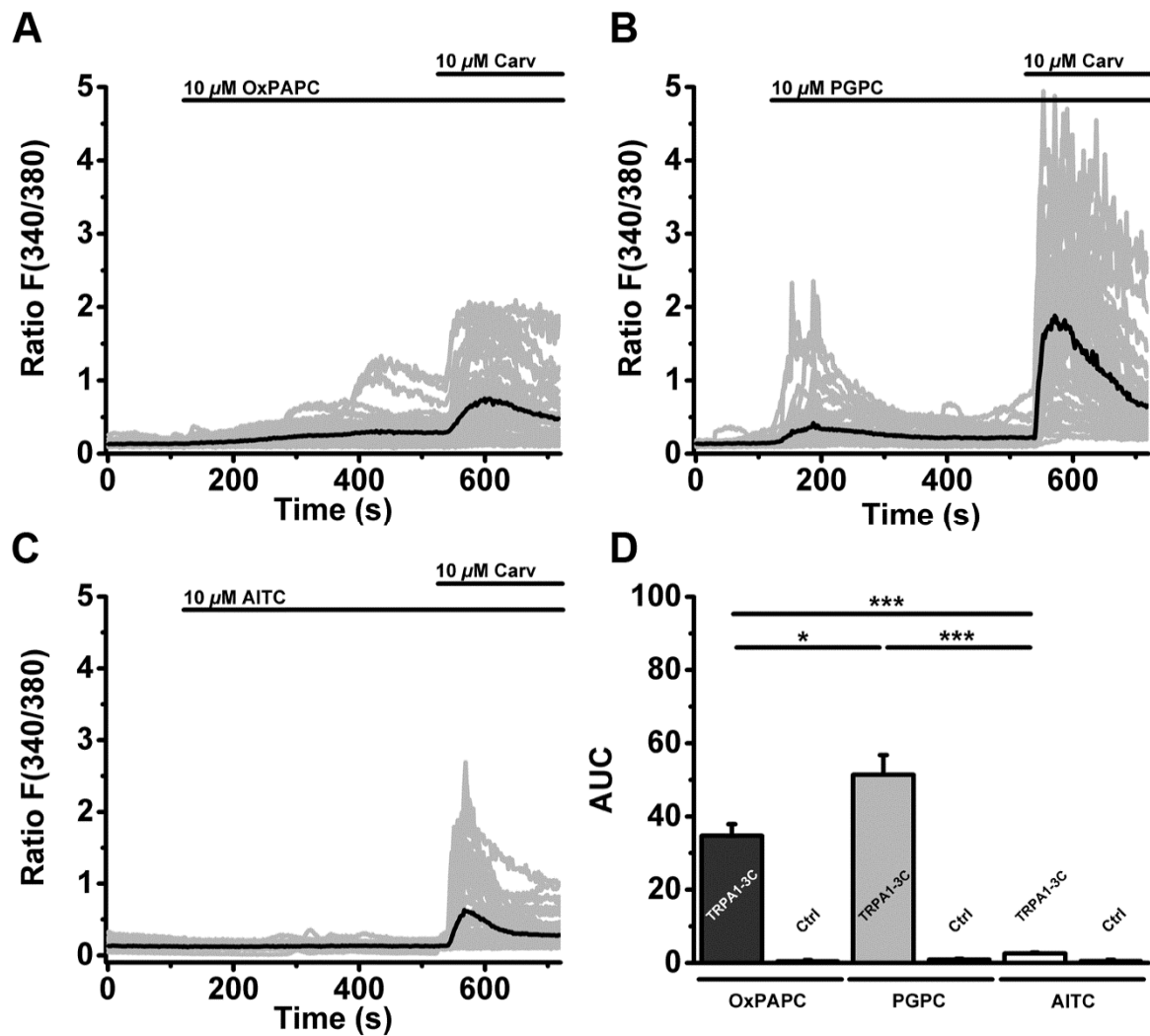
Figure 19: OxPAPC and PGPC can activate TRPA1 by an non-electrophilic mechanism. (A) Relative changes in $(Ca^{2+})_i$ of HEK293 expressing TRPA1-C3 induced by application of either OxPAPC (10 µM; mean of n = 50 cells), **(B)** PGPC (10 µM; mean of n = 50 cells), or **(C)** AITC (10 µM; mean of n = 50 cells) with consecutive addition of carvacrol (10 µM). Gray traces represent calcium responses (F(340/380)) of individual cells, black traces indicate means. **(D)** The relative calcium responses of HEK293 cells transfected with TRPA1-3C (TRPA1-3C) and untransfected control cells (Ctrl), stimulated with either OxPAPC, PGPC or AITC expressed as area under the curve (Ctrl; n = 5-6 of 3 cultures; data points are presented as means ± SEM; one-way ANOVA Holm-Sidak; $F_{(2,16)}$ = 42.33; *p ≤ 0.05, ***p < 0.001; modified after (Martin et al., 2018).

4.5.   Recombinant TRPV1 is modestly activated by OxPL

In addition to TRPA1, early experiments by our group showed that TRPV1 might be another target channel for OxPL. Initially, to investigate this, ratiometric calcium imaging was performed on HEK293 cells expressing recombinant rat TRPV1. After 120 s imaging time, OxPAPC (10 µM, 30 µM) or capsaicin (1 µM) were applied to stimulate TRPV1. TRPV1 calcium influx was inhibited after 540 s by application of the TRPV1 antagonist BCTC (1 µM).
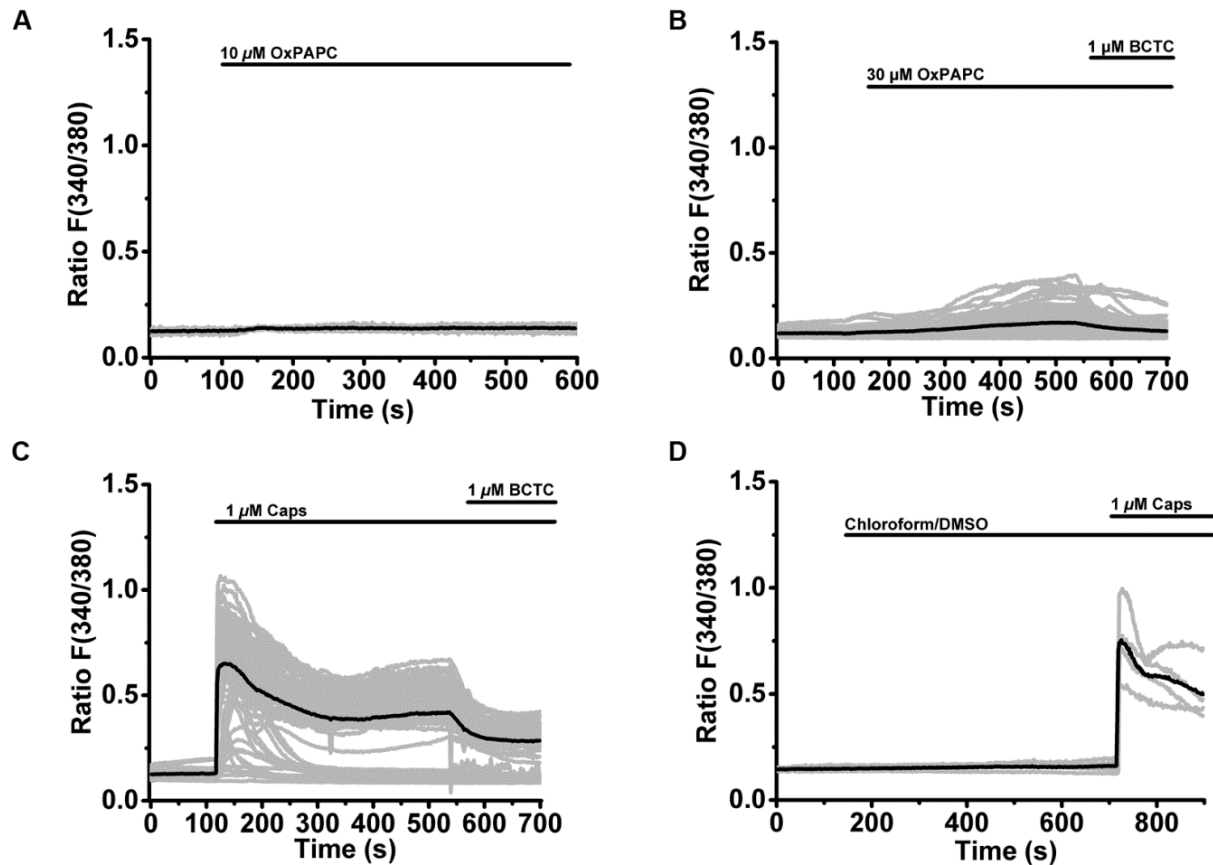
Figure 20: At a concentration of 30 µM OxPAPC evokes TRPV1-dependent calcium influx. Stimulation of HEK293$_{rTRPV1}$ cells with **(A)** 10 µM OxPAPC, **(B)** 30 µM OxPAPC or **(C)** 1 µM capsaicin. The agonists were added at 120 s after start of the measurement. The TRPV1 antagonist BCTC (1 µM) was added after 540 s. **(D)** Control measurements were performed by application of mock preparations of OxPL-solvents (chloroform and DMSO). Grey traces indicate single cell measurements. Black traces display the mean of all cells measured in one experiment.
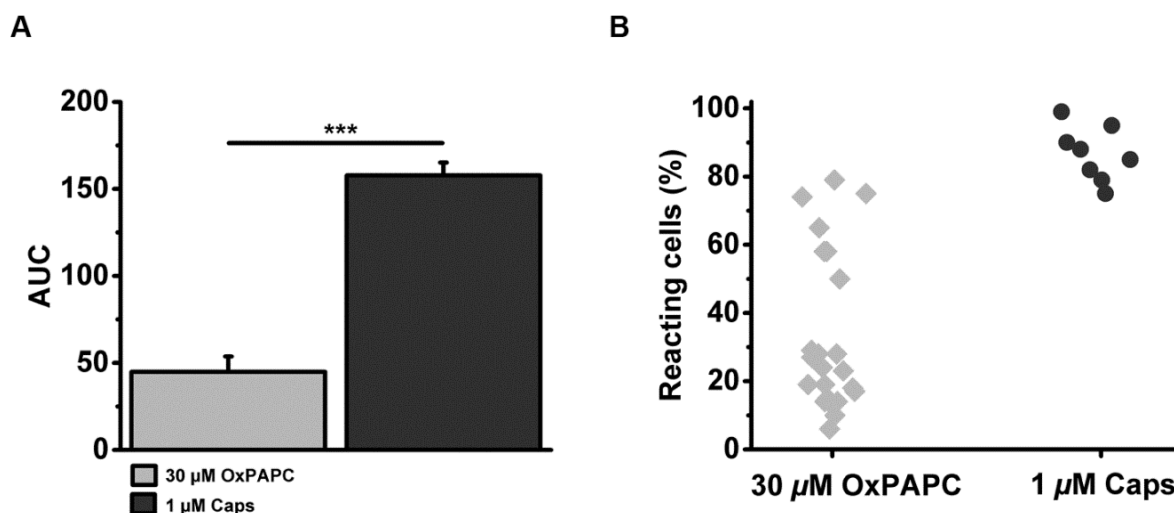
Figure 21: OxPAPC modestly activates HEK293$_{rTRPV1}$ cells. (A) Comparison of the AUC between HEK293 cells expressing rTRPV1 after stimulation with either 30 µM OxPAPC or 1 µM capsaicin (n = 8-22 separate experiments, mean ± SEM, one-way ANOVA post hoc Holm-Sidak, *** p ≤ 0.001). **(B)** Percentage of reacting cells after stimulation with either OxPAPC or capsaicin (n = 8-22 separate experiments).

In comparison to a capsaicin stimulus, OxPAPC induced a slower induction of calcium influx in rTRPV1-expressing cells (Fig. 20 B, C). In contrast to the measurements done on TRPA1, a 3-fold higher OxPAPC concentration (30 µM) was necessary to induce calcium influx via TRPV1. Recombinant HEK293 cells expressing stable rTRPV1 revealed only a modest influx of calcium with a delayed onset after addition of OxPAPC (30 µM) and a slight decrease upon inhibition with BCTC (1 µM; Fig. 20 B). Control measurements done with mock preparations of the corresponding solvents showed no increase in intracellular Ca^{2+}-concentrations (Fig. 20 D). The analysis of the percentage of OxPAPC-activated HEK293$_{rTRPV1}$ cells revealed a significantly lower percentage of reacting cells compared to capsaicin stimulations (Fig. 21). A substantial proportion of HEK293$_{rTRPV1}$ cells were not activated by OxPAPC at a concentration of 30 µM. Electrophysiological analysis of HEK293$_{rTRPV1}$ confirmed the calcium imaging results. Here, stimulation with 10 µM OxPAPC induced small TRPV1-mediated inward currents (Fig. 22). For control, stimulation with the TRPV1 agonist capsaicin led to a typical TRPV1 current. Even a 3-fold increase of the OxPAPC concentration (30 µM) could only induce rather small currents (Fig. 22).

These results show, that recombinant TRPV1 is a target for OxPAPC. However, at least in vitro, TRPA1 seems to be the preferred target of oxidized phospholipids.
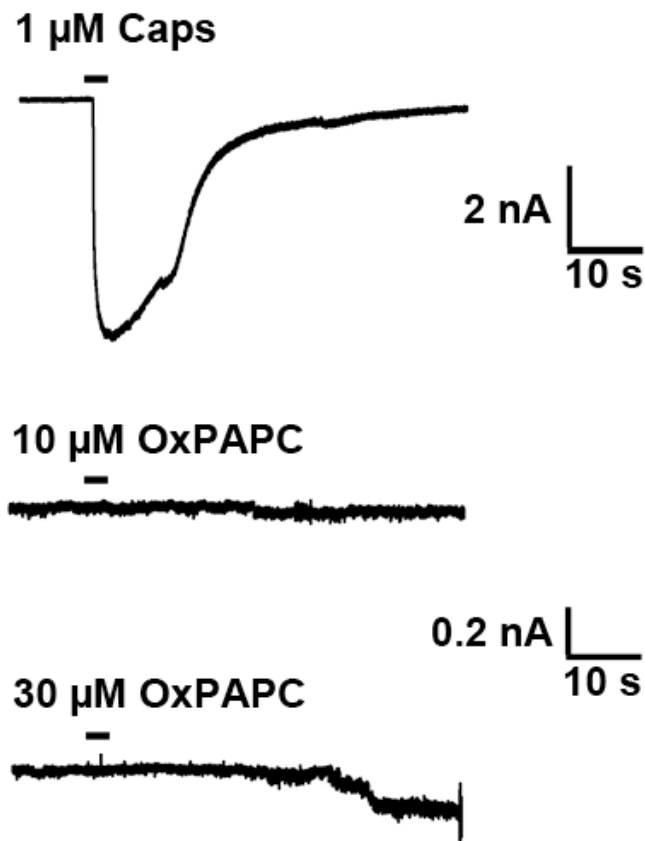
Figure 22: Oxidized phospholipids induce only very small inward currents in HEK293rTRPV1 **cells.** *Whole-cell* voltage clamp at -60 mV and the equivalent current responses after either capsaicin (1 µM) or OxPAPC (10 µM, 30 µM) stimulation. Measurements were performed for 60 s at RT. Agonist application occurred with an application pipette via pressure injection after 10 s (adapted after Oehler et al., 2017).

4.6. PGPC and POVPC are activators of TRPA1 and modestly activate TRPV1

Besides OxPAPC, other OxPL are produced by the reaction of ROS with PAPC. For instance during inflammation this chemical reaction generates a various number of irritants like 4-HNE, PGPC and POVPC. Furthermore, with the help of mass spectrometry, our group found additional OxPL (Oehler et al., 2017). Electrophysiological experiments performed with HEK293$_{hTRPA1}$ cells confirmed activation of TRPA1 with the OxPL compounds PGPC and POVPC (Fig.13, Fig 14). To further investigate activation of TRPA1 and TRPV1 by PGPC and POVPC, ratiometric calcium imaging was performed.
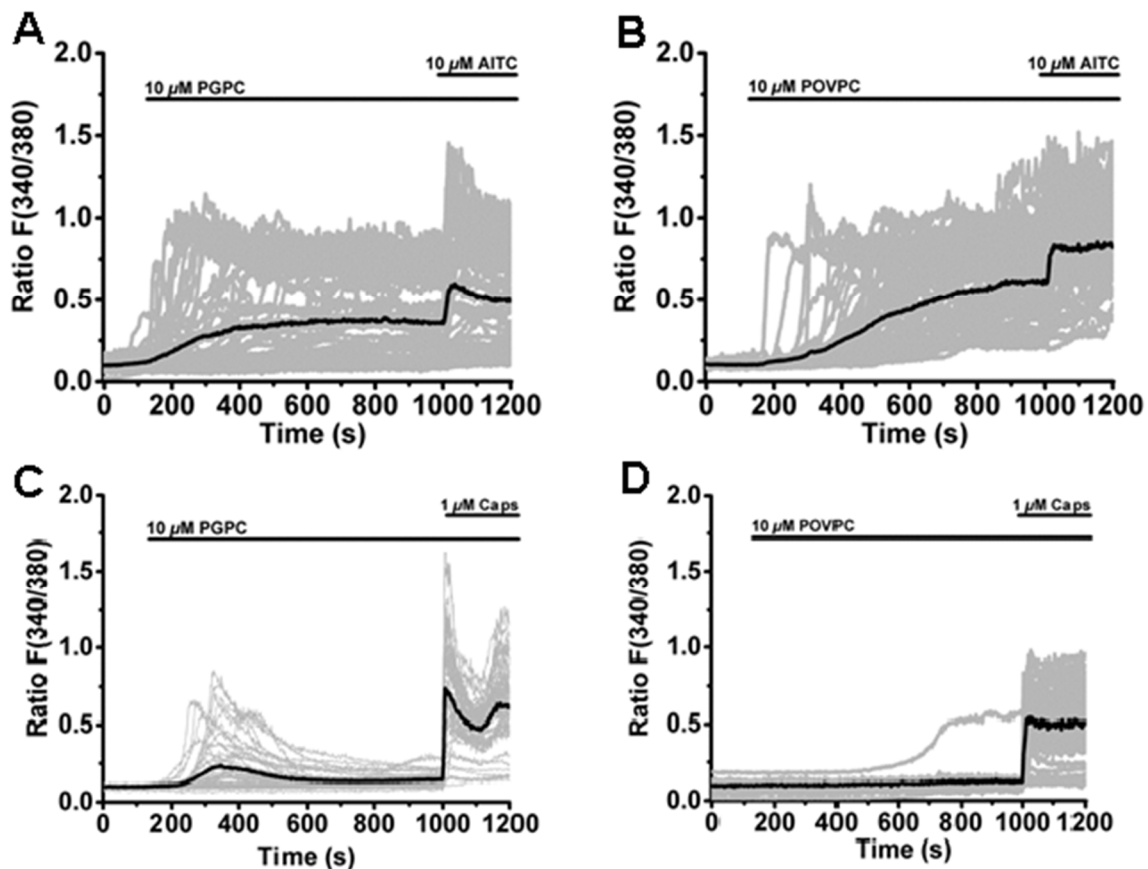
Figure 23: The OxPL PGPC and POVC induce calcium influx into HEK293$_{hTRPA1}$ and merely HEK293$_{rTRPV1}$ cells. (A) Representative traces showing the calcium increase after stimulation of HEK293$_{hTRPA1}$ with either 10 μM PGPC or **(B)** 10 μM POVPC. The addition of substances was performed 120 s after the start of the measurements. The TRPA1 agonist AITC (10 μM) was added after 540 s. Grey traces indicate single cell measurements, black traces display the mean of n = 50 cells measured in one experiment. **(C)** Representative ratio increase after stimulation of HEK293$_{rTRPV1}$ with either 10 μM PGPC or **(D)** 10 μM POVPC. The addition of substances was carried out 120 s after starting the measurements and the TRPV1 agonist capsaicin (1 μM) was added after 540 s. Grey traces indicate single cell measurements, black traces display the mean of all cells measured in one experiment.

In HEK293$_{hTRPA1}$, PGPC (10 µM) and POVPC (10 µM) evoked a long-lasting increase of intracellular calcium which exceeded the activation by the mixture OxPAPC. In comparison to TRPA1-mediated calcium influxes evoked by the TRPA1 agonist AITC, the PGPC and POVPC-induced calcium influx was delayed at equimolar concentrations (Fig. 23). In addition, the percentage of cells responding to a PGPC or POVPC stimulus was comparable to the percentage of cells responding to AITC. In comparison to TRPA1, PGPC (10 µM) and POVPC (10 µM) triggered only a modest activation of recombinant TRPV1 in HEK293 cells (Fig. 24). The percentage and the AUC of PGPC or POVPC activated HEK293$_{rTRPV1}$ cells compared to the prototypical TRPV1 agonist capsaicin was significantly lower (Fig. 24 B, D). In summary, *in vitro* reconstitution revealed that that the pure substances PGPC and POVPC, components of the OxPL mixture OxPAPC, can strongly activate TRPA1, while they only modestly activate TRPV1 (Oehler et al., 2017).
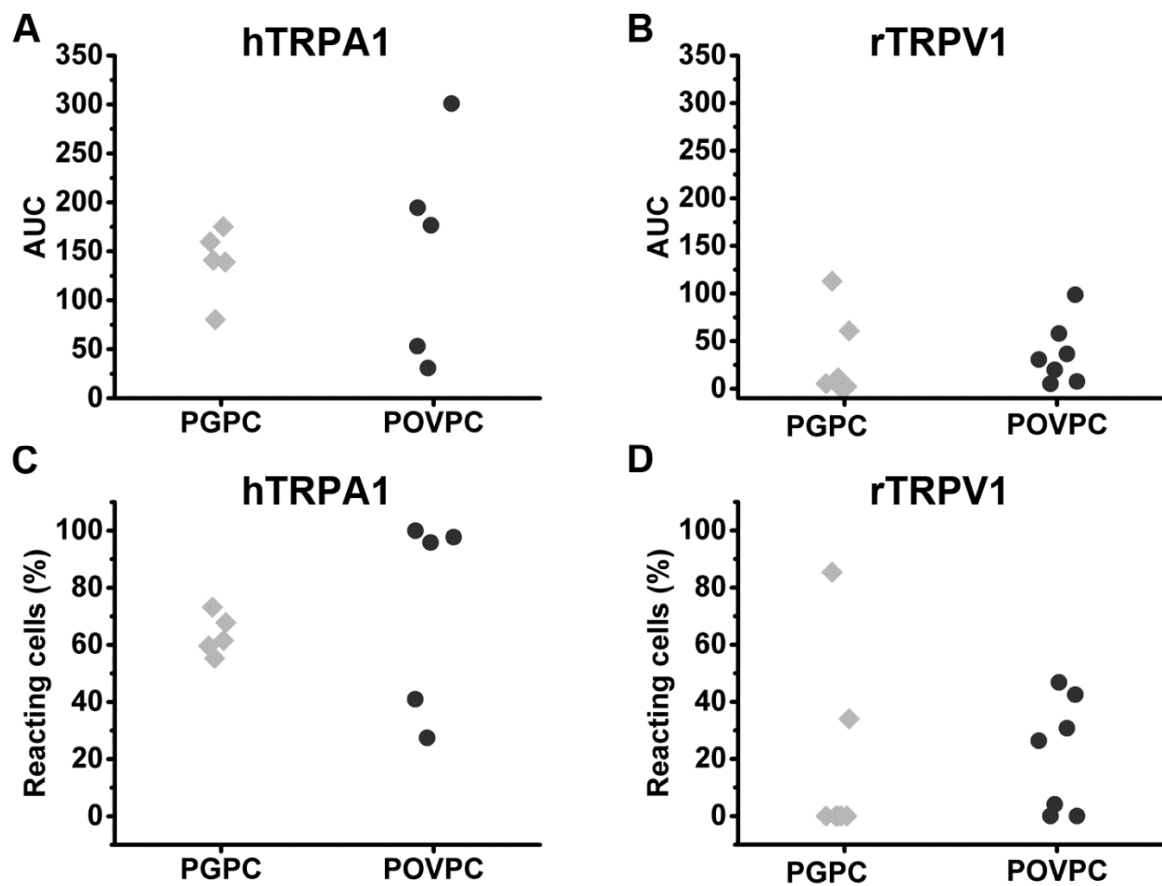
Figure 24: The OxPL compounds PGPC and POVPC activate TPRA1 and TRPV1 expressed in HEK293 cells. The AUC of HEK293$_{hTRPA1}$ **(A)** in comparison to **(B)** HEK293$_{rTRPV1}$ after stimulation with 10 µM PGPC or 10 µM POVPC is shown. **(C)** The amount of reacting cells to 10 µM PGPC or 10 µM in HEK293$_{hTRPA1}$ or **(D)** HEK293$_{rTRPV1}$ (n = 5-7 separate experiments, mean ± SEM).

4.7. TRPA1 and TRPV1 are expressed in cultured primary DRG neurons

The previous experiments suggest the TRP channels TRPA1 and TRPV1 as target receptors of oxidized phospholipids, at least when expressed in a recombinant cell system. Additionally in this thesis, neurons isolated from dorsal root ganglions (DRG) which natively express TRPA1 and TRPV1 channels were used for investigation of OxPL interaction on nociceptors. To find out whether our adult prepared DRG neurons express TRPV1 and TRPA1 protein, immunocytochemistry was performed. For this, a new specific antibody against TRPA1 (Novus Biologicals, Catalog #: NB110-40763) was used to identify TRPA1. Parallel experiments by our group confirmed that this antibody specifically detects recombinant TRPA1.
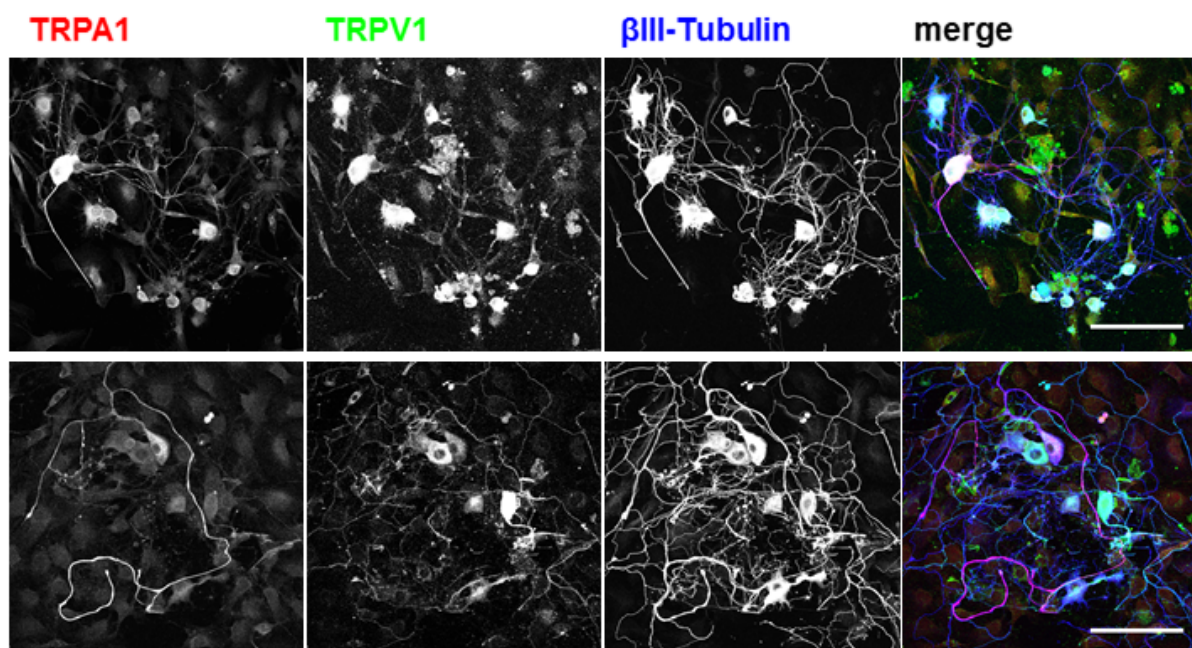
Figure 25: TRPA1 and TRPV1 are highly expressed in wildtypic primary DRG neurons. 48h old primary DRG cultures from C57Bl/6 wt mice were stained either with an antibody against TRPA1 (red). Furthermore, antibodies against TRPV1 (green) and βIII-Tubulin (blue) were used (Martin et al., 2018).

For investigation of the colocalization of TRPV1 and TRPA1, 48 h old cultured DRG neurons were stained for both TRP ion channels and the neuronal marker βIII-tubulin. The majority of the neurons expressed TRPV1 (Fig. 25, green), while the expression level of TRPA1 was high in single neurons. Both channels were seen in somatic and neuritic structures (Fig. 25, red). A large subset of neurons showed a weak immunoreactivity on TRPA1. A large proportion of the TRPA1-positive cells colocalized with anti-TRPV1 signals, thus confirming that adult-prepared DRG neurons coexpress TRPA1 and TRPV1, at least in a subset of cells. In summary, primary DRG neurons from adult mice express the target receptors of OxPL: TRPV1 and TRPA1.

4.8. The OxPAPC compound PGPC increases intracellular calcium in DRG neurons expressing TRPA1 and TRPV1

To establish a more defined neuronal stimulation with an OxPL, it was tested whether PGPC can serve as a prototypical OxPL compound. PGPC offers several advantages over OxPAPC mixtures: (1) It has a lower chemical reactivity and is a truncated end product during PAPC oxidation (Frühwirth et al., 2007; Bochkov et al., 2010); (2) it is not electrophilic, but activates typical physiological OxPL responses via TRPA1 (Oehler et al., 2017); (3) it shows an overall high biological activity (Bochkov et al., 2010; Stemmer and Hermetter, 2012), (4) provides more reliable stimulus conditions (see later), and (5) it is commercially available as a purified substance (Martin et al., 2018).

To further investigate the characteristics of PGPC-induced responses in DRG neurons, a slow ratiometric calcium imaging approach was performed with 24 h old DRG neurons. Stimulation of DRG neurons with AITC to stimulate TRPA1, and stimulations with capsaicin to activate TRPV1, confirmed the functional expression of both TRP channels in adult-prepared DRG neurons. PGPC stimulation of the neurons evoked a robust and sustained increase in intracellular calcium (Fig. 26 A, B). Stimulation of DRG neurons with PGPC generated rather heterogeneous calcium responses (Fig. 26 B). Upon PGPC application, while most neurons featured only brief increases in cytosolic calcium concentrations (e.g., blue and red traces; Fig. 26 B), some neurons showed a strong increase of cytosolic calcium (e.g., green trace; Fig. 26 B; (Martin et al., 2018). For control measurements, only bath solution was applied. Hereby, no cellular response was observed (n = 84 cells, two culture preparations; AUC: mean value = 0.05 ± 0.038 S.E.M).

Stimulation of DRG neurons with AITC and capsaicin increased the intracellular calcium influx as well (Fig. 26 A, B). Pre-incubations of DRG neurons with HC-030031, a TRPA1 antagonist, or BCTC, to antagonize TRPV1, inhibited the PGPC-induced calcium influx in most of the DRG neurons. (Fig. 26 C).
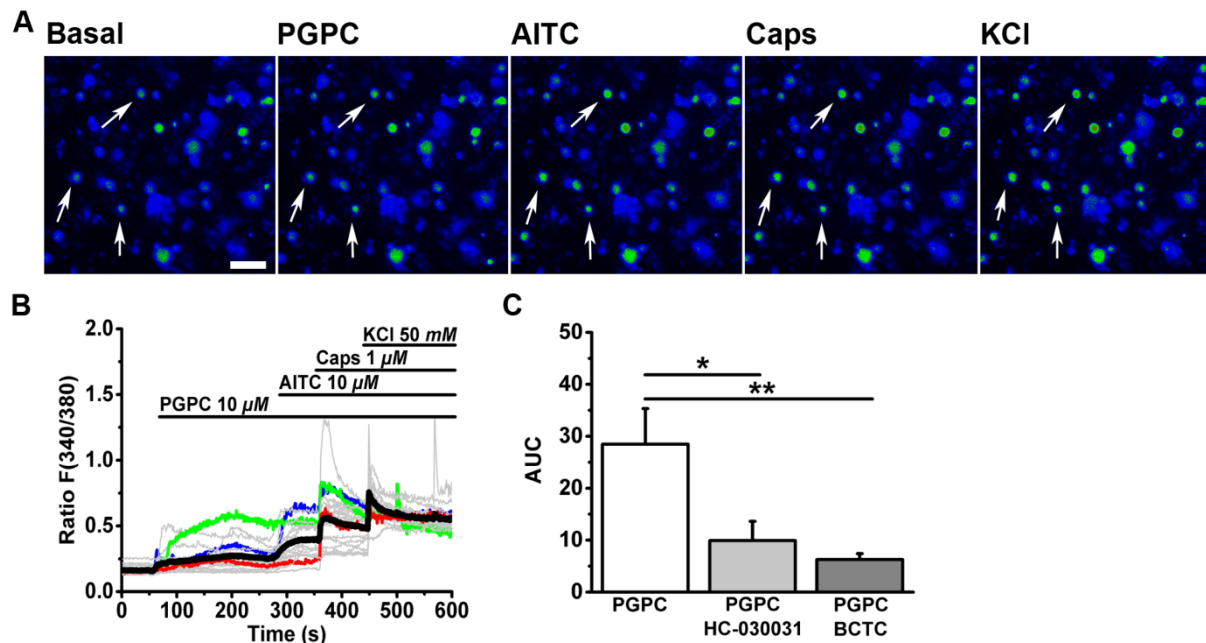
Figure 26: PGPC induces calcium influx in cultured sensory DRG neurons of mice. (A) Pseudo colored images representing calcium responses evoked by consecutive addition of PGPC (10 µM), AITC (10 µM), Caps (1 µM) and KCl (50 mM) in comparison to the start situation (Basal; scale bar = 100 µm). Murine DRG neurons were loaded with Fura-2-AM and measured at RT. Arrows indicate PGPC positive affected neurons. **(B)** Relative changes in $(Ca^{2+})_i$ evoked by consecutive application of PGPC (10 µM), AITC (10 µM), and capsaicin (1 µM) measured with Fura-2 in mouse DRG neurons. Grey traces indicate single cell calcium responses, ratio F(340/380). Black line: average of 50 cells. The AUC **(C)** of activated neurons by PGPC and control activators and their blockers (n = 5-8 separate experiments, mean ± SD, one-way ANOVA post hoc Holm-Sidak, * $p \leq 0.05$; modified after Martin et al., 2018).
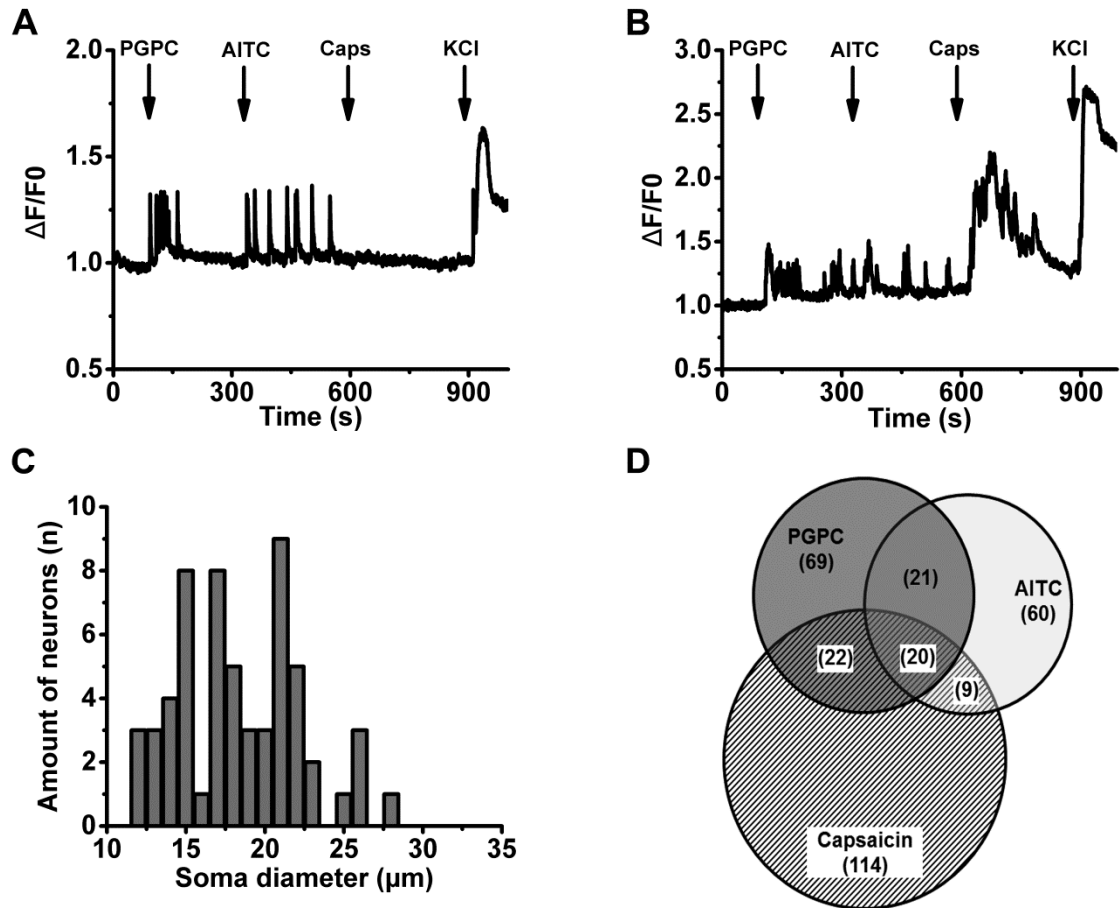
4.9. OxPL induce spike-like calcium transients in DRG neurons

Slow calcium imaging showed a surprising variability in the strength of the single cell calcium responses. To see whether this variability is due to differences in the response behavior of single neurons, a fast calcium imaging approach was established.

For this, the calcium indicator Oregon Green 488 BAPTA 1-AM (OGB) was used (Grienberger and Konnerth, 2012). OGB possesses a low affinity to free calcium ions (Kd≈170 nm), which makes it useful for capturing fast and rather small calcium transients (Ren et al., 2000), including spike-like calcium transients. Here, fast perfusion (5-fold chamber volume exchange) was established with the help of a peristaltic pump. This allowed rapidly adding and washing out applied agonists and antagonists. DRG neurons were tested upon TRPA1 and TRPV1 expression by stimulation with their agonists AITC and capsaicin. However, to prevent sensitization effects in the DRG neurons, they were first stimulated with PGPC, following AITC, capsaicin and KCl stimulation. Notably, PGPC and AITC were both carefully added via a pipette as they were not able to pass the perfusion tube. PGPC induced a robust calcium influx in about 22 % of the tested DRG neurons. Here, the experiments revealed that some neurons generated fast somatic, spike-like calcium transients after stimulation with PGPC which lasted 40 to 100 s (Fig. 27 A, B). Additionally, some neurons responded with spike-like behavior also after AITC stimulation (Fig. 27 A, B). However, the AITC stimulation was performed after stimulation with PGPC. An earlier study showed that PGPC-induced currents are quite long-lasting (Oehler et al., 2017). Possibly, PGPC-induced inward currents contribute to this AITC response behavior as observed in this experiment (Martin et al., 2018). Both, capsaicin and KCl were applied via a perfusion tube.

The onset of calcium influx took place within 200-400 ms after application when imaged at a speed of 5 Hz (200 ms acquisition time). From 307 KCl-positive DRG neurons, 69 reacted to PGPC. Of those, 22 were positive for capsaicin and 21 cells were positive for AITC only. 20 neurons were positive for all three substances. A minority of cells which were PGPC-negative reacted to the TRP agonists AITC and capsaicin. However, vice versa, the majority of AITC and capsaicin-reactive neurons were also activated the by PGPC stimulus. Surprisingly, an amount of 68 neurons reacted on PGPC, but neither on AITC nor on capsaicin.

To better define the sub-class of neurons reacting to PGPC, the soma diameter of DRG neurons was analyzed. Measurement of the cell diameter of OGB-labeled neurons showed that PGPC-responsive neurons had a small soma diameter (18.26 µm ± 1.95; Fig. 27 C), indicating that they belong to the small-diameter sensory neurons.

Figure 27: OxPL evokes repetitive, spike-like calcium transients in DRG neurons. (A, B) Representative fluorescence increase of murine DRG neurons loaded with Oregon Green BAPTA-1 AM. Calcium imaging was performed at10 Hz. Time-lapse imaging was performed under continuous perfusion with calcium imaging buffer. The agonists PGPC and AITC were added into the groove of the imaging chamber. Capsaicin and KCl solution were applied via the perfusion system. **(C)** The soma diameter in μm of PGPC-positive neurons. **(D)** Amount of DRG neurons reacting to PGPC, AITC and capsaicin displayed in a Venn-diagram (Martin et al., 2018).
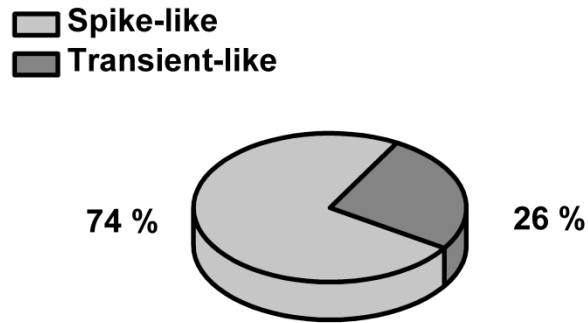
Figure 28: PGPC evokes two kinds of calcium transients. 74 % of all neurons show a spike-like calcium response after PGPC stimulation while 26 % show a transient-like activation (Martin et al., 2018).

The experiments revealed two characteristic response patterns of neurons on an acute PGPC stimulus (Fig. 28, 29). The majority (74 %) showed a spike-like response pattern (Fig. 29 A), while 26 % of the PGPC-rsponsive DRG neurons showed a transient-like (Fig. 29 B) calcium influx. The calcium spike behavior upon PGPC stimulation (Martin et al., 2018).
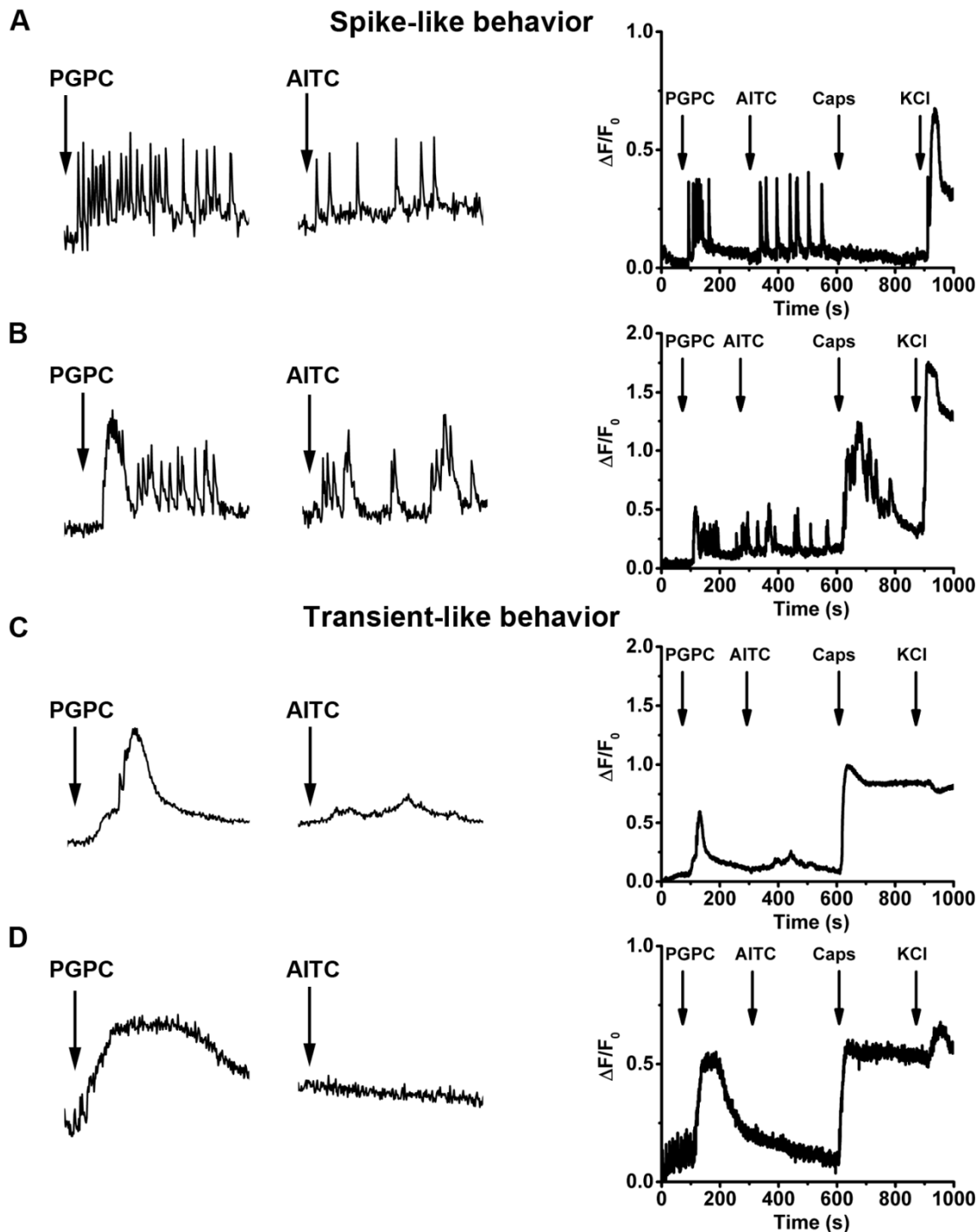
Figure 29: OxPL evokes repetitive, spike-like calcium transients in DRG neurons. (A) DRG neurons possessing a spike-like behavior after PGPC stimulation are displayed in comparison to neurons reacting with transient-like fluorescence increase (B). AITC-evoked responses are displayed next to PGPC-induced calcium responses. Neurons were loaded with Oregon Green BAPTA-1 AM and time-lapse imaging was performed under continuous perfusion with calcium imaging buffer. Overall graphs of the calcium imaging approach are shown on the right (modified after Martin et al., 2018).
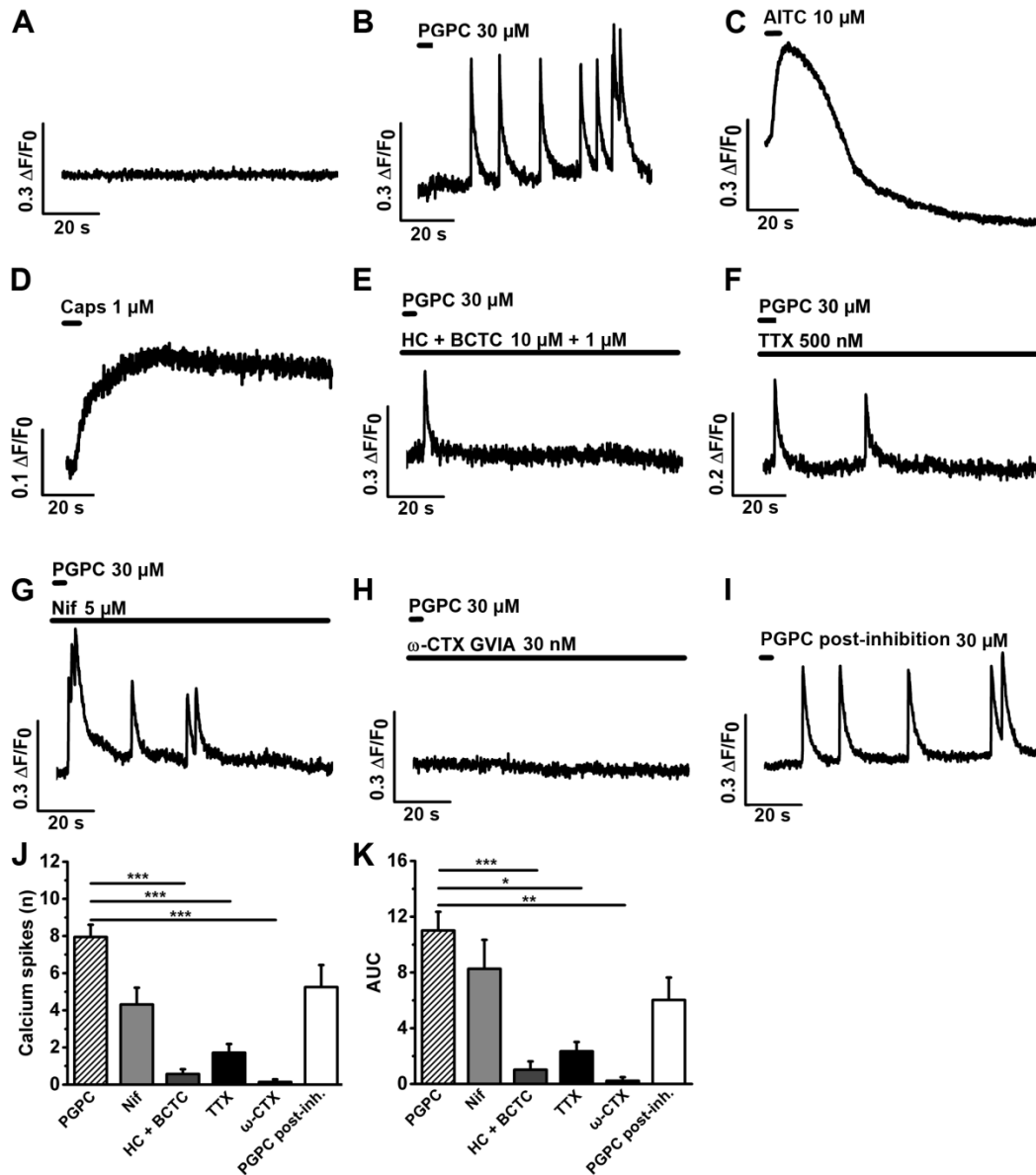
Figure 30: PGPC-induced calcium spike behavior is reduced by HC-030331 and BCTC, tetrodotoxin, and ω-conotoxin. (A) Representative calcium imaging trace of unstimulated DRG neurons. **(B-D)** Representative traces of calcium spike responses after local stimulation of either PGPC (30 µM, in B), AITC (10 µM, in C) or capsaicin (1 µM, in D). **(E-H)** Calcium traces of PGPC treated DRG neurons in presence of the prototypical inhibitors of TRPA1 and TRPV1 (both 10 µM HC-030331 and 1 µM BCTC, E), TTX (500 nM, F) to block TTX-sensitive voltage-gated sodium channels, nifedipine (5 µM, G) to inhibit L-type voltage-gated calcium channels or ω-CTX (GVIA, 30 nM, H). **(I)** Representative PGPC-induced calcium responses after washout of ω-CTX for 30 min. **(J)** Number of PGPC-induced calcium spikes under indicated conditions. **(K)** Analysis of the area under curve (AUC) of PGPC-induced calcium responses under indicated conditions. (J and K: PGPC: n = 70 cells; PGPC + HC-030331 + BCTC: n = 21; PGPC + TTX: n = 8; PGPC + nifedipine: n = 14; PGPC + ω-CTX (GVIA): n = 8. PGPC post-inhibition with ω-CTX: n = 8. Cells prepared from 3 mice; mean ± SEM; One-way ANOVA post hoc Holm-Sidak; ***p<0.001, **p<0.01; ***p<0.001; modified after Martin et al., 2018).

For further analysis of the dependency of PGPC-induced calcium spike behavior on voltage-gated calcium channels, DRG neurons were stimulated with an application pipette containing 30 µM PGPC (Fig. 30). To exclude spontaneous calcium spike activity, cells were imaged without stimulation before each experiment. Here, no activity was observed (Fig. 30 A). The local stimulation with PGPC triggered typical calcium spikes with a fast onset. PGPC-induced repetitive calcium spike signals were observed for a few tens of seconds (Fig. 33 B). Stimulation with the prototypical agonists of TRPA1 (AITC, 10 µM) and TRPV1 (Capsaicin, 1 µM) resulted in a calcium transient with a slow onset (Fig. 30 C, D). In case of AITC, a slowly decaying signal was observed. In contrast, capsaicin induced a long-lasting calcium transient in the neurons.

When a combination of TRPA1 (HC-030031, 10 µM) and TRPV1 (BCTC, 1 µM) antagonists was used, the number of calcium spikes induced by PGPC was diminished (Fig. 30 E-K). PGPC-induced calcium spikes were also inhibited in the presence of TTX and ω-conotoxin, a blocker of the high-voltage activated calcium channel $Ca_V2.2$ (30 mM, N-type; Catterall et al., 2005). The prototypical L-type Ca_V-channel blocker nifedipine (5 µM) failed to inhibit the PGPC-induced calcium spikes (Fig. 30 G-K). PGPC induced the calcium spike behavior in the stimulated neurons as well after a washout period of 30 min (Fig. 30 I-K). However, the recovery from CTX inhibition was not complete and the PGPC-stimulus was less efficient (t-test PGPC before inhibition versus PGPC post-inhibition: $p = 0.013$; (Martin et al., 2018). To sum it up, these experiments reveal the ability of PGPC to induce repetitive firing of voltage-dependent calcium spikes in a considerable proportion of DRG neurons.

4.10. OxPAPC increases the excitability of DRG neurons

In consideration of the enhanced TRP channel-mediated, spike-like calcium transients in DRG neurons caused by OxPL stimulation and considering that OxPL are produced as endogenous products during inflammation, the influence of OxPL on neuronal excitability was examined. For this, voltage- and current-clamp measurements of DRG-neurons were performed in *whole-cell* configuration under physiological conditions, at RT. The addition of OxPL occurred via an application pipette close to the cell with a pressure of 0.2 bar and an application time of 500 ms. Trains of action potentials were recorded from individual DRG neurons before and after focal and acute application of OxPL. Initially, the frequency of action potential firing of DRG neurons was investigated by eliciting repetitive action potentials with increasing current injections from 0 to 140 pA for a time period of one second subsequently followed by OxPAPC application in voltage-clamp modus at -60 mV for 60 seconds. Afterwards, potential changes of action potential frequency were recorded with increasing current injections from 0 to 140 pA for a time period of one second.
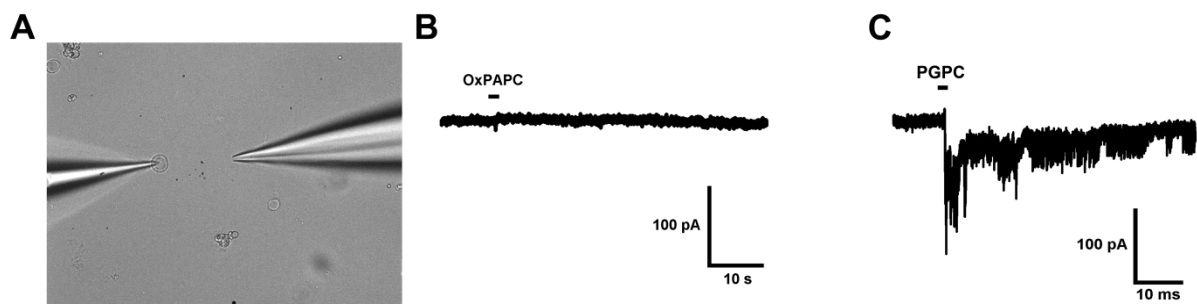
Figure 31: Acute OxPL stimuli induce only small inward currents in DRG neurons. (A) Exemplary image of the application of OxPL during electrophysiological measurements. On the left, the patch clamp pipette with the intracellular solution is seen. On the right, the application pipette is displayed. Representative inward currents are shown after stimulation of small-diameter DRG neurons with **(B)** 30 µM OxPAPC or **(C)** 30 µM PGPC at -60 mV. All measurements were done in *whole-cell* configuration in external bath solution.

OxPAPC induced no significant current induction when measured at -60 mV, while PGPC induced a small current (Fig. 31 B, C). To exclude the possibility that activation of pressure sensitive channels in the DRG neurons is caused by the pressure-assisted application method, control measurements were done by application of external bath solution to the neurons. Here, no increase in the action potential frequency was observed (Fig. 32).
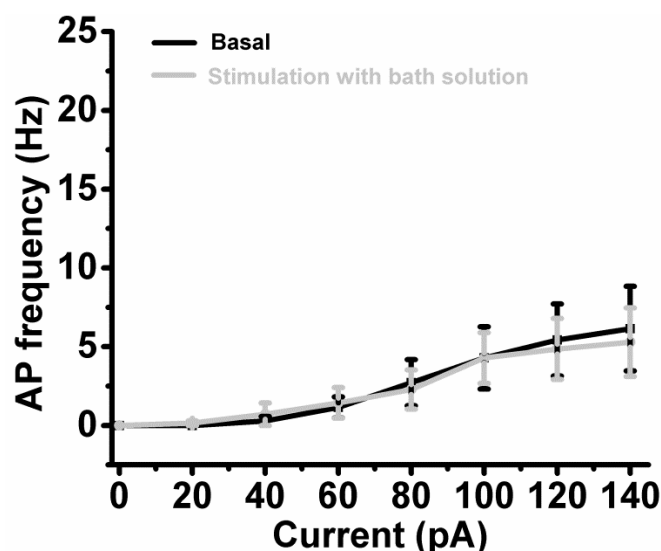
Figure 32: Stimulation with bath solution does not induce action potential firing in small-diameter sensory neurons. Bath solution was locally applied and currents were injected from 0 to 140 pA using 20 pA steps. The AP frequency was plotted against the time displaying basal and bath solution stimulated cells in comparison.

Table 6: Action potential frequency before (Basal) and after OxPAPC addition.

Current (pA)	Basal (n=6)	OxPAPC (n=6)
0	0 ± 0	0 ± 0
20	0 ± 0	1 ± 0.45
40	0.17 ± 0.17	3.67 ± 1.2
60	0.5 ± 0.5	6.17 ± 1.3
80	2.33 ± 1.41	8 ± 1.34
100	3.83 ± 1.78	9.67 ± 1.58
120	5.33 ± 2.16	12.33 ± 2.19
140	6.17 ± 2.23	14.67 ± 2.85

The frequency of action potential firing was significantly increased in OxPAPC stimulated neurons (table 6; e.g. at 80 pA current injection, OxPAPC; 8 APs ± 1.34, Fig. 33 B, C compared to basal measurements; 2.33 APs ± 1.41). Hereby, the curve progression shows a linear trend. The AP frequency of control and after OxPAPC stimulation conditions assimilates when pre-stimulated with a current of 120 pA or more (Fig. 33 C).

In summary, the OxPL compound mixture increases the excitability of DRG neurons, as indicated by an increased ease to fire action potentials upon moderate current injections.
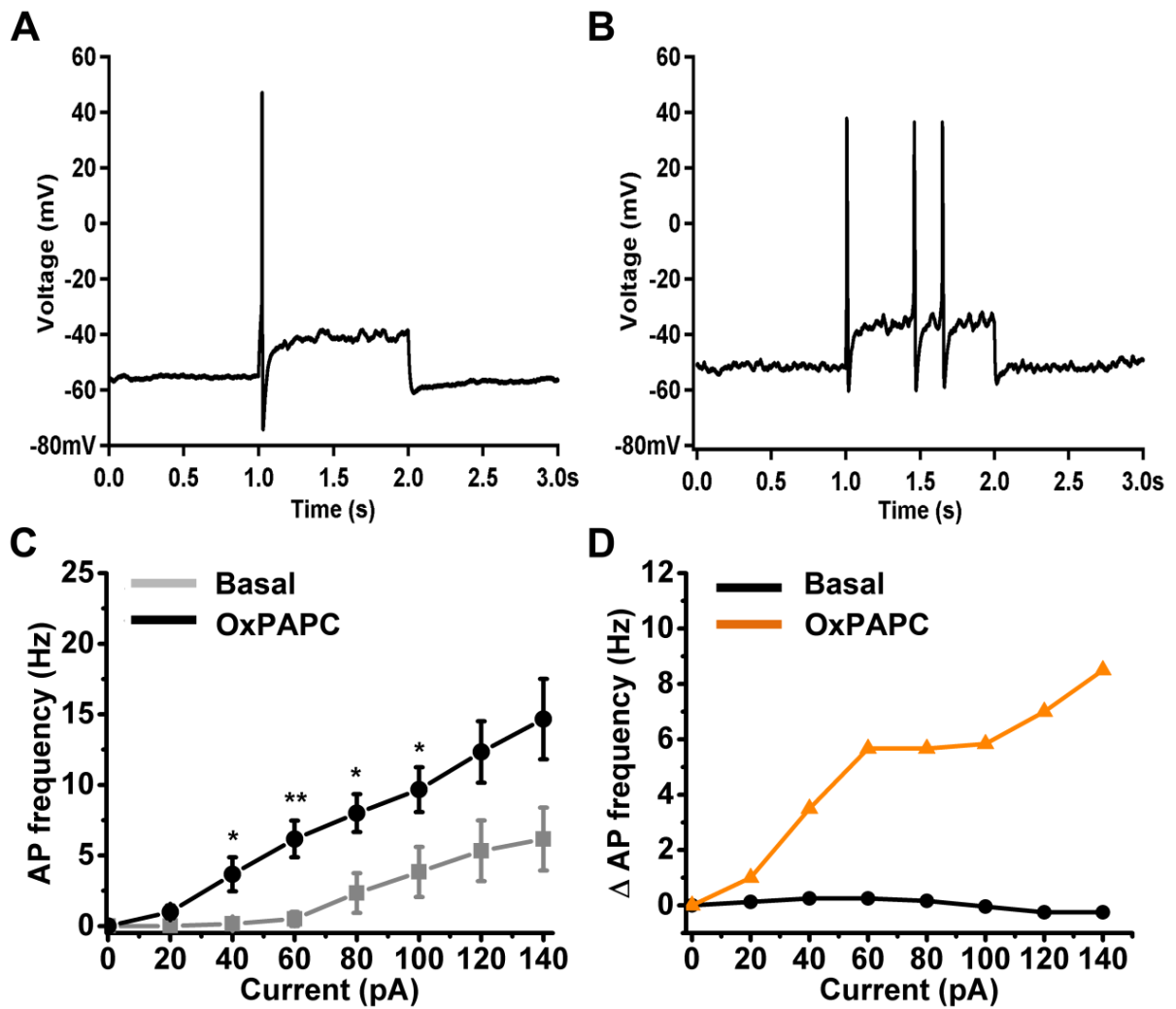
Figure 33: The OxPL mixture OxPAPC enhances the excitability of DRG neurons. (A) Representative train of action potentials, recorded from a murine DRG neuron in response to a 1 s current injection of 80 pA at rest (Basal, A) and after fast-pressure application of 30 µM OxPAPC **(B)**. **(C)** Action potential frequency obtained from experiments as shown in A and B before (Basal) and after OxPAPC (30 µM) stimulation as a function of injected current. **(D)** Changes of the firing frequency of DRG neurons (ΔAP frequency) induced by stimulation with 30 µM OxPAPC compared to the basal firing frequency (n = 6 from 4 mice; paired t-test; *$p < 0.05$; **$p < 0.001$). Lines connect data points; modified after Martin et al., 2018.

4.11. PGPC enhances excitability of DRG neurons

OxPAPC consists of a mixture of oxidized phospholipids, including POVPC and PGPC. Their precise composition depends on the level of PAPC oxidation and different products display different biological activities. In earlier results (Fig. 13; Fig 31) it was shown that PGPC induces long-lasting inward currents in both HEK293 cells stably expressing TRPA1 (Oehler et al., 2017) and DRG neurons. In order to test whether PGPC influences the action potential frequency, current clamp experiments were performed in DRG neurons.
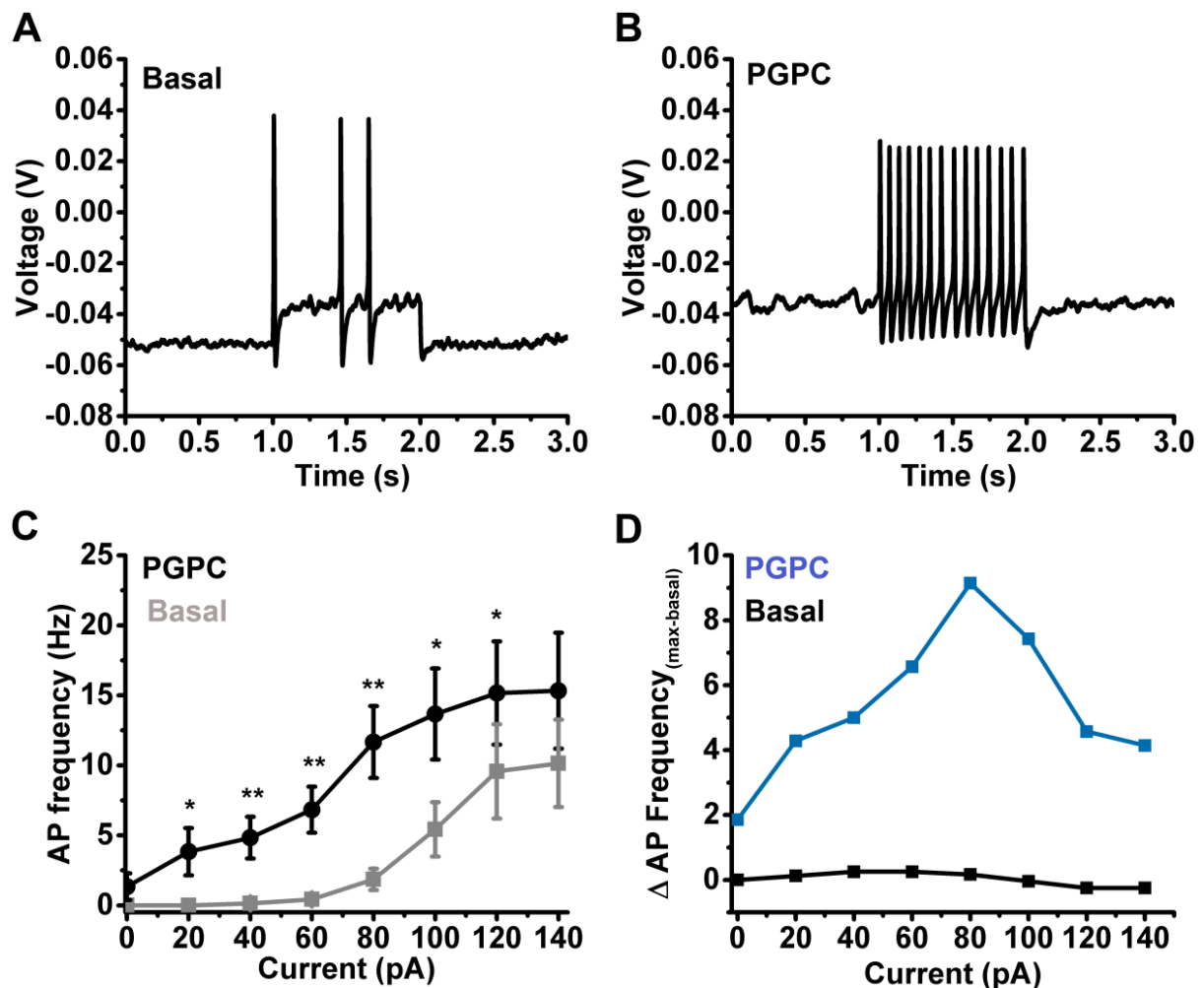
Figure 34: PGPC enhances the excitability of DRG neuron. (A) Representative trains of action potentials, recorded from murine DRG neurons in response to 1 s current injections of 80 pA before (A, Basal) and after (**B**, PGPC) application of PGPC. In **(C)** the action potential firing rate is displayed as a function of increased current injections. In **(D)** the difference of action potential frequency either before (black) or after PGPC stimulation (blue) are displayed. n=7; Data points represent mean values and significance between pairs of data was tested with a one-way ANOVA (*p<0.05; **p<0.001; Holm-Sidak; modified after Martin et al., 2018).

The addition of 30 µM PGPC was performed as described earlier. Compared to measurements under non-stimulated conditions, action potential firing frequency significantly increased at low current injections until they reached the maximal AP firing rate at 80 pA (Fig. 34 D). The curve progression shows a sigmoidal trend. The basal and PGPC-stimulated AP frequency assimilates when stimulated with 140 pA (Fig. 34 C).

Table 7: Action potential frequency before and after PGPC stimulation.

Current (pA)	Basal (n=7)	PGPC (n=7)
0	0 ± 0	1.86 ± 0.96
20	0 ± 0	4.29 ± 1.49
40	0.14 ± 1.4	5.14 ± 1.3
60	0.43 ± 0.2	7 ± 1.4
80	1.86 ± 0.77	11 ± 2.27
100	5.43 ± 1.94	12.86 ± 2.87
120	9.57 ± 3.37	14.14 ± 3.28
140	10.14 ± 3.13	14.29 ± 3.66
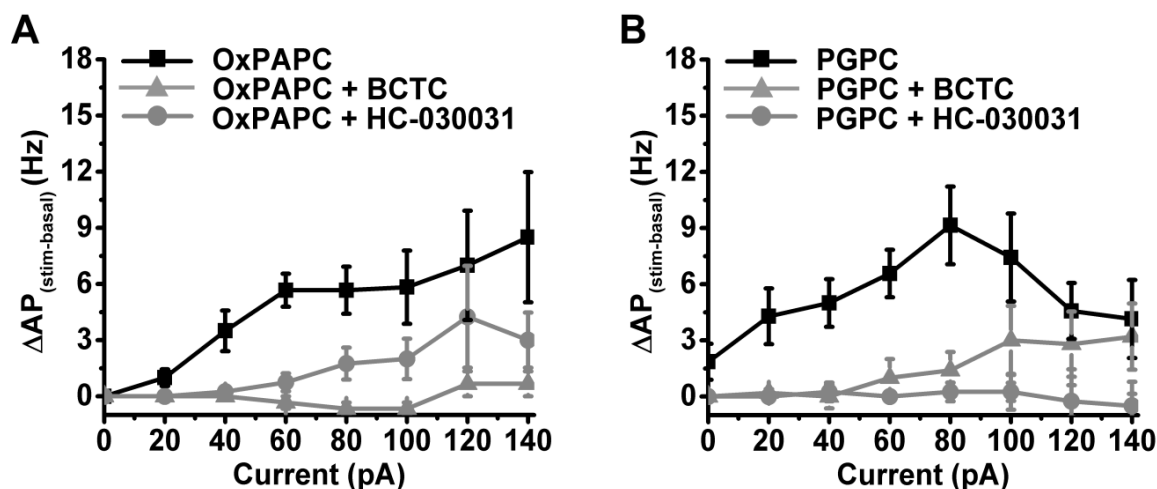
Figure 35: Inhibitors of TRPA1 and TRPV1 reduce OxPL-induced excitability. (A) Changes of the firing frequency of DRG neurons, $\Delta AP_{(stim-basal)}$, induced by stimulation with 30 µM OxPAPC in absence (OxPAPC) or presence of either 1 µM of the TRPV1 inhibitor BCTC or 10 µM of the TRPA1 inhibitor HC-030031 (10 µM; n = 3-6 from 3 mice; mean ± SEM; One-way ANOVA post hoc Holm-Sidak). **(B)** Changes of the firing frequency of DRG neurons, $\Delta AP_{(stim-basal)}$, induced by application of 30 µM PGPC in absence (PGPC) or presence of either 1 µM of the TRPV1 inhibitor BCTC or 10 µM of the TRPA1 inhibitor HC-030031 (n = 4-7 from 3 mice; mean ± SEM; One-way ANOVA post hoc Holm-Sidak; p-values s. table 8; modified after Martin et al., 2018).

OxPAPC and PGPC induced a current-dependent increase in the AP frequency and this increase was reduced by the TRPV1 inhibitor BCTC and the TRPA1 inhibitor HC-030031 (Fig. 35 A, B).

It was shown that PGPC serves as prototypical OxPL to ease excitability of primary DRG neurons upon current injection. This effect is reduced in presence of TRPA1 and TRPV1 inhibitors.

Table 8: Statistics of the difference of basal and PGPC respectively OxPAPC induced AP frequency ($\Delta AP_{(stim-basal)}$) as displayed in Figure 35 (modified after modified after Martin et al., 2018).

	PGPC	F-value	p-value	OxPAPC	F-value	p-value
0 pA	PGPC + HC-030031	F(2,15)=2.27	0.090*	OxPAPC + HC-030031	F(2, 12)=2.69	1
	PGPC + BCTC		0.11	OxPAPC + BCTC		1
	HC -030031+ BCTC		1	HC-030031 + BCTC		1
20 pA	PGPC + HC-030032	F(2,15)=4.74	0.022*	OxPAPC + HC-030031	F(2,12)=5.04	0.073
	PGPC + BCTC		0.025*	OxPAPC + BCTC		0.098
	HC -030031+ BCTC		0.91	HC-030031 + BCTC		1
40 pA	PGPC + HC-030033	F(2,15)=7.98	0.0038**	OxPAPC + HC-030031	F(2,12)=17.86	0.025*
	PGPC + BCTC		0.0081**	OxPAPC + BCTC		0.027*
	HC -030031+ BCTC		0.88	HC-030031 + BCTC		0.87
60 pA	PGPC + HC-030034	F(2,15)=10.73	0.0014**	OxPAPC + HC-030031	F(2,12)=17.86	0.00041***
	PGPC + BCTC		0.0029**	OxPAPC + BCTC		0.0009***
	HC -030031+ BCTC		0.58	HC-030031 + BCTC		0.41
80 pA	PGPC + HC-030035	F(2,15)=8.78	0.0032**	OxPAPC + HC-030031	F(2,12)=7.86	0.0037**
	PGPC + BCTC		0.0051**	OxPAPC + BCTC		0.029*
	HC -030031+ BCTC		0.67	HC-030031 + BCTC		0.21
100 pA	PGPC + HC-030036	F(2,15)=3.06	0.034*	OxPAPC + HC-030031	F(2,12)=3.56	0.029*
	PGPC + BCTC		0.14	OxPAPC + BCTC		0.13
	HC -030031+ BCTC		0.41	HC-030031 + BCTC		0.35
120 pA	PGPC + HC-030037	F(2,15)=2.36	0.049*	OxPAPC + HC-030031	F(2,12)=1.17	0.16
	PGPC + BCTC		0.22	OxPAPC + BCTC		0.45
	HC -030031+ BCTC		0.41	HC-030031 + BCTC		0.49
140 pA	PGPC + HC-030037	F(2, 15)=1.47	0.12	OxPAPC + HC-030031	F(2,12)=1.86	0.1
	PGPC + BCTC		0.23	OxPAPC + BCTC		0.2
	HC -030031+ BCTC		0.72	HC-030031 + BCTC		0.64

4.12. The role of Nav1.9 in OxPL-induced activation

The above described data raised the question, how the rather small excitatory action of OxPL can explain the rather strong pain-inducing function of OxPL *in vivo* (Oehler et al., 2017). This suggests that other ion channels contribute to the excitatory function of OxPL responses. Therefore, it was asked whether Na$_V$1.9, a voltage-gated sodium channel involved in DRG excitability and nociception (Baker et al., 2003; Maingret et al., 2008; Leipold et al., 2013; Leipold et al., 2015) is required as an amplifier for the OxPL-induced TRP responses. For this, primary neurons were prepared from a Na$_V$1.9 knockout mouse model (Östman et al., 2008) and it was tested whether Na$_V$1.9 deletion affects OxPL-induced action potential firing.
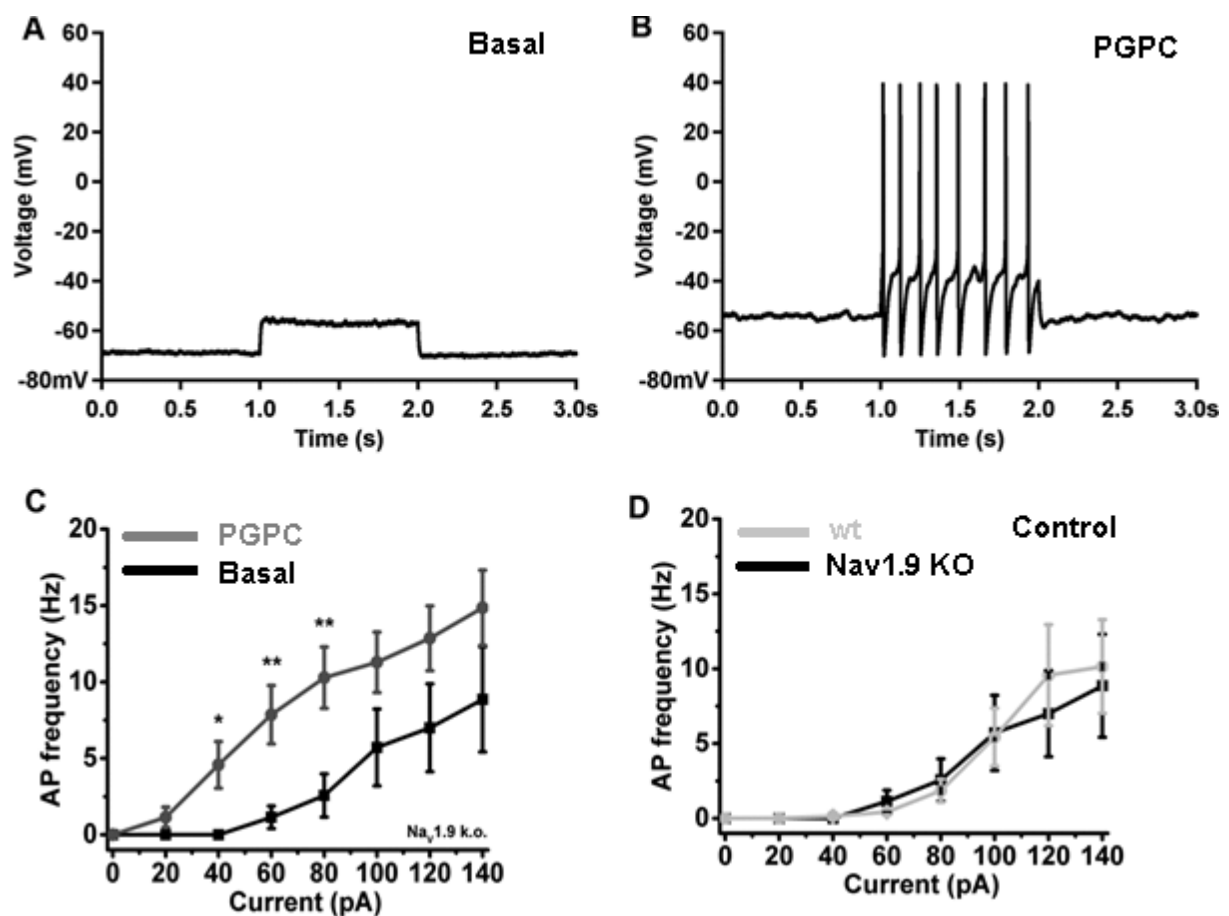
Figure 36: Na$_V$1.9, a DRG exciter, does not mediate OxPL induced pain. (A) Representative trains of action potentials, recorded from murine Na$_V$1.9 KO DRG neurons in response to 1 s current injections of 80 pA. **(B)** Frequency of the action potential firing rate after PGPC stimulation via application. In **(C)** the action potential firing rate is displayed as a function of increased current injections. In **(D)** the frequency of the action potential firing rate of Na$_V$1.9 KO DRG neurons is displayed in comparison to the wt control. Data points represent mean values and significance between pairs of data was tested with a one-way ANOVA (*p<0.05; **p<0.01; Holm-Sidak; modified after Martin et al., 2018).

In comparison to unstimulated cells (2.57 APs ± 1.41, 80 pA), PGPC induced an increase in the action potential firing frequency in $Na_V1.9$ k.o. DRG neurons (10.29 APs ± 2.01, at 80 pA current injection, Fig. 36 A-C). In this set of experiments, wildtypic and $Na_V1.9$-deficient neurons could not be distinguished in their responsiveness to a PGPC stimulus. Hereby, the curve progression retains the sigmoidal trend, which was also seen in the experiments with wildtypic DRG neurons and the frequency seen in the unstimulated $Na_V1.9$ KO neurons (5.71 APs ± 2.51) assimilates to PGPC stimulation measurements (11.29 APs ± 1.98) after current injection of 100 pA or more (Fig. 36 C). This suggests that $Na_V1.9$ is not an amplifier of PGPC-induced TRP responses in nociceptors, at least under steady state conditions.

4.13. Inflammatory mediators potentiate PGPC-induced stimuli

To address whether inflammatory mediators can affect OxPL stimulation, DRG neurons were treated with an inflammatory soup containing 5 nM bradykinin (BK), 100 nM histamine and 50 nM PGE_2. Ratiometric calcium imaging was performed on the neurons. As OxPL are generated under inflammatory conditions (Oehler et al., 2017), they would act together with other inflammatory mediators on DRG neurons (Baker et al., 2003). To test the impact of PGPC after treatment with single inflammatory mediators, primary DRG neurons were also exposed to BK or Forskolin (Forsk). Forskolin is a diterpene directly activating the adenylyl cyclase (Seamon et al., 1981). BK is an inflammatory peptide released from damaged tissue during inflammation or injury (Edery and Lewis, 1962; Hargreaves et al., 1988). It acts as an inflammation mediator on Bradykinin receptor 1 and furthermore as an exciter of sensory neurons (Levine et al. 1993 and Couture et al. 2001). First the effect of inflammatory soup on the PGPC response was investigated. When compared to measurements done under control conditions without inflammatory mediators (Fig. 37 A), PGPC stimulation led to an increased influx of calcium ions after treatment with inflammatory soup (Fig. 37 D). Both, the AUC (102.93 ± 24.43; Fig. 37 E) and the percentage of reacting neurons (62.11 % ± 9.38; Fig. 37 F) represent an increased responsiveness to PGPC under inflammatory conditions, compared to control, steady-state conditions (17 ± 4.66; 14.57 % ± 2.5). Pretreatment with BK resulted in an increased influx of Ca^{2+} into DRG neurons after stimulation with PGPC (Fig. 37 C). Both, the AUC (69.40 ± 22.00; Fig. 37) and the number of reactive neurons (38.7 % ± 8.11; Fig. 37 B) verified an increased stimulation potency of the OxPL compound PGPC after BK treatment. Pretreatment with Forskolin also increased the PGPC-responsiveness of DRG neurons (Fig. 37 D). Both, the AUC (56.06 ± 15.56; Fig. 37 A) and the number of PGPC-positive neurons (27.61 % ± 6.85, Fig. 37 B) are increased by Forskolin. In summary, inflammatory mediators potentiate the OxPL-induced activation of DRG neurons.
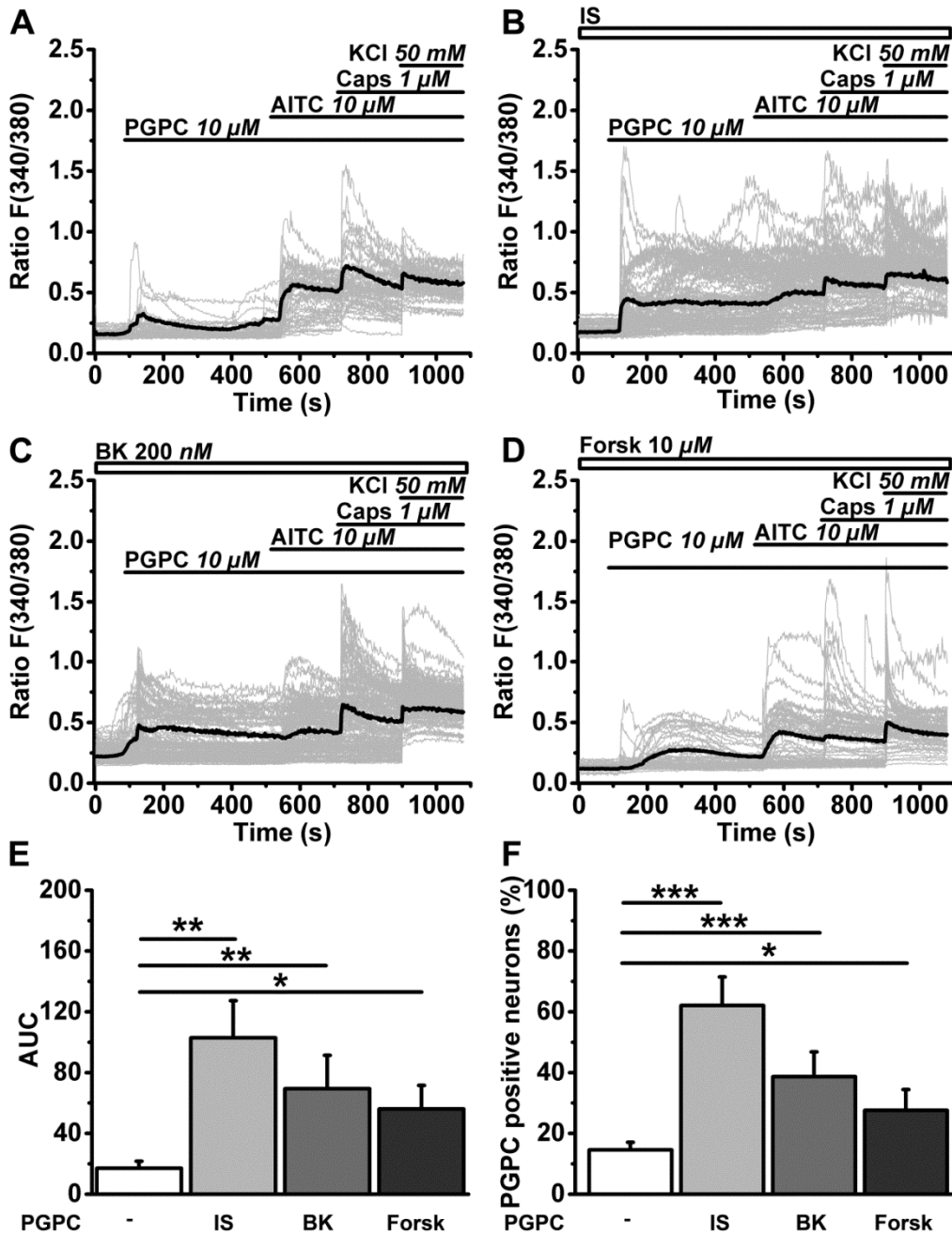
Figure 37: Inflammatory mediators promote OxPL-induced activation. (A) Relative changes in $(Ca^{2+})_i$ in wild-type DRG neurons loaded with Fura-2-AM, expressed as florescence ratio F(340/380) as a function of time. Application of agonists PGPC (10 µM), AITC (10 µM), Caps (1 µM) and KCl (50 mM) are indicated with horizontal bars. Grey traces are calcium responses of 50 individual cells; the black trace represents the mean response of al experiments. **(B, C, D)** Identical experiments as shown in A, but after preincubation of cells with either Inflammatory soup (IS, B), Bradykinin (BK, C), Forskolin (Forsk, D). **(E)** Integrated calcium responses from experiments shown in A-D (n = 6-8 from 3 mice; mean ± SEM; One-way ANOVA post hoc Holm-Sidak; $F_{(3,26)}$ = 3.84; *p = 0.045; **p = 0.0029). **(F)** The percentage of neurons reacting to PGPC stimulation following treatment with inflammatory mediators (n = 6-8 from 3 mice; mean ± SEM; One-way ANOVA post hoc Holm-Sidak; $F_{(3,26)}$ = 15.45; *p<0.05; **p<0.001; Martin et al., 2018)(Martin et al., 2018).

4.14. Inflammatory mediators recruit Na$_V$1.9 to potentiate the OxPL function

As an enhanced OxPL-function in the presence of inflammatory mediators was obvious, it was asked whether Na$_V$1.9 needs this condition to influence the action potential frequency in DRG neurons in response to an OxPL stimulus. Recent studies suggest Na$_V$1.9 as the driving force of action potential firing under inflammatory conditions as it is responsible for persistent sodium currents in DRG neurons. These can be increased by intracellular GTP or by non-hydrolysable GTP analogs (Baker et al., 2003; Östmann et al., 2008). Additionally, an exogenously applied inflammatory soup is able to rapidly potentiate Na$_V$1.9 channel activity to increase AP firing in response to appropriate electrical stimulation (Maingret et al., 2008). In order to examine the role of Na$_V$1.9 in PGPC-induced activation of nociceptors during long term exposure to inflammatory mediators, *whole-cell* patch-clamp measurements were performed on DRG neurons. Compared to measurements under control conditions without inflammatory mediators (Fig. 38 A), PGPC stimulation of wt DRG neurons leads to a potentiated action potential frequency after treatment with inflammatory soup (Fig. 38 A). Hereby, the effect of PGPC-induced firing is significantly increased. This effect was fully lost in Na$_V$1.9-deficient neurons (Fig. 38). Furthermore, the resting membrane potential of DRG neurons was compared between DRG neurons pretreated with IS and those incubated in medium alone. While there was no significant difference in the resting membrane potential (RMP) in neither wt nor Na$_V$1.9 k.o. neurons, the inflammatory soup caused an increased RMP of both wt and Na$_V$1.9 k.o. neurons. However, this effect was much stronger in wildtypic DRG neurons, indicating that Na$_V$1.9 has a role in the modulation of the threshold of the membrane potential under inflammatory conditions.

In the past, Na$_V$1.9 has been shown to induce cell-autonomous calcium spikes in growth cones and somata of primary motoneurons, which is persistent with the hypothesis that the persistent sodium currents driven by Na$_V$1.9 trigger a local excitation cascade (Subramanian et al., 2012; Wetzel et al., 2013). This results in calcium spikes driven by voltage-activated calcium channels (Wetzel et al., 2013). In theory, when local PGPC-stimulation induces receptor potentials, the persistent sodium current by Na$_V$1.9 should be able to drive repetitive calcium spikes. In order to test this theory, PGPC-induced calcium signals were measured with fast calcium imaging and wildtypic and Na$_V$1.9 KO DRG neuron responses with or without treatment with inflammatory mediators were compared (Fig. 39). Pseudo colored images represent a calcium imaging series of DRG neurons loaded with OGB (Fig. 39 A). Wildtypic small-diameter neurons responded with an enhanced number of calcium spikes upon treatment with inflammatory mediators (Fig. 39 A, B, D). On the contrary, the inflammatory-mediator dependent elevation in calcium spike frequency was fully lost in Na$_V$1.9 KO neurons (Fig. 39 F).
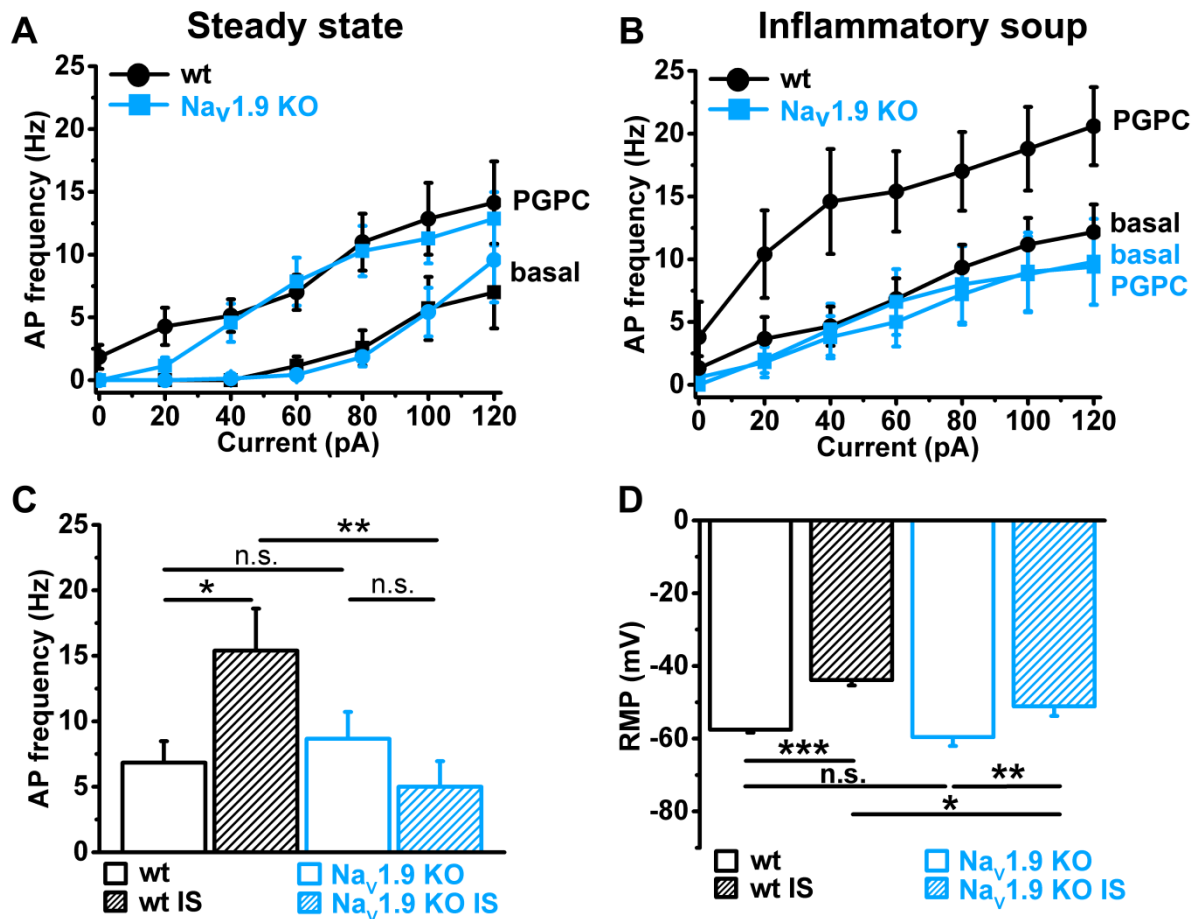
Figure 38: Inflammatory mediators recruit Na$_V$1.9 to potentiate OxPL function. (A) Frequency of action potential firing of wild-type and Na$_V$1.9 KO neurons in response to variable current injections ranging from 0 to120 pA before (Basal) and after stimulation with 30 µM PGPC under steady state conditions (mean ± SEM; *n* = 7 from 6 mice; statistics see table 3). **(B)** Action potential frequencies of wild-type (black lines) and Na$_V$1.9 KO DRG (blue lines) in response to variable current injections before (basal) and after application of 30 µM PGPC and pretreatment with inflammatory soup (*n* = 5 from 5 mice (wild-type); *n* = 5 from 3 mice (Na$_V$1.9 KO); mean ± SEM; statistics see table 3). **(C)** Frequency of action potentials obtained during 60 pA current injections for 1 s from wild-type (black lines) and Na$_V$1.9 KO DRG (blue lines) neurons after PGPC application without or with pretreatment of cells with inflammatory soup (IS; *n* = 5-7 of 3 mice; mean ± SEM; one-way ANOVA; post hoc Holm-Sidak; $F_{(3,21)}$ = 3.86; *p=0.014; **p=0.0054). **(D)** Resting membrane potential (RMP) of wild-type and Na$_V$1.9 KO DRG neurons obtained under either steady state conditions (wt: *n* = 19; Na$_V$1.9 KO: *n* = 12) or after pretreatment with inflammatory soup (wt: *n* = 8; Na$_V$1.9 KO *n* = 9; mean ± SEM; one-way ANOVA; post hoc Holm-Sidak; $F_{(3, 46)}$ = 13.34; *p<0.019; **p=0.0029; ***p=3.95E-06; modified after Martin et al., 2018).

Table 9: Statistics of wt and Na$_V$1.9 KO DRG neurons stimulated either with PGPC or PGPC and inflammatory soup (IS) as displayed in figure 38 (adapted after Martin et al., 2018).

		0 pA	20 pA	40 pA	60 pA
<u>Steady state</u>	<u>Steady state</u>	$F_{(3, 27)}=3.73$	$F_{(3, 27)}=6.14$	$F_{(3, 27)}=7.67$	$F_{(3, 27)}=9.66$
Basal wt	**PGPC wt**	0.012*	0.0011**	0.0018**	0.00083***
Basal wt	**Basal Na$_V$1.9 KO**	1	1	0.92	0.69
Basal Na$_V$1.9 KO	**PGPC Na$_V$1.9 KO**	0.012*	0.012*	0.0037**	0.001**
PGPC wt	**PGPC Na$_V$1.9 KO**	1	0.33	0.69	0.63
<u>IS</u>	<u>IS</u>	$F_{(3,20)}=1.23$	$F_{(3,20)}=3.62$	$F_{(3,20)}=4.07$	$F_{(3,20)}=3.79$
Basal wt	**PGPC wt**	0.24	0.032*	0.012*	0.020*
Basal wt	**Basal Na$_V$1.9 KO**	0.52	0.53	0.81	0.58
Basal Na$_V$1.9 KO	**PGPC Na$_V$1.9 KO**	0.78	0.95	0.94	0.94
PGPC wt	**PGPC Na$_V$1.9 KO**	0.15	0.013*	0.011*	0.018*
		80 pA	**100 pA**	**120 pA**	
<u>Steady state</u>	<u>Steady state</u>	$F_{(3, 27)}=8.11$	$F_{(3, 27)}=2.61$	$F_{(3, 27)}=1.20$	
Basal wt	**PGPC wt**	0.002**	0.042*	0.17	
Basal wt	**Basal Na$_V$1.9 KO**	0.77	0.93	0.76	
Basal Na$_V$1.9 KO	**PGPC Na$_V$1.9 KO**	0.002**	0.092	0.29	
PGPC wt	**PGPC Na$_V$1.9 KO**	0.77	0.64	0.54	
<u>IS</u>	<u>IS</u>	$F_{(3,20)}=2.89$	$F_{(3,20)}=2.55$	$F_{(3,20)}=3.065$	
Basal wt	**PGPC wt**	0.047*	0.072	0.052	
Basal wt	**Basal Na$_V$1.9 KO**	0.56	0.56	0.5	
Basal Na$_V$1.9 KO	**PGPC Na$_V$1.9 KO**	0.83	0.96	0.93	
PGPC wt	**PGPC Na$_V$1.9 KO**	0.028*	0.031*	0.02*	

Consistently, only small diameter DRG neurons were affected by PGPC. As the calcium spikes correlated with the acute, local PGPC stimulation, the stimulus was needed to induce spiking behavior of the DRG neurons. Notably, a pretreatment with inflammatory mediators alone was not sufficient to drive a long-lasting or permanent spike behavior of the small-diameter neurons (Martin et al., 2018).

In summary, these results indicate that in the presence of inflammatory mediators Na$_V$1.9 potentiates OxPL responses. Na$_V$1.9 seems to contribute to an increased RMP under inflammatory conditions, indicating that a persistent inward current by Na$_V$1.9 mediates an increased excitability under inflammatory conditions. Thus, the channel contributes to an increased responsiveness of an acute TRP-mediated, PGPC-induced inward current.
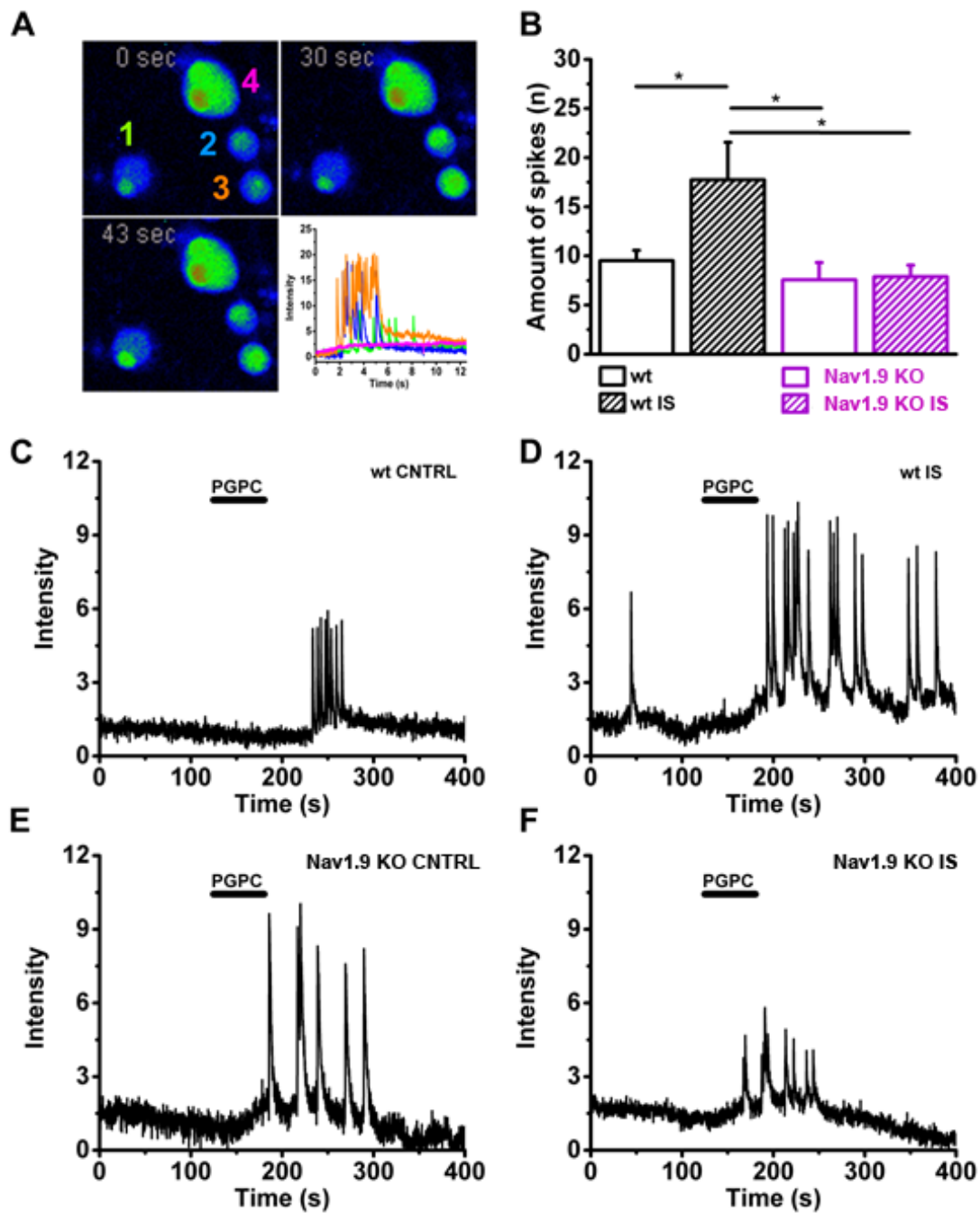
Figure 39: Inflammatory mediators enhance PGPC-induced and Na$_V$1.9 dependent calcium spikes in DRG neurons. (A) Pseudo colored images representing a calcium imaging series of DRG neurons loaded with OGB. Calcium evoked spiking of DRG neurons after preincubation with inflammatory mediators and after stimulation with PGPC (10 µM; 30 s, 43 s) are displayed in comparison to the start situation (0 sec). The reaction of the four appropriate cells imaged in the experiment is shown on the lower right. **(B)** Single calcium traces of the cells stimulated with PGPC monitored in (A). **(C)** Spiking behavior of wt DRG neurons after pretreatment with inflammatory mediators and stimulation with PGPC. **(D)** Comparison between the number of spikes between inflammatory mediator treated and non-treated DRG neurons as well as between wt and Na$_V$1.9 KO neurons. (n=9-35; n=5; mean ± SEM; Two-way-ANOVA, Holm-Sidak; *p<0.05; **p<0.001; ***p<0.0001; modified after Martin et al., 2018).

5 Discussion

Pain is an important protective mechanism of the body to ensure survival (Dubin and Patapoutian, 2010). Hereby, inflammatory pain is the crucial response mechanism to restore homeostasis after tissue damage by trauma or environmental agents (Viana, 2016). A broad range of mechanisms occur during inflammatory pain, including immune cell infiltration into the damaged area and the activation of various receptors and ion channels by inflammatory mediators to trigger the healing process. Frequently, inflammatory pain is accompanied by allodynia and hypersensitivity which causes pain by contact with harmless stimuli (Serhan, 2010). Typical therapeutics to treat inflammatory pain are non-steroidal anti-inflammatory drugs (NSAID). Non-steroidal anti-inflammatory drugs target enzymes responsible for the formation of prostaglandins. Therapeutics such as Aspirin or Ibuprofen are among the most widely used painkillers worldwide. Despite their unequivocal effectiveness, NSAIDs are also responsible for serious side effects such as gastric bleeding, renal failure or heart attacks. This restricts the use of NSAIDs indicating the need for alternative treatment options (Trelle et al., 2011; Sudano et al., 2012). In order to develop new therapeutic approaches, it is necessary to better understand the molecular mechanisms underlying nociception leading to inflammatory pain.

The major components of cellular membranes and lipoproteins are phospholipids (Singer and Nicolson, 1972). During inflammatory processes phagocytes produce ROS, which can oxidize phospholipids. Subsequent chemical reactions can lead to the formation of a variety of OxPL substances including the OxPL metabolites OxPAPC, PGPC, POVPC and PEIPC (Freigang, 2016). OxPL have a role in atherosclerosis, sepsis, acute lung injury and even Parkinson's or Alzheimer's (Furnkranz et al., 2005; Usui et al., 2009). In two recent studies, experimental evidence was found that oxidized phospholipids (OxPL) are generated in inflamed paw tissue (Liu et al., 2016; Oehler et al., 2017), suggesting OxPL as a potential target candidate for the treatment of inflammatory pain. With the help of electrophysiological and calcium imaging techniques it is shown in this thesis, that OxPL induce activation of TRPA1 and TRPV1 in small-diameter DRG neurons (Oehler et al., 2017) an effect which is potentiated after pretreatment of DRG neurons with inflammatory mediators (Martin et al., 2018). It is also shown that inflammatory mediators potentiate the responsiveness of small sensory neurons to oxidized phospholipids. Notably, this effect is mediated by the sodium channel $Na_V1.9$, which behaves like a switch to mediate between resting or inflamed conditions. This is of high clinical relevance, because blocking oxidized phospholipid-mediated TRP channel activation can efficiently treat acute and chronic inflammatory pain, as our research group could identify in the course of this study (Oehler et al., 2017).

Furthermore, since human Na$_V$1.9 has been shown to mediate painful and painless channelopathies (Leipold et al., 2013; Zhang et al., 2013; Huang et al., 2014, 2017; Woods et al., 2014; Han et al., 2015), this study provides new insights into the mechanism by which NaV1.9 amplifies stimuli of endogenous irritants under inflammatory conditions.

5.1. Primary DRG neurons are a useful model system for investigations on the molecular mechanism of inflammatory pain

In this thesis, primary DRG neurons from adult C57BL/6Jmice (Doppler et al., 2016) were used for investigations of the novel inflammation mediator OxPL. As the expression profile of important pain-mediating receptors changes during development (McMahon et al., 1994), primary DRG neurons were prepared from adult mice. Adult rodents are also used in pain behaviour experiments and therefore one can expect a better correlation between the results obtained in vitro versus in vivo. Our DRG cultures were confirmed to express the critical OxPL target channels TRPV1 and TRPA1 and we could also a high protein abundance of the voltage-gated sodium channel Na$_V$1.9 under non-inflammatory, as well as inflammatory conditions.

5.2. TRPA1 and TRPV1 are target channels for OxPL-induced activation

In nociception, the transient receptor potential channels TRPA1 and TRPV1 are of distinguished importance (Caterina et al., 2000; Bautista et al., 2006; Dhaka et al., 2006; Basbaum et al., 2009; Gangadharan and Kuner, 2013a). Both channels participate in the detection of noxious chemical agents on pain-signaling sensory neurons, thus activating pain pathways to initiate avoidance behaviors and facilitate inflammation by release of neuropeptides. The channels are polymodal receptors and amongst others sensitive to ROS and peroxidized lipids (Bautista et al., 2006; Patwardhan et al., 2010). TRPA1 itself has a broad range of activators including aldehydes, alkenales, tear gases (Bessac and Jordt, 2008) and electrophilic compounds like AITC or allicin. Furthermore, a large quantity of compounds like carvacrol, menthol, thymol or nicotine, which are not covalently activating the TRPA1 channel, but can interact with it (Viana and Ferrer-Montiel, 2009; Chen and Hackos, 2015). It is possible to activate TRPA1 by low pH (de la Roche et al., 2013) and polyunsaturated fatty acids (Motter and Ahern, 2012). In addition, the channel has an outstanding role in clinical treatment, due to its involvement in therapeutic actions (Fajardo et al., 2008; Andersson et al., 2011; Fusi et al., 2014; Kozai et al., 2015). TRPA1 can build complexes with TRPV1 channels, modifying their gating properties (Akopian, 2011). A recent study revealed that this modulation is regulated by TMEM100, a membrane adaptor protein, resulting in prominent changes of TRPA1 activity (Weng et al., 2015).

An additional modulatory mechanism of TRPA1 function is the translocation of channels in the plasma membrane in response to agonists (Schmidt et al., 2009). The OxPL mixture OxPAPC as well as the single compounds PGPC and POVPC used in this thesis robustly activated TRPA1, both in recombinant cells and natively expressed primary DRG neurons. In these experiments, OxPL triggered TRPV1 responses as well, but they were diminutive, suggesting TRPA1 as the preferred target channel of OxPL. The addition of the TRPA1 agonist HC-030031 inhibited OxPL-induced calcium influx, currents as well as action potential firing of small-diameter sensory neurons. These experiments confirm that TRPA1 is a target receptor channel for the acute excitatory action of OxPL on nociceptive sensory neurons (Oehler et al., 2012; Martin et al., 2018).

It is known that gating of TRPA1 occurs via covalent modification of lysine and cysteine residues at the N-terminus of the channel (Hinman et al., 2006; Macpherson et al., 2007; Eberhardt et al., 2012b). Several of those cysteines are located nearby the transmembrane segment S1 (Paulsen et al., 2015). However, some residues are located in the transmembrane core of the channel where they are surrounded by a lipid environment. This could be important for reaction with lipophilic electrophiles and might serve as target location for the interaction with OxPL. TRPA1 is known to have mechanosensitive properties but TRPV1 does not show such characteristics (Kwan et al., 2006; Saghy et al., 2015).

Thus, the stronger effect of OxPL on TRPA1 might be explained by the integration of OxPL into the cell membrane, which might affect only those proteins being sensitive to mechanical pressure, hence TRPA1.The precise characteristics of OxPL activation were shown via a fast calcium imaging approach, where the endogenous irritants evoked repetitive, spike-like calcium transients in primary adult DRG neurons. Here, the data show that PGPC-positive DRG neurons also respond to AITC, capsaicin or both agonists. These results suggest that both TRPA1 and TRPV1 are molecular targets of OxPL-induced activation. Although, not all PGPC positive neurons react to TRPA1 or TRPV1 agonists, thus raising the question whether other receptors or excitatory mechanisms are sensitive for OxPL as well. Additionally, it was shown that BCTC, an antagonist for TRPV1, inhibits the calcium influx induced by OxPL in DRG neurons, suggesting that TRPV1 is a target channel of OxPL. However, the strong inhibition cannot be explained by the constrain of TRPV1 alone as recombinant measurements done in stable expressing $HEK293_{rTRPV1}$ cell lines showed only modest activation of TRPV1 by OxPL even though in this cell system, channels are overexpressed. One explanation for the inhibition by BCTC could be its non-selectivity for merely TRPV1 and its inhibition effect on other receptors expressed in DRG neurons. Here, TRPC5 seems to be an appropriate target channel (Al-Shawaf et al., 2010; Zimmermann et al., 2011).

Some studies revealed besides TRPC5 the prostaglandin-E4-receptors as objective channels of OxPL-induced activation (Al-Shawaf et al., 2010; Zimmermann et al., 2011; Oskolkova et al., 2017). Both channels should further be investigated for interactions with PGPC or additional OxPL. Furthermore, other channels could be activated either by force by lipid effects due to integration of OxPL into the cell membrane or by desensitization and subsequent reduction of the TRP channels agonist effect. A desensitization effect after stimulation with other agonists is common for TRP channels (Akopian et al., 2007; Ruparel et al., 2008) leading to the assumption that the amount of triple positive cells for OxPL and both TRP control stimuli is much higher than noted. Due to the usage of calcium imaging, only those channels being either cation or calcium-selective have to be considered for this events. So far, little is known about the interaction of OxPL with other receptors on nociceptors or other types of sensory neurons.

5.3. Interaction mechanisms of oxidized phospholipids with cell membranes and membrane proteins

To analyze how oxidized phospholipids can interact with TRP channels, a closer look has to be taken at the molecular structure of OxPL and their reactive residues. It is known, that oxidized phospholipids contain a saturated fatty acyl chain (Position *sn*-1) as well as an oxidized fatty acid residue found in position *sn*-2. Via fragmentation reactions phospholipid *sn*-2-aldehydes like PGPC or POVPC are formed. PGPC is a truncated phospholipid with a conical molecular shape and the oxidation product of PAPC (Stemmer and Hermetter, 2012). The molecule contains a short, polar oxidized acyl chain and is amphipathic, thus allowing fast and polar insertion in artificial membrane-like lipid-water layers. Hereby, possible interactions of OxPL with amino- or thiol groups of proteins located in the membrane are controlled by their molecular lipid mobility, the orientation of the functional aldehyde group and the steric restriction (Stemmer and Hermetter, 2012). Their sole long hydrophobic acyl chain is coupled to the phospholipid phase due to the amphiphilic characteristic of the molecule. In this context, the polarity of the acyl chain allows the molecule to fold back to either the surface or the membrane layer leading to a possible interaction with TRPA1 and TRPV1 (Podrez et al., 2002; Wong-Ekkabut et al., 2007; Greenberg et al., 2008; Khandelia and Mouritsen, 2009). In this context, it is shown that the negatively charged carboxylate group of PGPC stretches into the water phase.

Due to its conical structure, PGPC is able to form positive membrane curvatures causing functional as well as structural consequences like facilitation of membrane vesicles or the alteration of proteins that prefer a specific membrane environment (Epand et al., 2009; Rhode et al., 2009; Smith et al., 2009).

In experiments done with PGPC carrying a fluorescent tag, this tag was shown to integrate within milliseconds into lipid patches. As consequence, an increase of a release of cytosolic vesicles was triggered (Rhode et al., 2009). Due to the polar characteristic of OxPL, it can be assumed that they can be transported through the aqueous phase of the membrane bilayer. This uptake of OxPL has been studied by fluorescence microscopy by usage of fluorescent lipid analogs or by utilizing albumin-bound or biotin-tagged OxPL (Glass and Witztum, 2001; Gugiu et al., 2008). Furthermore, the amphipathic characteristic of these molecules leads to an easy and spontaneous exchange between the cell surfaces as well as proteins and lipoproteins (Stemmer et al., 2012).

The likely integration of PGPC into the lipid bilayer of plasma membranes and following modulation of functional properties of lipids and proteins in the membrane (Stemmer and Hermetter, 2012) might induce a mechanical activation of TRPA1 (Kwan et al., 2006; Jansson et al., 2013; Saghy et al., 2015). This idea of mechanical activation was supported by the here shown finding that the chemically stable OxPL PGPC activates a TRPA1-3C mutant (Macpherson et al., 2007) lacking the characteristic binding site for electrophile agonists of TRPA1 (Martin et al., 2018).

5.4. OxPL trigger action potential firing in primary sensory neurons

Via *whole-cell* patch clamp recording in the current-clamp mode, it was verified that local application of PGPC and OxPAPC on primary DRG neurons induces an enhanced action potential firing rate upon current injection (Fig. 33, 34). This enhanced firing rate, which is reduced while using TRPA1 and TRPV1 antagonists, can be explained by a decreased voltage threshold after PGPC addition due to the activation of the receptor potential channels TRPA1 and TRPV1. The subsequent calcium influx increases the membrane potential leading to a consecutive earlier activation of the voltage-gated sodium channels $Na_V1.9$, $Na_V1.8$ and $Na_V1.7$. Activation of TRP channels in their small-diameter DRG neurons confirms the findings performed with recombinant $HEK293_{hTRPA1}$ and $HEK293_{rTRPV1}$. Thus, it was shown that PGPC has an elevating effect on the excitability of DRG neurons (Fig. 34) and it suggested that efficient OxPL function needs an underlying excitatory current which is needed to amplify the OxPL signal. Therefore we assumed that $Na_V1.9$ has a role in threshold mediation given that the channel is responsible for excitation effects within the range of the resting membrane potential (RMP) in C-fibers (Baker et al., 2003; Maingret et al., 2008; Östman et al., 2008; Basbaum et al., 2009). Surprisingly, the involvement of $Na_V1.9$ as threshold mediator under steady-state conditions showed no effects, as PGPC still triggered an increased AP firing frequency in *SCN11^{-/-}* mice. Additionally, no change of resting membrane potential was observed indicating that $Na_V1.9$ has no role in amplifying

OxPL stimuli under these healthy conditions. The mechanism of OxPL-induced nociceptor activation under steady state conditions might occur as following: A given amount of OxPL develops under steady state conditions and is able to interact with nociceptive sensory neurons via TRPA1 and TRPV1. OxPL induce the influx of cations especially calcium ions by activating the TRP channels TRPA1 and modestly TRPV1. In this case, the activation of the TRP channels is moderate. As discussed above, PGPC might integrate into cell membranes and induces an activation of the TRP channels in an indirect manner. Subsequently, the membrane potential is increased and the excitation threshold decreased, therefore activating the voltage-gated sodium channels $Na_V1.8$ and $Na_V1.7$ (Fig. 40). APs induced by these channels would be powerful enough to activate voltage-gated calcium channels.

5.5. Inflammatory mediators recruit $Na_V1.9$ to potentiate the OxPL function in primary sensory DRG neurons

As OxPLs are present in tissue and generated at higher levels during inflammation, it seems plausible that a specific mechanism helps to differentiate between healthy steady-state and inflammatory conditions. This thesis suggests that $Na_V1.9$ is an essential element of a switch mechanism to distinguish between the healthy state and the diseased inflammatory condition. As a result, OxPL stimuli would show a higher potency in terms of TRP channel activation during inflammatory conditions. Data indicate an increased expression rate and quantity of $Na_V1.9$ under inflammatory conditions (Bennett and Woods, 2014; Fischer et al., 2017). However, the mRNA expression (Subramanian et al., 2012) and immunoreactivity (this study) of this unique VGSC is high at steady-state. This argues against the possibility that increased PGPC stimuli under inflammatory conditions depended solely on enhanced $Na_V1.9$ expression.

In the presence of inflammatory mediators the effect of PGPC-induced calcium influx via TRPA1 and TRPV1 is increased (Fig. 37). Furthermore, the action potential firing rate after PGPC addition to wt DRG neurons, treated with inflammatory mediators, was enhanced in comparison to equally treated sensory neurons harvested from $Na_V1.9$ KO (Fig. 38). This indicates that inflammatory mediators engage $Na_V1.9$ as threshold modulator in DRG sensory neurons. Furthermore, TRPA1 and TRPV1 induced receptor potentials are crucial for the induction of action potentials in DRG neurons, since no increased action potential firing occurred while blocking both channels with their antagonists. These findings indicate an enhanced activation of $Na_V1.9$ under inflammatory conditions and support the concept that $Na_V1.9$ is at least partially involved in the hyperexcitability of DRG neurons during inflammation.

Data from other studies, showing a reduced inflammation-induced hyperalgesia in $Na_V1.9$ KO mice, support these results (Priest et al., 2005; Östman et al., 2008). Furthermore, inflammatory mediators, causing an increase in GTP, can influence $Na_V1.9$ properties (Baker et al., 2003). Mediators of inflammation iniate an increased excitability of nociceptors and some studies suggest that an increase in $Na_V1.9$ function causes an increase in DRG excitability, thus causing a higher rate of action potential firing (Maingret et al., 2008). In this study, the authors used inflammatory mediators as acute stimulus on DRG neurons, revealing that they only have an effect on $Na_V1.9$ while used in combination.

Inflammatory mediators augment the resting membrane potential of DRG sensory neurons and $Na_V1.9$ contributes to this effect. Additionally, a brief PGPC stimulus induced a long-lasting calcium-spike behavior of small DRG neurons (Fig. 27, 39). This suggests that $Na_V1.9$ integrates TRP-mediated receptor potentials to mediate the increased action potential firing. Furthermore, an important feature of $Na_V1.9$ is its ability to offer persistent sodium currents (Cummins et al., 1999; Herzog et al., 2001). These sodium currents likely drive the observed calcium spike behavior observed in this study. Indeed, this effect was already shown in motoneurons, where $Na_V1.9$ triggered calcium spikes in a spontaneous and cell-autonomous manner (Subramanian et al., 2012; Wetzel et al., 2013).

Inflammatory mediators can be categorized as classic mediators such as bradykinin, ATP or NGF or as modulators such as BDNF (brain-derived neurotrophic factor) or substance P. In this context, the integration and activation of $Na_V1.9$ into the excitation machinery by signaling cascades leaves room for speculation. Here, the signaling pathways of the neurotrophin receptors for BDNF and NGF might be potential candidates as they are powerful enough to drive long-lasting excitability effects as well as growth effects and translational changes. This has already been described for several types of neurons (Blum et al., 2002; Subramanian et al., 2012; Wetzel et al., 2013; Sasi et al., 2017).

In summary, this thesis gives evidence that an inflammatory soup recruits $Na_V1.9$ to potentiate OxPL-induced function via TRPA1 and TRPV1 channels. During inflammation, nearly twice the amount of OxPL are generated and found in subcutaneous tissue (Oehler et al., 2017).
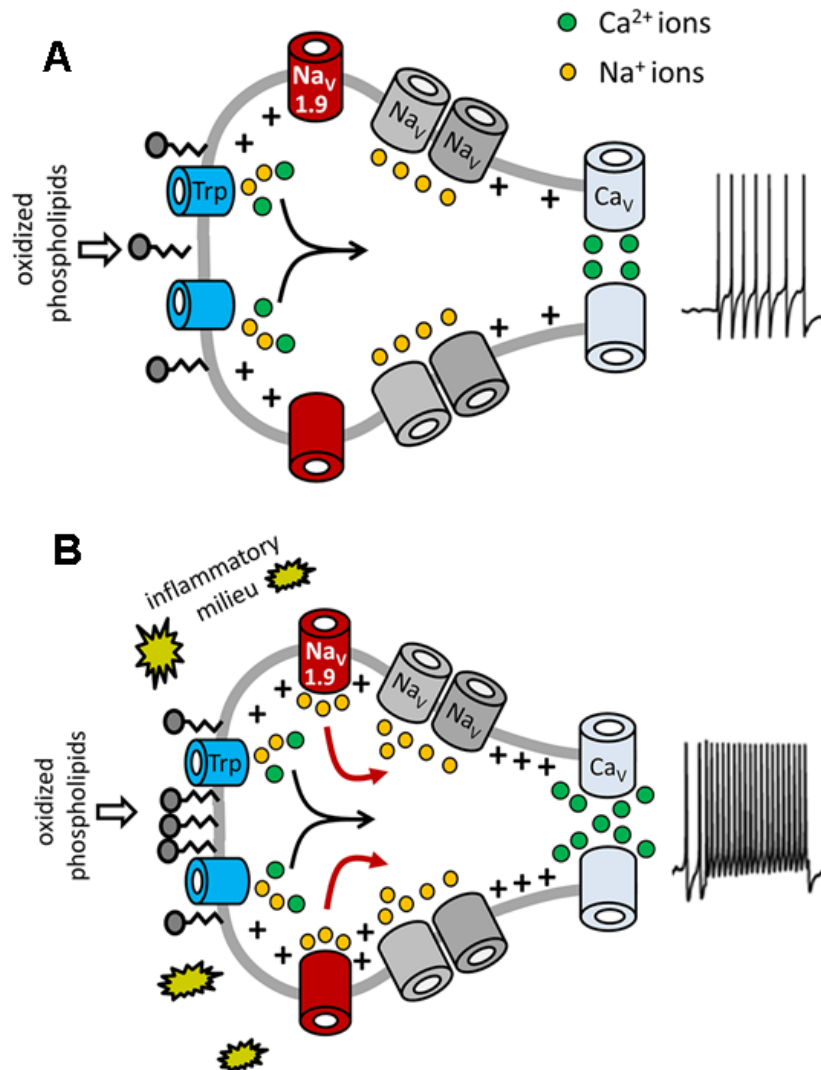
Figure 40: Potentiation of OxPL-induced TRP activation by Na$_V$1.9. (A) A given amount of OxPL develops under steady state conditions and is able to interact with nociceptive sensory neurons via TRPA1 and TRPV1. In this case, the activation of the TRP channels is moderate. PGPC might integrate into cell membranes and might thus induce an activation of the TRP channels in an indirect manner. The increased receptor potentials induce the activation of Na$_V$1.7, Na$_V$1.8 and Na$_V$1.9 and an AP firing is triggered (Martin et al., 2018). **(B)** During inflammation, nearly twice the amount of OxPL are generated and found in subcutaneous tissue (Oehler et al., 2017). Besides, produced inflammatory mediators can additionally sensitize peripheral sensory neurons and interact with other receptors and channels expressed on the nociceptors. Hence yet unknown signaling cascades enhance the Na$_V$1.9 activation. Then, the persistent sodium current of this unique subthreshold active channel potentiates the OxPL-induced receptor potentials via the TRP channels. An enhanced action potential firing rate is enhanced by voltage gated sodium channels (Na$_V$1.7, Na$_V$1.8) in the nociceptor and it responds with an elevated fast calcium spikes. This model suggests Na$_V$1.9 as a master switch distinguishing between the healthy steady state and inflammated condition. Hereby, the channel integrates chemical irritants increasing the nociceptor response during inflammation (Martin et al., 2018).

Inflammatory mediators can additionally sensitize peripheral sensory neurons and sensitize other receptors and channels expressed on the sensory neurons. Hence yet unknown signaling cascades enhance the $Na_V1.9$ activation and the persistent sodium current of this unique subthreshold active channel potentiates the OxPL-mediated receptor potentials via the TRP channels.

An increased action potential firing rate is triggered by voltage gated sodium channels ($Na_V1.7$, $Na_V1.8$) in the nociceptor which triggers the elevated calcium spiking. In conclusion, the data suggest $Na_V1.9$ as master switch distinguishing between resting excitability and increased excitability under inflammatory conditions.

6 Conclusion

In conclusion, the present thesis reveals the OxPL-induced activation of both transient receptor potential channels TRPA1 and TRPV1 expressed in small diameter DRG sensory neurons. Hereby, the function of TRPV1 is puzzling as recombinant TRPV1 is only modestly activated by OxPL. OxPL initate hyperexcitability in primary DRG neurons by influencing the decrease of their excitation threshold *in vitro*. When mimicking an inflammatory environment with an inflammatory soup, the PGPC-induced excitation of primary nociceptors in potentiated, thus indicating a connection between hyperalgesia generated by OxPL and inflammation-initiated sensitization of DRG neurons.

The voltage-gated sodium channel $Na_V 1.9$ seems to be almost inactive under steady state conditions, whereas, it does play an essential role in the threshold mediation after recruitment by inflammatory mediators. This stresses the significance of this unique subthreshold active voltage-gated sodium channel as a mediator of excitability and as an integrator for chemical irritant stimuli during inflammation. In this model, $Na_V 1.9$ serves as an essential and non-redundant master switch distinguishing between resting excitability and excitability under inflammatory conditions.

7 Outlook

The important discovery of mutations in $Na_V1.9$ in human patients suffering from either painful neuropathy, episodic pain syndromes or even a complete loss of pain perception, emphasizes the importance of $Na_V1.9$ as potential target channel to treat pain (Leipold et al., 2013; Zhang et al., 2013; Huang et al., 2014, 2017; Woods et al., 2014; Han et al., 2015). However, it has to be considered that this unique voltage-gated sodium channel is not only functionally important in nociceptors. The L811P mutation of $Na_V1.9$ was shown to lead to severe gastrointestinal symptoms such as intestinal dysmotility. This is in accordance with the function of $Na_V1.9$ in myenteric sensory neurons of rodents (Rugiero et al., 2003). Additionally, it serves as an excitability mediator in motoneurons. Here, $Na_V1.9$ triggers cell-autonomous calcium spikes in growth cones to support activity-dependent axon elongation (Subramanian et al., 2012; Wetzel et al., 2013). These calcium spikes are reduced in preclinical models that mimic spinal muscular atrophy (Jablonka et al., 2007; Wetzel et al., 2013). Furthermore, signs of delayed motor development as well as muscular weakness are in accordance with a function in the maintenance or development of the motor system (Woods et al.; Subramanian et al., 2012; Leipold et al., 2013). Thus, before systemically applied therapeutics targeting $Na_V1.9$ can become safe, a deeper knowledge of the molecular activation cascade upstream of $Na_V1.9$ is needed (Martin et al., 2018).

8 References

Akopian AN (2011) Regulation of nociceptive transmission at the periphery via TRPA1-TRPV1 interactions. Curr Pharm Biotechnol 12:89-94.

Akopian AN, Ruparel NB, Jeske NA, Hargreaves KM (2007) Transient receptor potential TRPA1 channel desensitization in sensory neurons is agonist dependent and regulated by TRPV1-directed internalization. J Physiol 583:175-193.

Al-Shawaf E, Naylor J, Taylor H, Riches K, Milligan CJ, O'Regan D, Porter KE, Li J, Beech DJ (2010) Short-term stimulation of calcium-permeable transient receptor potential canonical 5-containing channels by oxidized phospholipids. Arterioscler Thromb Vasc Biol 30:1453-1459.

Andersson DA, Gentry C, Moss S, Bevan S Transient Receptor Potential A1 Is a Sensory Receptor for Multiple Products of Oxidative Stress: J Neurosci. 2008 Mar 5;28(10):2485-94. doi:10.1523/JNEUROSCI.5369-07.2008.

Andersson DA, Gentry C, Alenmyr L, Killander D, Lewis SE, Andersson A, Bucher B, Galzi JL, Sterner O, Bevan S, Hogestatt ED, Zygmunt PM (2011) TRPA1 mediates spinal antinociception induced by acetaminophen and the cannabinoid Delta(9)-tetrahydrocannabiorcol. Nature communications 2.

Andre E, Campi B, Materazzi S, Trevisani M, Amadesi S, Massi D, Creminon C, Vaksman N, Nassini R, Civelli M, Baraldi PG, Poole DP, Bunnett NW, Geppetti P, Patacchini R (2008) Cigarette smoke-induced neurogenic inflammation is mediated by alpha,beta-unsaturated aldehydes and the TRPA1 receptor in rodents. J Clin Invest 118:2574-2582.

Anliker B, Chun J (2004) Lysophospholipid G protein-coupled receptors. J Biol Chem 279:20555-20558.

Atzori L, Bannenberg G, Corriga AM, Lou YP, Lundberg JM, Ryrfeldt A, Moldeus P (1992) Sulfur dioxide-induced bronchoconstriction via ruthenium red-sensitive activation of sensory nerves. Respiration 59:272-278.

Averill S, McMahon SB, Clary DO, Reichardt LF, Priestley JV (1995) Immunocytochemical localization of trkA receptors in chemically identified subgroups of adult rat sensory neurons. Eur J Neurosci 7:1484-1494.

Babes A, Zorzon D, Reid G (2004) Two populations of cold-sensitive neurons in rat dorsal root ganglia and their modulation by nerve growth factor. Eur J Neurosci 20:2276-2282.

Baker MD, Chandra SY, Ding Y, Waxman SG, Wood JN (2003) GTP-induced tetrodotoxin-resistant Na+ current regulates excitability in mouse and rat small diameter sensory neurones. J Physiol 548:373-382.

Bandell M, Story GM, Hwang SW, Viswanath V, Eid SR, Petrus MJ, Earley TJ, Patapoutian A (2004) Noxious cold ion channel TRPA1 is activated by pungent compounds and bradykinin. Neuron 41:849-857.

Barabas ME, Kossyreva EA, Stucky CL (2012) TRPA1 is functionally expressed primarily by IB4-binding, non-peptidergic mouse and rat sensory neurons. PloS one 7:e47988.

Basbaum AI, Bautista DM, Scherrer G, Julius D (2009) Cellular and molecular mechanisms of pain. Cell 139:267-284.

Bautista DM, Jordt SE, Nikai T, Tsuruda PR, Read AJ, Poblete J, Yamoah EN, Basbaum AI, Julius D (2006) TRPA1 mediates the inflammatory actions of environmental irritants and proalgesic agents. Cell 124:1269-1282.

Bennett DL, Woods CG (2014) Painful and painless channelopathies. Lancet Neurol 13:587-599.

Bessac BF, Jordt SE (2008) Breathtaking TRP channels: TRPA1 and TRPV1 in airway chemosensation and reflex control. Physiology 23:360-370.

Blum R, Kafitz KW, Konnerth A (2002) Neurotrophin-evoked depolarization requires the sodium channel Na(V)1.9. Nature 419:687-693.

Bochkov VN, Oskolkova OV, Birukov KG, Levonen AL, Binder CJ, Stockl J (2010) Generation and biological activities of oxidized phospholipids. Antioxid Redox Signal 12:1009-1059.

Bretscher P, Egger J, Shamshiev A, Trotzmuller M, Kofeler H, Carreira EM, Kopf M, Freigang S (2015) Phospholipid oxidation generates potent anti-inflammatory lipid mediators that mimic structurally related pro-resolving eicosanoids by activating Nrf2. EMBO molecular medicine 7:593-607.

Catala A (2009) Lipid peroxidation of membrane phospholipids generates hydroxy-alkenals and oxidized phospholipids active in physiological and/or pathological conditions. Chem Phys Lipids 157:1-11.

Caterina MJ, Schumacher MA, Tominaga M, Rosen TA, Levine JD, Julius D (1997) The capsaicin receptor: a heat-activated ion channel in the pain pathway. Nature 389:816-824.

Caterina MJ, Leffler A, Malmberg AB, Martin WJ, Trafton J, Petersen-Zeitz KR, Koltzenburg M, Basbaum AI, Julius D (2000) Impaired nociception and pain sensation in mice lacking the capsaicin receptor. Science 288:306-313.

Catterall WA, Goldin AL, Waxman SG (2005) International Union of Pharmacology. XLVII. Nomenclature and structure-function relationships of voltage-gated sodium channels. Pharmacological reviews 57:397-409.

Chen J, Hackos DH (2015) TRPA1 as a drug target--promise and challenges. Naunyn Schmiedebergs Arch Pharmacol 388:451-463.

Cheng JK, Ji RR (2008) Intracellular signaling in primary sensory neurons and persistent pain. Neurochem Res 33:1970-1978.

Clapham DE (2007) SnapShot: mammalian TRP channels. Cell 129:220.

Cummins TR, Rush AM, Estacion M, Dib-Hajj SD, Waxman SG (2009) Voltage-clamp and current-clamp recordings from mammalian DRG neurons. Nat Protoc 4:1103-1112.

Cummins TR, Dib-Hajj SD, Black JA, Akopian AN, Wood JN, Waxman SG (1999) A novel persistent tetrodotoxin-resistant sodium current in SNS-null and wild-type small primary sensory neurons. The Journal of neuroscience : the official journal of the Society for Neuroscience 19:RC43.

Davies SS, Pontsler AV, Marathe GK, Harrison KA, Murphy RC, Hinshaw JC, Prestwich GD, Hilaire AS, Prescott SM, Zimmerman GA, McIntyre TM (2001) Oxidized alkyl phospholipids are specific, high affinity peroxisome proliferator-activated receptor gamma ligands and agonists. J Biol Chem 276:16015-16023.

de la Roche J, Eberhardt MJ, Klinger AB, Stanslowsky N, Wegner F, Koppert W, Reeh PW, Lampert A, Fischer MJ, Leffler A (2013) The molecular basis for species-specific activation of human TRPA1 protein by protons involves poorly conserved residues within transmembrane domains 5 and 6. J Biol Chem 288:20280-20292.

Dhaka A, Viswanath V, Patapoutian A (2006) Trp ion channels and temperature sensation. Annu Rev Neurosci 29:135-161.

Dib-Hajj S, Black JA, Cummins TR, Waxman SG (2002) NaN/Nav1.9: a sodium channel with unique properties. Trends Neurosci 25:253-259.

Dib-Hajj SD, Black JA, Waxman SG (2015) NaV1.9: a sodium channel linked to human pain. Nat Rev Neurosci 16:511-519.

Dib-Hajj SD, Yang Y, Black JA, Waxman SG (2013) The Na(V)1.7 sodium channel: from molecule to man. Nat Rev Neurosci 14:49-62.

Dib-Hajj SD, Black JA, Cummins TR, Kenney AM, Kocsis JD, Waxman SG (1998) Rescue of alpha-SNS sodium channel expression in small dorsal root ganglion neurons after axotomy by nerve growth factor in vivo. J Neurophysiol 79:2668-2676.

Djouhri L, Lawson SN (2004) Abeta-fiber nociceptive primary afferent neurons: a review of incidence and properties in relation to other afferent A-fiber neurons in mammals. Brain Res Brain Res Rev 46:131-145.

Doppler K, Appeltshauser L, Villmann C, Martin C, Peles E, Kramer HH, Haarmann A, Buttmann M, Sommer C (2016) Auto-antibodies to contactin-associated protein 1 (Caspr) in two patients with painful inflammatory neuropathy. Brain 139:2617-2630.

Dubin AE, Patapoutian A (2010) Nociceptors: the sensors of the pain pathway. J Clin Invest 120:3760-3772.

Eberhardt MJ, Filipovic MR, Leffler A, de la Roche J, Kistner K, Fischer MJ, Fleming T, Zimmermann K, Ivanovic-Burmazovic I, Nawroth PP, Bierhaus A, Reeh PW, Sauer SK (2012a) Methylglyoxal activates nociceptors through transient receptor potential channel A1 (TRPA1): a possible mechanism of metabolic neuropathies. The Journal of biological chemistry 287:28291-28306.

Eberhardt MJ, Filipovic MR, Leffler A, de la Roche J, Kistner K, Fischer MJ, Fleming T, Zimmermann K, Ivanovic-Burmazovic I, Nawroth PP, Bierhaus A, Reeh PW, Sauer SK (2012b) Methylglyoxal activates nociceptors through transient receptor potential channel A1 (TRPA1): a possible mechanism of metabolic neuropathies. J Biol Chem 287:28291-28306.

Edery H, Lewis GP (1962) Inhibition of plasma kininase activity at slightly acid ph. Br J Pharmacol Chemother 19:299-305.

Epand RF, Mishra VK, Palgunachari MN, Anantharamaiah GM, Epand RM (2009) Anti-inflammatory peptides grab on to the whiskers of atherogenic oxidized lipids. Biochim Biophys Acta 9:25.

Faber CG, Hoeijmakers JG, Ahn HS, Cheng X, Han C, Choi JS, Estacion M, Lauria G, Vanhoutte EK, Gerrits MM, Dib-Hajj S, Drenth JP, Waxman SG, Merkies IS (2012) Gain of function Nanu1.7 mutations in idiopathic small fiber neuropathy. Ann Neurol 71:26-39.

Fajardo O, Meseguer V, Belmonte C, Viana F (2008) TRPA1 channels: novel targets of 1,4-dihydropyridines. Channels 2:429-438.

Fischer BD, Ho C, Kuzin I, Bottaro A, O'Leary ME (2017) Chronic exposure to tumor necrosis factor in vivo induces hyperalgesia, upregulates sodium channel gene expression and alters the cellular electrophysiology of dorsal root ganglion neurons. Neurosci Lett 653:195-201.

Fischer MJ, Btesh J, McNaughton PA (2013) Disrupting sensitization of transient receptor potential vanilloid subtype 1 inhibits inflammatory hyperalgesia. The Journal of neuroscience : the official journal of the Society for Neuroscience 33:7407-7414.

Flower R, Gryglewski R, Herbaczynska-Cedro K, Vane JR (1972) Effects of anti-inflammatory drugs on prostaglandin biosynthesis. Nat New Biol 238:104-106.

Freigang S (2016) The regulation of inflammation by oxidized phospholipids. Eur J Immunol 46:1818-1825.

Furnkranz A, Schober A, Bochkov VN, Bashtrykov P, Kronke G, Kadl A, Binder BR, Weber C, Leitinger N (2005) Oxidized phospholipids trigger atherogenic inflammation in murine arteries. Arteriosclerosis, thrombosis, and vascular biology 25:633-638.

Fusi C, Materazzi S, Benemei S, Coppi E, Trevisan G, Marone IM, Minocci D, De Logu F, Tuccinardi T, Di Tommaso MR, Susini T, Moneti G, Pieraccini G, Geppetti P, Nassini R (2014) Steroidal and non-steroidal third-generation aromatase inhibitors induce pain-like symptoms via TRPA1. Nature communications 5.

Gangadharan V, Kuner R (2013a) Pain hypersensitivity mechanisms at a glance. Disease models & mechanisms 6:889-895.

Gangadharan V, Kuner R (2013b) Pain hypersensitivity mechanisms at a glance. Dis Model Mech 6:889-895.

Glass CK, Witztum JL (2001) Atherosclerosis. the road ahead. Cell 104:503-516.

Greenberg ME, Li XM, Gugiu BG, Gu X, Qin J, Salomon RG, Hazen SL (2008) The lipid whisker model of the structure of oxidized cell membranes. J Biol Chem 283:2385-2396.

Grienberger C, Konnerth A (2012) Imaging calcium in neurons. Neuron 73:862-885.

Gugiu BG, Mouillesseaux K, Duong V, Herzog T, Hekimian A, Koroniak L, Vondriska TM, Watson AD (2008) Protein targets of oxidized phospholipids in endothelial cells. J Lipid Res 49:510-520.

Guimarães EL, Best J, Dollé L, Najimi M, Sokal E, van Grunsven LA Mitochondrial uncouplers inhibit hepatic stellate cell activation: BMC Gastroenterol. 2012;12:68. doi:10.1186/1471-230X-12-68.

Hamill OP, Marty A, Neher E, Sakmann B, Sigworth FJ (1981) Improved patch-clamp techniques for high-resolution current recording from cells and cell-free membrane patches. Pflugers Arch 391:85-100.

Han C, Yang Y, de Greef BT, Hoeijmakers JG, Gerrits MM, Verhamme C, Qu J, Lauria G, Merkies IS, Faber CG, Dib-Hajj SD, Waxman SG (2015) The Domain II S4-S5 Linker in Nav1.9: A Missense Mutation Enhances Activation, Impairs Fast Inactivation, and Produces Human Painful Neuropathy. Neuromolecular Med 17:158-169.

Hansson GK, Hermansson A (2011a) The immune system in atherosclerosis. Nat Immunol 12:204-212.

Hansson GK, Hermansson A (2011b) The immune system in atherosclerosis. Nature immunology 12:204-212.

Hargreaves KM, Troullos ES, Dionne RA, Schmidt EA, Schafer SC, Joris JL (1988) Bradykinin is increased during acute and chronic inflammation: therapeutic implications. Clin Pharmacol Ther 44:613-621.

Heinricher MM, Tavares I, Leith JL, Lumb BM (2009) Descending control of nociception: Specificity, recruitment and plasticity. Brain Res Rev 60:214-225.

Herzog RI, Cummins TR, Waxman SG (2001) Persistent TTX-resistant Na+ current affects resting potential and response to depolarization in simulated spinal sensory neurons. J Neurophysiol 86:1351-1364.

Hinman A, Chuang HH, Bautista DM, Julius D (2006) TRP channel activation by reversible covalent modification. Proc Natl Acad Sci U S A 103:19564-19568.

Huang EJ, Reichardt LF (2001) Neurotrophins: roles in neuronal development and function. Annu Rev Neurosci 24:677-736.

Huang J, Vanoye CG, Cutts A, Goldberg YP, Dib-Hajj SD, Cohen CJ, Waxman SG, George AL, Jr. (2017) Sodium channel NaV1.9 mutations associated with insensitivity to pain dampen neuronal excitability. J Clin Invest 22.

Huang J, Yang Y, Zhao P, Gerrits MM, Hoeijmakers JG, Bekelaar K, Merkies IS, Faber CG, Dib-Hajj SD, Waxman SG (2013) Small-fiber neuropathy Nav1.8 mutation shifts activation to

hyperpolarized potentials and increases excitability of dorsal root ganglion neurons. The Journal of neuroscience : the official journal of the Society for Neuroscience 33:14087-14097.

Huang J, Han C, Estacion M, Vasylyev D, Hoeijmakers JG, Gerrits MM, Tyrrell L, Lauria G, Faber CG, Dib-Hajj SD, Merkies IS, Waxman SG (2014) Gain-of-function mutations in sodium channel Na(v)1.9 in painful neuropathy. Brain 137:1627-1642.

Imai Y et al. (2008) Identification of oxidative stress and Toll-like receptor 4 signaling as a key pathway of acute lung injury. Cell 133:235-249.

Jablonka S, Beck M, Lechner BD, Mayer C, Sendtner M (2007) Defective Ca2+ channel clustering in axon terminals disturbs excitability in motoneurons in spinal muscular atrophy. J Cell Biol 179:139-149.

Ji RR, Xu ZZ, Gao YJ (2014) Emerging targets in neuroinflammation-driven chronic pain. Nat Rev Drug Discov 13:533-548.

Jordt SE, Tominaga M, Julius D (2000) Acid potentiation of the capsaicin receptor determined by a key extracellular site. Proc Natl Acad Sci U S A 97:8134-8139.

Jordt SE, Bautista DM, Chuang HH, McKemy DD, Zygmunt PM, Hogestatt ED, Meng ID, Julius D (2004) Mustard oils and cannabinoids excite sensory nerve fibres through the TRP channel ANKTM1. Nature 427:260-265.

Khandelia H, Mouritsen OG (2009) Lipid gymnastics: evidence of complete acyl chain reversal in oxidized phospholipids from molecular simulations. Biophys J 96:2734-2743.

Kozai D, Sakaguchi R, Ohwada T, Mori Y (2015) Deciphering Subtype-Selective Modulations in TRPA1 Biosensor Channels. Curr Neuropharmacol 13:266-278.

Kumar V, Sharma A (2008) Innate immunity in sepsis pathogenesis and its modulation: new immunomodulatory targets revealed. J Chemother 20:672-683.

Kumazawa T, Mizumura K, Koda H, Fukusako H (1996) EP receptor subtypes implicated in the PGE2-induced sensitization of polymodal receptors in response to bradykinin and heat. J Neurophysiol 75:2361-2368.

Kwan KY, Allchorne AJ, Vollrath MA, Christensen AP, Zhang DS, Woolf CJ, Corey DP (2006) TRPA1 contributes to cold, mechanical, and chemical nociception but is not essential for hair-cell transduction. Neuron 50:277-289.

Latorre R, Zaelzer C, Brauchi S (2009) Structure-functional intimacies of transient receptor potential channels. Q Rev Biophys 42:201-246.

Lee H, Shi W, Tontonoz P, Wang S, Subbanagounder G, Hedrick CC, Hama S, Borromeo C, Evans RM, Berliner JA, Nagy L (2000) Role for peroxisome proliferator-activated receptor alpha in oxidized phospholipid-induced synthesis of monocyte chemotactic protein-1 and interleukin-8 by endothelial cells. Circ Res 87:516-521.

Lee S, Birukov KG, Romanoski CE, Springstead JR, Lusis AJ, Berliner JA (2012a) Role of phospholipid oxidation products in atherosclerosis. Circ Res 111:778-799.

Lee S, Birukov KG, Romanoski CE, Springstead JR, Lusis AJ, Berliner JA (2012b) Role of phospholipid oxidation products in atherosclerosis. Circulation research 111:778-799.

Leipold E, Hanson-Kahn A, Frick M, Gong P, Bernstein JA, Voigt M, Katona I, Oliver Goral R, Altmüller J, Nürnberg P, Weis J, Hübner CA, Heinemann SH, Kurth I (2015) Cold-aggravated pain in humans caused by a hyperactive NaV1.9 channel mutant. Nature communications 6:10049.

Leipold E et al. (2013) A de novo gain-of-function mutation in SCN11A causes loss of pain perception. Nat Genet 45:1399-1404.

Li R, Mouillesseaux KP, Montoya D, Cruz D, Gharavi N, Dun M, Koroniak L, Berliner JA (2006) Identification of prostaglandin E2 receptor subtype 2 as a receptor activated by OxPAPC. Circ Res 98:642-650.

Lin CR, Amaya F, Barrett L, Wang H, Takada J, Samad TA, Woolf CJ (2006) Prostaglandin E2 receptor EP4 contributes to inflammatory pain hypersensitivity. J Pharmacol Exp Ther 319:1096-1103.

Liu B, Tai Y, Caceres AI, Achanta S, Balakrishna S, Shao X, Fang J, Jordt SE (2016) Oxidized Phospholipid OxPAPC Activates TRPA1 and Contributes to Chronic Inflammatory Pain in Mice. PloS one 11.

Liu T, Ji RR Oxidative stress induces itch via activation of transient receptor potential subtype ankyrin 1 (TRPA1) in mice: Neurosci Bull. 2012 Apr;28(2):145-54.

Macpherson LJ, Dubin AE, Evans MJ, Marr F, Schultz PG, Cravatt BF, Patapoutian A (2007) Noxious compounds activate TRPA1 ion channels through covalent modification of cysteines. Nature 445:541-545.

Maingret F, Coste B, Padilla F, Clerc N, Crest M, Korogod SM, Delmas P (2008) Inflammatory mediators increase Nav1.9 current and excitability in nociceptors through a coincident detection mechanism. J Gen Physiol 131:211-225.

Malin SA, Davis BM, Molliver DC (2007) Production of dissociated sensory neuron cultures and considerations for their use in studying neuronal function and plasticity. Nat Protoc 2:152-160.

Martin C, Stoffer C, Mohammadi M, Hugo J, Leipold E, Oehler B, Rittner HL, Blum R (2018) NaV1.9 Potentiates Oxidized Phospholipid-Induced TRP Responses Only under Inflammatory Conditions. Frontiers in Molecular Neuroscience 11.

McMahon SB, Armanini MP, Ling LH, Phillips HS (1994) Expression and coexpression of Trk receptors in subpopulations of adult primary sensory neurons projecting to identified peripheral targets. Neuron 12:1161-1171.

McNamara CR, Mandel-Brehm J, Bautista DM, Siemens J, Deranian KL, Zhao M, Hayward NJ, Chong JA, Julius D, Moran MM, Fanger CM (2007) TRPA1 mediates formalin-induced pain. Proc Natl Acad Sci U S A 104:13525-13530.

Medzhitov R (2008) Origin and physiological roles of inflammation. Nature 454:428-435.

Merskey H and Bogduk N. Part III: Pain Terms, A Current List with Definitions and Notes on Usage" (pp 209-214) Classification of Chronic Pain, Second Edition, IASP Task Force on Taxonomy, edited by H. Merskey and N. Bogduk, IASP Press, Seattle, ©1994.

Millan MJ (1999) The induction of pain: an integrative review. Prog Neurobiol 57:1-164.

Moriyama T, Higashi T, Togashi K, Iida T, Segi E, Sugimoto Y, Tominaga T, Narumiya S, Tominaga M (2005) Sensitization of TRPV1 by EP1 and IP reveals peripheral nociceptive mechanism of prostaglandins. Mol Pain 1:3.

Motter AL, Ahern GP (2012) TRPA1 is a polyunsaturated fatty acid sensor in mammals. PloS one 7:19.

Oehler B, Scholze A, Schaefer M, Hill K (2012) TRPA1 is functionally expressed in melanoma cells but is not critical for impaired proliferation caused by allyl isothiocyanate or cinnamaldehyde. Naunyn-Schmiedeberg's archives of pharmacology 385:555-563.

Oehler B, Kistner K, Martin C, Schiller J, Mayer R, Mohammadi M, Sauer R-S, Filipovic MR, Nieto FR, Kloka J, Pflücke D, Hill K, Schaefer M, Malcangio M, Reeh PW, Brack A, Blum R, Rittner HL (2017) Inflammatory pain control by blocking oxidized phospholipid-mediated TRP channel activation. Scientific Reports 7:5447.

Oskolkova O, Gawlak G, Tian Y, Ke Y, Sarich N, Son S, Andreasson K, Bochkov VN, Birukova AA, Birukov KG (2017) Prostaglandin E receptor-4 receptor mediates endothelial barrier-enhancing and anti-inflammatory effects of oxidized phospholipids. Faseb J 1.

Östman JA, Nassar MA, Wood JN, Baker MD (2008) GTP up-regulated persistent Na+ current and enhanced nociceptor excitability require NaV1.9. J Physiol 586:1077-1087.

Patapoutian A, Reichardt LF (2001) Trk receptors: mediators of neurotrophin action. Curr Opin Neurobiol 11:272-280.

Patwardhan AM, Akopian AN, Ruparel NB, Diogenes A, Weintraub ST, Uhlson C, Murphy RC, Hargreaves KM (2010) Heat generates oxidized linoleic acid metabolites that activate TRPV1 and produce pain in rodents. The Journal of clinical investigation 120:1617-1626.

Paulsen CE, Armache JP, Gao Y, Cheng Y, Julius D (2015) Structure of the TRPA1 ion channel suggests regulatory mechanisms. Nature 520:511-517.

Pedersen SF, Owsianik G, Nilius B (2005) TRP channels: an overview. Cell Calcium 38:233-252.

Pereira WE, Hoyano Y, Summons RE, Bacon VA, Duffield AM (1973) Chlorination studies. II. The reaction of aqueous hypochlorous acid with alpha-amino acids and dipeptides. Biochim Biophys Acta 313:170-180.

Petho G, Reeh PW (2012) Sensory and signaling mechanisms of bradykinin, eicosanoids, platelet-activating factor, and nitric oxide in peripheral nociceptors. Physiol Rev 92:1699-1775.

Petho G, Derow A, Reeh PW (2001) Bradykinin-induced nociceptor sensitization to heat is mediated by cyclooxygenase products in isolated rat skin. Eur J Neurosci 14:210-218.

Pflucke D, Hackel D, Mousa SA, Partheil A, Neumann A, Brack A, Rittner HL (2013) The molecular link between C-C-chemokine ligand 2-induced leukocyte recruitment and hyperalgesia. The journal of pain : official journal of the American Pain Society 14:897-910.

Podrez EA, Poliakov E, Shen Z, Zhang R, Deng Y, Sun M, Finton PJ, Shan L, Gugiu B, Fox PL, Hoff HF, Salomon RG, Hazen SL (2002) Identification of a novel family of oxidized phospholipids that serve as ligands for the macrophage scavenger receptor CD36. J Biol Chem 277:38503-38516.

Priest BT, Murphy BA, Lindia JA, Diaz C, Abbadie C, Ritter AM, Liberator P, Iyer LM, Kash SF, Kohler MG, Kaczorowski GJ, MacIntyre DE, Martin WJ (2005) Contribution of the tetrodotoxin-

resistant voltage-gated sodium channel NaV1.9 to sensory transmission and nociceptive behavior. Proc Natl Acad Sci U S A 102:9382-9387.

Raja SN, Meyer RA, Campbell JN (1988) Peripheral mechanisms of somatic pain. Anesthesiology 68:571-590.

Ren Y, Ridsdale A, Coderre E, Stys PK (2000) Calcium imaging in live rat optic nerve myelinated axons in vitro using confocal laser microscopy. Journal of neuroscience methods 102:165-176.

Rhode S, Grurl R, Brameshuber M, Hermetter A, Schutz GJ (2009) Plasma membrane fluidity affects transient immobilization of oxidized phospholipids in endocytotic sites for subsequent uptake. J Biol Chem 284:2258-2265.

Ricciotti E, FitzGerald GA (2011) Prostaglandins and inflammation. Arterioscler Thromb Vasc Biol 31:986-1000.

Rugiero F, Mistry M, Sage D, Black JA, Waxman SG, Crest M, Clerc N, Delmas P, Gola M (2003) Selective expression of a persistent tetrodotoxin-resistant Na+ current and NaV1.9 subunit in myenteric sensory neurons. The Journal of neuroscience : the official journal of the Society for Neuroscience 23:2715-2725.

Ruparel NB, Patwardhan AM, Akopian AN, Hargreaves KM (2008) Homologous and heterologous desensitization of capsaicin and mustard oil responses utilize different cellular pathways in nociceptors. Pain 135:271-279.

Rush AM, Waxman SG (2004) PGE2 increases the tetrodotoxin-resistant Nav1.9 sodium current in mouse DRG neurons via G-proteins. Brain Res 15:264-271.

Saghy E, Szoke E, Payrits M, Helyes Z, Borzsei R, Erostyak J, Janosi TZ, Setalo G, Jr., Szolcsanyi J (2015) Evidence for the role of lipid rafts and sphingomyelin in Ca2+-gating of Transient Receptor Potential channels in trigeminal sensory neurons and peripheral nerve terminals. Pharmacol Res 100:101-116.

Sasi M, Vignoli B, Canossa M, Blum R (2017) Neurobiology of local and intercellular BDNF signaling. Pflugers Arch 469:593-610.

Schmidt M, Dubin AE, Petrus MJ, Earley TJ, Patapoutian A (2009) Nociceptive signals induce trafficking of TRPA1 to the plasma membrane. Neuron 64:498-509.

Schulze A, Oehler B, Urban N, Schaefer M, Hill K (2013) Apomorphine is a bimodal modulator of TRPA1 channels. Molecular pharmacology 83:542-551.

Seamon KB, Padgett W, Daly JW (1981) Forskolin: unique diterpene activator of adenylate cyclase in membranes and in intact cells. Proc Natl Acad Sci U S A 78:3363-3367.

Serhan CN (2010) Novel lipid mediators and resolution mechanisms in acute inflammation: to resolve or not? Am J Pathol 177:1576-1591.

Singer SJ, Nicolson GL (1972) The fluid mosaic model of the structure of cell membranes. Science 175:720-731.

Smith HL, Howland MC, Szmodis AW, Li Q, Daemen LL, Parikh AN, Majewski J (2009) Early stages of oxidative stress-induced membrane permeabilization: a neutron reflectometry study. J Am Chem Soc 131:3631-3638.

Sostres C, Gargallo CJ, Arroyo MT, Lanas A (2010) Adverse effects of non-steroidal anti-inflammatory drugs (NSAIDs, aspirin and coxibs) on upper gastrointestinal tract. Best Pract Res Clin Gastroenterol 24:121-132.

Stein C, Baerwald C (2014) Opioids for the treatment of arthritis pain. Expert Opin Pharmacother 15:193-202.

Stemmer U, Hermetter A (2012) Protein modification by aldehydophospholipids and its functional consequences. Biochimica et biophysica acta 1818:2436-2445.

Stemmer U, Ramprecht C, Zenzmaier E, Stojcic B, Rechberger G, Kollroser M, Hermetter A (2012) Uptake and protein targeting of fluorescent oxidized phospholipids in cultured RAW 264.7 macrophages. Biochim Biophys Acta 4:706-718.

Story GM, Peier AM, Reeve AJ, Eid SR, Mosbacher J, Hricik TR, Earley TJ, Hergarden AC, Andersson DA, Hwang SW, McIntyre P, Jegla T, Bevan S, Patapoutian A (2003) ANKTM1, a TRP-like channel expressed in nociceptive neurons, is activated by cold temperatures. Cell 112:819-829.

Subramanian N, Wetzel A, Dombert B, Yadav P, Havlicek S, Jablonka S, Nassar MA, Blum R, Sendtner M (2012) Role of Na(v)1.9 in activity-dependent axon growth in motoneurons. Hum Mol Genet 21:3655-3667.

Sudano I, Flammer AJ, Roas S, Enseleit F, Noll G, Ruschitzka F (2012) Nonsteroidal antiinflammatory drugs, acetaminophen, and hypertension. Curr Hypertens Rep 14:304-309.

Tominaga M, Caterina MJ, Malmberg AB, Rosen TA, Gilbert H, Skinner K, Raumann BE, Basbaum AI, Julius D (1998) The cloned capsaicin receptor integrates multiple pain-producing stimuli. Neuron 21:531-543.

Tomura H, Mogi C, Sato K, Okajima F (2005) Proton-sensing and lysolipid-sensitive G-protein-coupled receptors: a novel type of multi-functional receptors. Cell Signal 17:1466-1476.

Trelle S, Reichenbach S, Wandel S, Hildebrand P, Tschannen B, Villiger PM, Egger M, Juni P (2011) Cardiovascular safety of non-steroidal anti-inflammatory drugs: network meta-analysis. Bmj 11.

Trevisani M, Siemens J, Materazzi S, Bautista DM, Nassini R, Campi B, Imamachi N, Andre E, Patacchini R, Cottrell GS, Gatti R, Basbaum AI, Bunnett NW, Julius D, Geppetti P (2007) 4-Hydroxynonenal, an endogenous aldehyde, causes pain and neurogenic inflammation through activation of the irritant receptor TRPA1. Proc Natl Acad Sci U S A 104:13519-13524.

Usui K, Hulleman JD, Paulsson JF, Siegel SJ, Powers ET, Kelly JW (2009) Site-specific modification of Alzheimer's peptides by cholesterol oxidation products enhances aggregation energetics and neurotoxicity. Proceedings of the National Academy of Sciences of the United States of America 106:18563-18568.

Vane JR (1971) Inhibition of prostaglandin synthesis as a mechanism of action for aspirin-like drugs. Nat New Biol 231:232-235.

Verge VM, Richardson PM, Benoit R, Riopelle RJ (1989) Histochemical characterization of sensory neurons with high-affinity receptors for nerve growth factor. J Neurocytol 18:583-591.

Viana F (2016) TRPA1 channels: molecular sentinels of cellular stress and tissue damage. J Physiol 594:4151-4169.

Viana F, Ferrer-Montiel A (2009) TRPA1 modulators in preclinical development. Expert Opin Ther Pat 19:1787-1799.

Walton KA, Hsieh X, Gharavi N, Wang S, Wang G, Yeh M, Cole AL, Berliner JA (2003) Receptors involved in the oxidized 1-palmitoyl-2-arachidonoyl-sn-glycero-3-phosphorylcholine-mediated synthesis of interleukin-8. A role for Toll-like receptor 4 and a glycosylphosphatidylinositol-anchored protein. J Biol Chem 278:29661-29666.

Weng HJ, Patel KN, Jeske NA, Bierbower SM, Zou W, Tiwari V, Zheng Q, Tang Z, Mo GC, Wang Y, Geng Y, Zhang J, Guan Y, Akopian AN, Dong X (2015) Tmem100 Is a Regulator of TRPA1-TRPV1 Complex and Contributes to Persistent Pain. Neuron 85:833-846.

Wetzel A, Jablonka S, Blum R (2013) Cell-autonomous axon growth of young motoneurons is triggered by a voltage-gated sodium channel. Channels 7:51-56.

Wong-Ekkabut J, Xu Z, Triampo W, Tang IM, Tieleman DP, Monticelli L (2007) Effect of lipid peroxidation on the properties of lipid bilayers: a molecular dynamics study. Biophys J 93:4225-4236.

Woods CG, Babiker MO, Horrocks I, Tolmie J, Kurth I The phenotype of congenital insensitivity to pain due to the NaV1.9 variant p.L811P: Eur J Hum Genet. 2015 May;23(5):561-3. doi: 10.1038/ejhg.2014.166. Epub 2014 Aug 13.

Woolf CJ, Costigan M (1999) Transcriptional and posttranslational plasticity and the generation of inflammatory pain. Proc Natl Acad Sci U S A 96:7723-7730.

Woolf CJ, Ma Q (2007) Nociceptors--noxious stimulus detectors. Neuron 55:353-364.

Wright DE, Snider WD (1995) Neurotrophin receptor mRNA expression defines distinct populations of neurons in rat dorsal root ganglia. J Comp Neurol 351:329-338.

Zeller I, Srivastava S (2014) Macrophage functions in atherosclerosis. Circulation research 115:e83-85.

Zhang XY, Wen J, Yang W, Wang C, Gao L, Zheng LH, Wang T, Ran K, Li Y, Li X, Xu M, Luo J, Feng S, Ma X, Ma H, Chai Z, Zhou Z, Yao J, Zhang X, Liu JY (2013) Gain-of-function mutations in SCN11A cause familial episodic pain. Am J Hum Genet 93:957-966.

Zimmermann K, Lennerz JK, Hein A, Link AS, Kaczmarek JS, Delling M, Uysal S, Pfeifer JD, Riccio A, Clapham DE (2011) Transient receptor potential cation channel, subfamily C, member 5 (TRPC5) is a cold-transducer in the peripheral nervous system. Proc Natl Acad Sci U S A 108:18114-18119.

9 Affidavit

Affidavit

I hereby confirm that my thesis entitled "Oxidized phospholipids and their role in neuronal excitation" is the result of my own work. I did not receive any help or support from commercial consultants. All sources and / or materials applied are listed and specified in the thesis.

Furthermore, I confirm that this thesis has not yet been submitted as part of another examination process neither in identical nor in similar form.

Würzburg,

Place, Date   Signature

Eidesstattliche Erklärung

Hiermit erkläre ich an Eides statt, die Dissertation „Oxidierte Phospholipide und ihre Funktion in neuronaler Erregbarkeit" eigenständig, d.h. insbesondere selbständig und ohne Hilfe eines kommerziellen Promotionsberaters, angefertigt und keine anderen als die von mir angegebenen Quellen und Hilfsmittel verwendet zu haben.

Ich erkläre außerdem, dass die Dissertation weder in gleicher noch in ähnlicher Form bereits in einem anderen Prüfungsverfahren vorgelegen hat.

Würzburg,

Ort, Datum   Unterschrift

Data of following chapters have already been published:

- 4.1, 4.2, 4.5, 4.6:

  Oehler B, Kistner K, **Martin C**, Schiller J, Mayer R, Mohammadi M, Sauer RS, Filipovic MR, Nieto FR, Kloka J, Pflucke D, Hill K, Schaefer M, Malcangio M, Reeh PW, Brack A, Blum R, Rittner HL (2017) Inflammatory pain control by blocking oxidized phospholipid-mediated TRP channel activation. Scientific reports 7:5447.

- 4.7 - 4.15:

  Martin C, Stoffer C, Mohammadi M, Hugo J, Leipold E, Oehler B, Rittner HL, Blum R. $Na_V1.9$ potentiates oxidized phospholipid-induced TRP responses. Frontiers in Molecular Neuroscience, Jan 2018, doi: 10.3389/fnmol.2018.00007.

Experiments, data analysis and writing of the present thesis were done by myself with the following exceptions:

- Chapter 4.8, 4.10 and 4.15: Experiments were performed in collaboration with Carolin Stoffer, Institute of Clinical Neurobiology, in the course of her master thesis under my supervision and supervision by the primary supervisor PD Dr. Robert Blum.

10 Curriculum Vitae

Personal

Corinna Martin born on June 12th 1990 in Rüsselsheim

Scientific experience

08/14-today   PhD student, Institute of Clinical Neurobiology, University Hospital of Würzburg

10/12-07/14   Master of Science in Biomolecular Engineering, TU Darmstadt

10/09-09/12   Bachelor of Science in Biomolecular Engineering, TU Darmstadt

Education

08/01-06/09   Abitur at Max-Planck Gymnasium, Rüsselsheim

Honors and awards

08/2015   Neuroscience Research Award 2015, GSLS, University of Würzburg

05/2017   Poster Prize, IZKF Retreat Kloster Banz, University Hospital of Würzburg

Publications

Martin C, Stoffer C, Mohammadi M, Hugo J, Leipold E, Oehler B, Rittner HL, Blum R. $Na_V1.9$ potentiates oxidized phospholipid-induced TRP responses only under inflammatory conditions. Front. Mol. Neurosci. doi: 10.3389/fnmol.2018.00007

Oehler B, Kistner K, **Martin C**, Schiller J, Mayer R, Mohammadi M., Sauer RS, Filipovic MR, Nieto FR., Kloka J, Pflucke D, Hill K, Schaefer M, Malcangio M, Reeh PW, Brack A, Blum R, and Rittner HL. Inflammatory pain control by blocking oxidized phospholipid-mediated TRP channel activation. Scientific Reports 7, 5447. doi:10.1038/s41598-017-05348-3.

Doppler K, Appeltshauser L, Villmann C, **Martin C**, Peles E, Krämer HH, Haarmann A, Buttmann M, Sommer C. Auto-antibodies to contactin-associated protein 1 (Caspr) in two patients with painful inflammatory neuropathy. Brain, 2016 Oct; 139(Pt 10):2617-2630.

Siotto F, **Martin C**, Rauh O, Van Etten JL, Schroeder I, Moroni A, Thiel G. Viruses infecting marine picoplancton encode functional potassium ion channels. Virology. 2014 Oct;466-467:103-11. doi: 10.1016/j.virol.2014.05.002.

Publications under review

Mohammadi M, Oehler B, Kloka J, **Martin C**, Brack A, Blum R, Rittner HL. Activation of TRPA1 leads to a subsequent production of OxPAPC and pain behavior.
In revision, British Journal of Pharmacology (status: 29.01.2018)

Prada J, Sasi M, **Martin C**, Jablonka S, Dandekar T, Blum R. An open source tool for automatic spatiotemporal assessment of calcium transients and local 'signal-close-to-noise' activity in calcium imaging data. In revision, PLOS Computational Biology (status: 29.01.2018)

Conferences and speeches

11 - 12 Oct 2017; 12th International Symposium organized by the Doctoral Researchers of the Graduate School of Life Sciences "Eureka", Würzburg. Contribution: Talk; "Oxidized phospholipids and their role in neuronal excitation and inflammatory pain"

22 - 25 Mar 2017; 12th Neuroscience Meeting of the German Neuroscience Society Göttingen. Contribution: Poster; "OxPL acutely increase the firing rate of DRG neurons and induce pain behavior"

12 - 13 Oct 2016; 11th International Symposium organized by the Doctoral Researchers of the Graduate School of Life Sciences "Eureka", Würzburg. Contribution: Poster; "Oxidized phospholipids acutely increase the firing rate of dorsal root ganglia (DRG) neurons"

14 - 15 Oct 2015; 10th International Symposium organized by the Doctoral Researchers of the Graduate School of Life Sciences "Eureka", Würzburg. Contribution: Poster; "Pain induced action of oxidized phospholipids: Mechanism of neuronal excitation in DRG neurons"

11 Acknowledgement